TEXTILE RESEARCH JOURNAL

Publication of

TEXTILE RESEARCH INSTITUTE

VOLUME XXIX AUGUST 1959 NUMBER 8

TEXTILE RESEARCH JOURNAL

VOL. XXIX *August 1959* NUMBER 8

Editor: **Richard K. Toner**

Production Editor: **Candida Frenking**

Advisory Board

Herbert J. Ball
Earl E. Berkley
John Boulton
C. H. Fisher
Walter J. Hamburger
Milton Harris
R. M. Hoffman
Harold P. Lundgren
Herman Mark
Edward R. Schwarz
George Switlyk
Helmut Zahn

TEXTILE RESEARCH JOURNAL, published monthly at Prince and Lemon Streets, Lancaster, Pa., is devoted to the interest of research in textile and allied industries. It is published by Textile Research Institute.

Manuscripts and communications should be sent to the Publications Department, P.O. Box 625, Princeton, N. J.

Second-class postage paid at Lancaster, Pa.

Subscription rates: $25.00 per year; additional for postage, 50 cents to Canada, $1.00 to all other countries. Single copies, $2.50 each.

Contents copyrighted © 1959 by Textile Research Institute Advertising rates supplied on request.

IN THIS ISSUE

Studies in the Adsorption of Arylamides of 2-Hydroxy-3-Naphthoic Acid and Related Compounds by Cellulosic Fibers. *E. H. Daruwalla and R. H. Mehra* 595

Mechanics of Elastic Performance of Textile Materials. Part XIV: Some Aspects of Bending Rigidity of Singles Yarns. *Milton M. Platt, William G. Klein, and Walter J. Hamburger* 611

An Application of a Sequential Type Analysis to Field Tests. *H. R. Rush* 628

A Study of Blended Woolen Structures. Part V: Methods of Within-Section Blend Analysis. *Myron J. Coplan and William G. Klein* 632

Thermal Comfort of Clothing of Varying Fiber Content. *Jane E. Werden, M. K. Fahnestock, and Ruth L. Galbraith* 640

The Effects of Wear and Laundering on the Wrinkling of Fabrics. *P. R. Wilkinson and R. M. Hoffman* 652

Procion Dye Staining for Differentiation of Skin and Core of Viscose Rayon Fibers. *Koichi Kato* 661

LETTER TO THE EDITOR

The Effect of Alkali on the Extractability of Wool Proteins; Evidence Against Disulfide Exchange as an Explanation for the Reduction in Solubility. *J. M. Swan* 665

Book Reviews 668

REPRINT REQUESTS SHOULD BE DIRECTED TO THE AUTHORS
SEE ARTICLES FOR ADDRESSES

CHEMISTS

Various degree levels with appropriate experience

POLYMER RESEARCH CHEMISTS

1. To conduct exploratory research on polymerizable materials, methods and routes of polymerization and polymeric products. Characterization of the polymers, both chemical and physical, is an important function in this work.

2. Senior men combining strong theoretical background with good practical experience in plastics properties, processing and use. Prefer R&D man with 8 or more years experience involving responsibilities for complex programs including the guidance of technical people.

PHYSICAL RESEARCH CHEMISTS

1. To investigate properties of new polymers and fibers for assessing ultimate potentiality in end use applications.

2. To investigate microstructure of polymers and fibers, for selecting new polymers, converting polymers to fibers, and predicting and controlling fiber products.

ANALYTICAL CHEMIST

For non-routine analytical and method development work. Wet analysis, as well as instrumental analysis, is included.

CHEMISTS or CHEMICAL ENGINEERS

1. To conduct laboratory work on application, development and technical service on monomers, alkyds, plasticizers, synthetic lubricants, resins and allied fields.

2. To conduct research on the conversion of new polymers to fibers, and to explore new methods for producing fibers.

Celanese's research facilities are located in modern surroundings in residential Summit, New Jersey, a favored living community in the metropolitan New York City area. Nearby colleges and universities, as well as other industrial research laboratories provide ample opportunities for professional association and individual growth.

Please send complete details regarding education, work experience and salary requirements to D. J. W. Cogger.

Celanese CORP OF AMERICA

SUMMIT NEW JERSEY

AUGUST 1959
VOL. XXIX NO. 8

TEXTILE RESEARCH JOURNAL

Studies in the Adsorption of Arylamides of 2-Hydroxy-3-Naphthoic Acid and Related Compounds by Cellulosic Fibers

E. H. Daruwalla and R. H. Mehra

Department of Chemical Technology, University of Bombay, Bombay 19, India

Abstract

Adsorption of arylamides of 2-hydroxy-3-naphthoic acid and related compounds by a variety of cellulosic fibers under different conditions of application such as varying alkali concentration and sodium chloride concentration of the impregnating liquor, temperature, etc. is studied. Limitations of Marshall and Peters thermodynamic treatment for calculation of affinity values are indicated and a modified thermodynamic treatment is developed for calculation of affinity values in which consideration is given to the simultaneous adsorption of hydroxyl ions, from sodium hydroxide used, on the accessible hydroxyl groups in the fiber substance. In case of three arylamides, heats of adsorption and entropy changes during application have also been calculated. Correlation between affinity values of arylamides and their chemical constitution has been established.

Introduction

Although many investigators have studied the uptake of arylamides of 2-hydroxy-3-naphthoic acid and related compounds (azoic coupling components) by cellulosic fibers under different experimental conditions, quite a few discrepancies exist between their results [8, 20, 22, 28]. Furthermore, the subject matter has not been treated from the point of view of simultaneous changes in the dye bath concentration of free alkali and of azoic coupling component during application, and the thermodynamic treatments for the adsorption of these components on different cellulosic fibers have remained neglected as compared with extensive experimental work carried out in the fundamental studies in the adsorption of direct cotton and leuco vat dyes by cellulose fiber substances. By use of the technique developed by Daruwalla and Desai [4] for the estimation of free alkali and of arylamide in the aqueous alkaline solutions of these compounds, it was possible to study the changes in the treating solution as a result of uptake of these compounds by a variety of cellulosic fibers under different conditions such as alkali concentration, electrolyte concentration, temperature, etc. From the data thus obtained, a suitable treatment is developed for the determination of affinity values for selected arylamides, and in some cases heats of reaction and entropy changes during application have also been calculated.

Experimental Materials and Methods

Arylamides of 2-hydroxy-3-naphthoic acid and related compounds used in the present work are shown in Table I.

Purification of the commercial samples of these compounds was according to the method recommended by Spiegler [31]. Purity of these compounds was determined from their melting points and analysis of the elements present. All other chemicals used were of Analar quality.

Fiber Substance

Standard cellulose. 20's single yarn prepared from Indian cotton was used. After careful purification by standard procedure, it had the following specifications

Copper number [9]	0.03
Fluidity in cuprammonium hydroxide solution (0.5%) [2]	3.72 poises^{-1}
Carboxyl content as determined by iodometric method [21]	0.783 meq./100 g.

Mercerized cellulose. Standard cellulose made from 2/30's yarn from Indian cotton was mercerized using sodium hydroxide concentration of 25.5% (wt./wt.) at a temperature of 15° C. During mercerization the sample was allowed to shrink during initial stages of impregnation and then stretched to its original length, in which state it was kept for 2 min., squeezed, and washed with hot water, followed by cold water rinsing. Traces of alkali were removed by a treatment with 0.25% hydrochloric acid for 10 min. The specimen was then thoroughly washed with running distilled water till free from acid, squeezed, and dried at room temperature.

Viscose rayon. The commercial bright sample (120/40) was washed with distilled water to remove glycerol present and then dried at room temperature.

Cuprammonium rayon. A commercial sample (40/30) was given the same preliminary treatment as that in the case of viscose rayon.

All the fiber substances were stored in an atmosphere of 65% RH at 30° C.

Application of Azoic Coupling Component from its Aqueous Alkaline Solution

Cellulosic fiber (1 g.; allowance made for moisture regain) was treated at 30 ± 1° C. with definite volumes of sodium hydroxide solutions of the azoic coupling component and of free alkali required, with or without additions of different quantities of sodium chloride. All throughout the period of application, stoppered conical flasks (Pyrex) containing the azoic coupling component solutions were agitated under standard conditions on a shaker which gave 75 uniform shakes per minute. The flasks were kept on the shaker for different lengths of time, and the amount of azoic coupling component and excess sodium hydroxide remaining in solution were determined by the method of Daruwalla and Desai [4].

During the study of application at higher temperatures, Pyrex flasks fitted with water condensers were used; the flasks were kept in a thermostat at a definite temperature without providing any agitation to the material or the solution. Agitation of liquor was found unnecessary because equilibrium conditions were obtained within 1 min. of application.

In order to check whether the amount of azoic coupling component exhausted from the solution corresponded with that adsorbed by the fiber, fiber substance containing the azoic coupling component was transferred to a gooch crucible (AG—3 × 4) and the fiber was completely sucked dry under vacuum. The azoic coupling component was then completely stripped from a known weight of the fiber using an alkaline solution of 25% pyridine; the amount of coupling component in the stripping solution was estimated by the gravimetric method [1]. It was observed that within the limits of experimental error the amount of azoic coupling component present on the fiber as determined from the stripping solution was the same as that estimated from the exhausted liquor after the application.

Experimental Results and Discussion

Effect of Increasing Concentration of Sodium Hydroxide in the Impregnating Solution on the Uptake of Free Sodium Hydroxide and of Arylamide by Standard Cellulose

All ten azoic coupling components were studied. The concentration of the coupling component in each case was kept constant at 5 g./l. while the concentration of free alkali in the impregnating solution was increased from 10 to 200 millimoles per liter. The liquor : material ratio was 40 : 1 and the temperature of treatment was 30 ± 1° C. Results obtained indicate that with an increase in the concentration of free alkali in the impregnating solution, the equilibrium adsorption of all the arylamides studied does not increase appreciably but the equilib-

rium adsorption of free alkali shows a progressive increase. In few cases, a slight increase in adsorption of the arylamide is observed in the initial stages of increasing alkali concentration. Figures 1 and 2 show the results of equilibrium adsorption of selected arylamides and of free alkali by standard cellulose respectively when the concentration of sodium hydroxide in the treating solution was progressively increased.

These results of the present work are in agreement with those of the work of Moryganov and Rostovtsev [20] and of Dunn [5], who indicated practically no change in equilibrium adsorption of arylamides with an increase in the alkali concentration of the

TABLE I. Arylamides of 2-Hydroxy-3-Naphthoic Acid and their Molecular Weights and Melting Points

No.	Chemical name	Constitution	Color Index: Azoic coupling component no.	Color Index: Constitution no.	Molecular weight	Melting point, °C.
1.	Phenylamide of 2-hydroxy-3-naphthoic acid	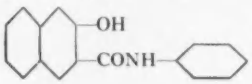	2	37505	263	249
2.	4′-Methoxy phenylamide of 2-hydroxy-3-naphthoic acid	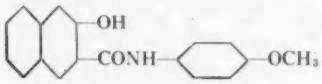	11	37535	293	230
3.	2′-Methylphenylamide of 2-hydroxy-3-naphthoic acid	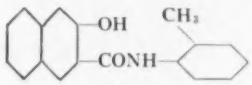	18	37520	277	194
4.	1′-Naphthylamide of 2-hydroxy-3-naphthoic acid	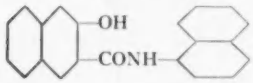	4	37560	313	223
5.	2′-Methyl-4′-chlorophenylamide of 2-hydroxy-3-naphthoic acid	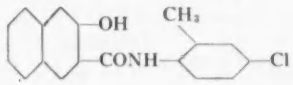	8	37525	311.5	243
6.	2′–4′-Dimethoxy-5′-chlorophenylamide of 2-hydroxy-3-naphthoic acid	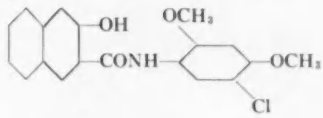	12	37550	357.5	194
7.	4′-Chlorophenylamide of 2-hydroxy-3-naphthoic acid	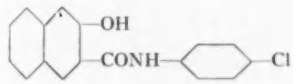	10	37510	297.5	264
8.	2′-Naphthylamide of 2-hydroxy-3-naphthoic acid	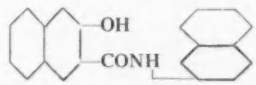	7	37565	313	244
9.	2′–5′-Dimethoxy-4′-chlorophenylamide of 2-hydroxy-3-naphthoic acid	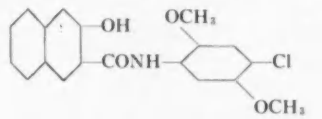	23	37555	357.5	189
10.	4′-Chlorophenylamide of 2-hydroxy-carbazole-3-carboxylic acid	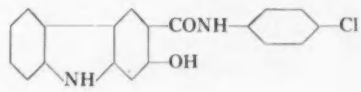	15	37600	336.5	259

solution. It is reasonable to assume that the alkaline solutions of arylamides of 2-hydroxy-3-naphthoic acid used in the present investigation exist in a state approaching that of molecular dispersion; thus their transfer from the bath onto the fiber takes place very readily. This is substantiated by the fact that in all cases equilibrium conditions are attained within 5 min. at 30 ± 1° C. and within 1 min. at 60° C. and higher temperatures. Furthermore, addition of dispersing agents such as a sodium salt of oleyl sulfate (Lissapol C) and a sodium salt of oleyl taurate (Igepon T), which are very effective in bringing about disaggregation of direct cotton and leuco vat dyes, does not alter either the rate of uptake of the arylamides or the amount adsorbed at equilibrium.

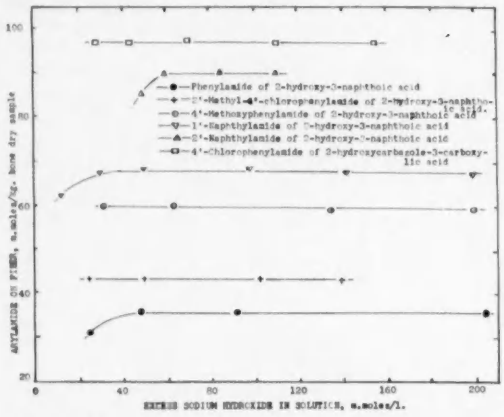
—●—Phenylamide of 2-hydroxy-3-naphthoic acid
—+—2'-Methyl-4'-chlorophenylamide of 2-hydroxy-3-naphthoic acid.
—○—4'-Methoxyphenylamide of 2-hydroxy-3-naphthoic acid.
—▽—1'-Naphthylamide of 2-hydroxy-3-naphthoic acid
—▲—2'-Naphthylamide of 2-hydroxy-3-naphthoic acid
—□—4'-Chlorophenylamide of 2-hydroxycarbazole-3-carboxylic acid
ARYLAMIDE ON FIBER, n.moles/g. bone dry sample
EXCESS SODIUM HYDROXIDE IN SOLUTION, n.moles/l.

Fig. 1. Effect of sodium hydroxide concentration in solution on equilibrium adsorption of arylamides.

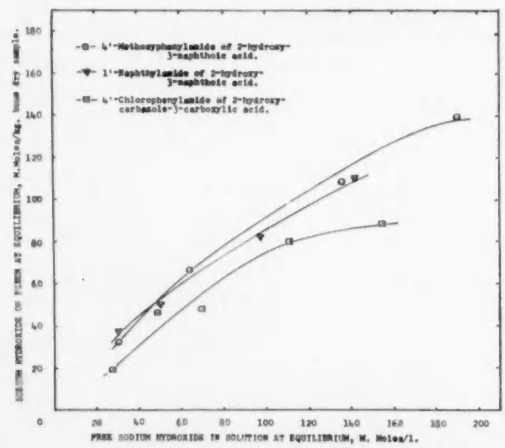
-○- 4'-Methoxyphenylamide of 2-hydroxy-3-naphthoic acid.
-▽- 1'-Naphthylamide of 2-hydroxy-3-naphthoic acid.
-□- 4'-Chlorophenylamide of 2-hydroxy-carbazole-3-carboxylic acid.
SODIUM HYDROXIDE ON FIBER AT EQUILIBRIUM, M.Moles/Kg. bone dry sample.
FREE SODIUM HYDROXIDE IN SOLUTION AT EQUILIBRIUM, M. Moles/l.

Fig. 2. Relation between sodium hydroxide in solution and on fiber at equilibrium.

Within the range of alkali concentration studied, it has been shown that swelling of the cellulosic fiber is very little altered (longitudinal swelling only of the order of 1% at free alkali concentration of 10 g./l. [23]). Thus, no appreciable change is likely to be expected in the adsorption of azoic coupling components within the range of alkali concentration studied.

With respect to free alkali adsorption by the fiber substance, the hydroxyl groups in cellulose are the main active sites responsible for adsorption. With an increase in the sodium hydroxide concentration in solution, an increased adsorption at these sites is to be expected, a phenomenon similar to that observed in all adsorption mechanisms. In most cases the isotherms representing free alkali concentration in the fiber to that in solution at equilibrium are of Freundlich type with their log-log plots linear in shape (Figures 2 and 3). Similar adsorption isotherms have been obtained by several previous workers also [3, 13, 24].

Effect of Increasing Concentration of Sodium Chloride in the Impregnating Solution on the Uptake of Arylamide and Free Sodium Hydroxide by Standard Cellulose

In this set of experiments the concentration of arylamide was kept constant at 5 g./l. and sodium hydroxide concentration was also constant (moles of arylamide : moles of sodium hydroxide = 1 : 4) while the concentration of sodium chloride was changed from 5 to 100 g./l. keeping the liquor : material ratio

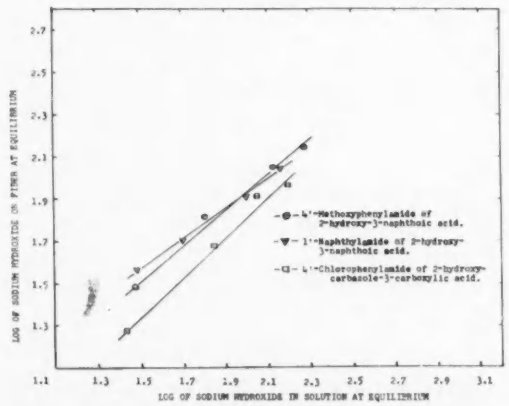
-●- 4'-Methoxyphenylamide of 2-hydroxy-3-naphthoic acid.
-▽- 1'-Naphthylamide of 2-hydroxy-3-naphthoic acid.
-□- 4'-Chlorophenylamide of 2-hydroxy-carbazole-3-carboxylic acid.
LOG OF SODIUM HYDROXIDE ON FIBER AT EQUILIBRIUM
LOG OF SODIUM HYDROXIDE IN SOLUTION AT EQUILIBRIUM

Fig. 3. Logarithmic plots of sodium hydroxide in solution and on fiber.

at 40:1 and temperature of treatment at 30 ± 1° C. Sodium chloride additions in different amounts to the treating liquor leads to an increase in the rate of adsorption and in the adsorption at equilibrium of both the arylamides as well as of free alkali with all the arylamides studied. Figures 4 and 5 show the equilibrium adsorption values for selected arylamides and for free alkali from treating solutions with increasing amounts of sodium chloride. The initial increase in the adsorption of an arylamide can be explained on the basis of the same arguments as those suggested for the adsorption of direct cotton dyes by cellulose from baths containing different amounts of an electrolyte. Cellulose in water acquires a negative surface charge and ions of arylamide formed in the solution as a result of dissociation of its sodium salt also carry a negative charge. The electrical repulsion forces between negatively charged fiber surface and negatively charged arylamide ions are responsible for prevention of arylamide ions approaching the fiber surface. With the addition of sodium chloride, the concentration of sodium ions in the solution is progressively increased, with the result that the negative surface potential at the fiber surface is diminished and the negative charge on the arylamide ion is screened by the cloud of positively charged sodium ions surrounding these ions. This in turn facilitates approach of the arylamide ions to the fiber surface, resulting in a marked increase in rate of adsorption as well as the equilibrium adsorption by the substrate. When values of the increase in equilibrium adsorption of different arylamides for a corresponding increase in equilibrium uptake of Chrysophenine G and Chlorazol Sky Blue FF from dye baths where the sodium chloride concentration is increased from 5 to 10 g./l. are compared [32], it is found that the effect of electrolyte is maximum in the case of Chlorazol Sky Blue FF (31% increase), intermediate with Chrysophenine G (26% increase), and least with the arylamides (19% increase). This is, however, natural because a dye anion of Chlorazol Sky Blue FF carries four negative charges, that of Chrysophenine G has two negative charges, and the anions of the arylamides studied carry only a single negative charge. Thus, the effect of electrolyte in reducing the repulsion forces will increase with increasing charge on the anions.

Among the different arylamides studied, the effect of increased adsorption is more marked with arylamides of high substantivity, intermediate with those

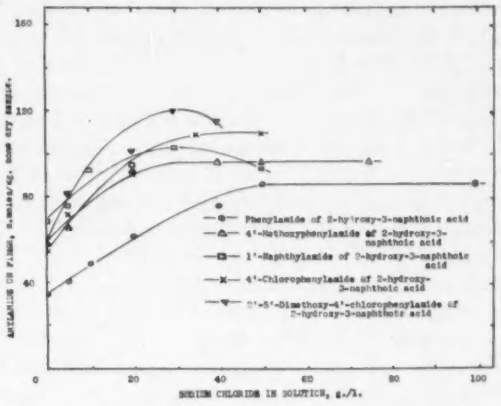

Fig. 4. Effect of sodium chloride in solution on equilibrium adsorption of arylamides.

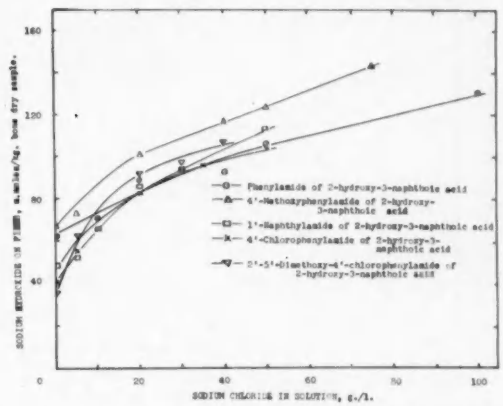

Fig. 5. Effect of sodium chloride on equilibrium adsorption of sodium hydroxide with different arylamides.

of moderate substantivity, and least with those of low substantive coupling components. This could be explained on the basis that although with all arylamides the addition of electrolyte will reduce the electrical repulsion forces, only those possessing sufficient secondary valency forces or hydrogen bonding forces will be readily adsorbed at suitable sites in the fiber substance, whereas those with low residual valency forces will be influenced the least.

Reduction in equilibrium adsorption of some of the arylamides after a certain stage of sodium chloride concentration in the solution (Figure 4) is due to the formation of larger aggregates which by virtue of their large size are unable to diffuse through capillaries of water-swollen cellulosic fibers. This is supported by the fact that this decrease is noticed to

a maximum extent in case of those arylamides in which the tendency for aggregate formation is greatest [27]. Previous workers have indicated that at low concentration of alkali in the solution, the hydroxyl ions of sodium hydroxide are adsorbed on the hydroxyl groups of cellulose, whereas at higher concentrations of alkali, chemical reaction between hydroxyl groups of cellulose and sodium hydroxide takes place with the formation of soda cellulose [3, 13, 23, 24]. Thus, free sodium hydroxide will behave in the same way as an arylamide and will show increased adsorption at specific sites with progressive reduction in the electrical charge at the fiber surface. The present results are in agreement with those of Rath [27], Marsson [16], Moryganov and Rostovtsev [20], and Nabar et al. [22].

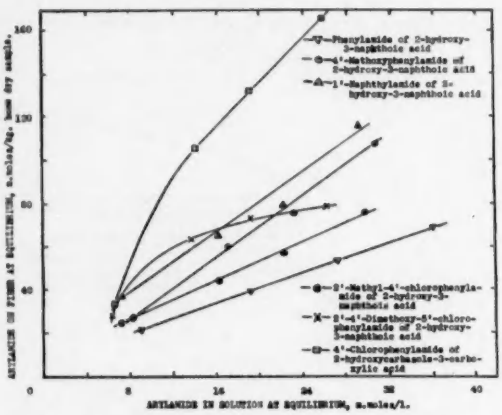

Fig. 6. Effect of varying concentration of an arylamide in solution on its equilibrium adsorption on fiber.

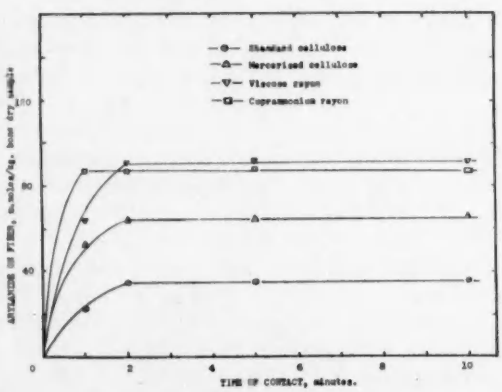

Fig. 7. Adsorption of phenylamide of 2-hydroxy-3-naphthoic acid on different cellulosic fibers.

Effect of Increasing Concentration of Arylamide in the Treating Liquor on the Uptake of Arylamide by Standard Cellulose

Arylamide numbers 1, 2, 4, 5, 6, and 10 were studied; the ratio of moles of arylamide to moles of sodium hydroxide in the solution was always kept constant at 1:4. The concentration of arylamide was varied from 6 to 40 millimoles per liter, liquor: material ratio was 40:1, and temperature of treatment was 30 ± 1° C. Results in Figure 6 indicate the relation between arylamide concentration in fiber and in solution at equilibrium with increasing arylamide concentration in bath. These results indicate that with increasing amount of arylamide in the solution, the equilibrium adsorption of all the azoic coupling components increases; in the case of some of the arylamides the shape of the isotherms resembles Freundlich adsorption isotherms, while with others the shape is more or less linear (Figure 6). The linear isotherms were obtained in case of arylamides of low and medium affinity where the distribution of the arylamide between the fiber phase and solution phase depends on the ionic concentrations in the two phases and on the charge at the fiber surface.

Effect of Substrate

With three arylamides studied (1, 4, and 10) on standard cellulose, mercerized cellulose, viscose rayon, and cuprammonium rayon, the effect is the same in that under standard conditions of arylamide concentration (5 g./l.), alkali concentration (moles

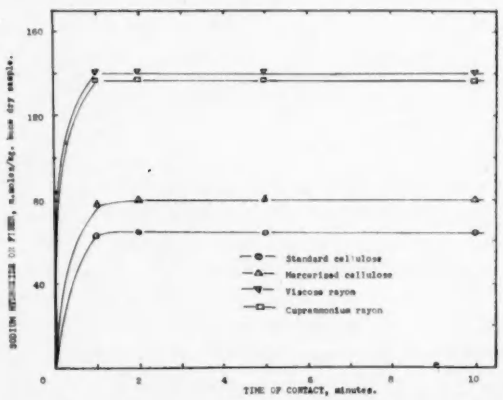

Fig. 8. Adsorption of sodium hydroxide on different cellulosic fibers with phenylamide of 2-hydroxy-3-naphthoic acid.

of arylamide : moles of sodium hydroxide 1 : 4), liquor : material ratio 40 : 1, and temperature of treatment 30 ± 1° C., the rate of uptake as well as the amount adsorbed at equilibrium of arylamide and of free alkali increases in the order standard cellulose < mercerized cellulose < regenerated cellulosic fibers. Figures 7 and 8 represent the results obtained with phenylamide of 2-hydroxy-3-naphthoic acid.

Regarding the effect of increasing alkali concentration (e.g., from 20 to 150 m.moles/l.) or sodium chloride concentration (e.g., from 5 to 50 g./l.) on the rate of adsorption as well as equilibrium adsorption of different arylamides on different fiber substances, it was observed that with an increase in concentration of free alkali the equilibrium adsorption of any of the arylamides does not increase in case of any of the fiber substance studied but equilibrium adsorption of free sodium hydroxide shows a progressive increase under identical conditions of application. However, with increasing amounts of sodium chloride, with all the fibers studied there is a marked increase in the rate of adsorption and also in the amount adsorbed at equilibrium of the arylamide as well as of free alkali. The increase is more marked on regenerated cellulosic fibers, intermediate with mercerized cellulose, and least with standard cellulose (Figure 9 and 10).

These differences in adsorption of arylamides and of alkali can be readily explained on the basis of accessible hydroxyl groups in the intermicellar surfaces where adsorption of these compounds takes place. During mercerization, the original crystal structure is disrupted by action of sodium hydroxide, as indicated by Heyn [10]; a new network of crystallites with much shorter periodicity is formed, resulting in an increase in the reactive fraction and a lower degree of crystallinity. Similarly, in case of regenerated rayons, disruption of original crystal structure and re-formation of new ones takes place during dissolution of cellulose and subsequent coagulation in the spinning bath. The structural changes are more pronounced in regenerated rayons than in mercerized cellulose. Thus, with an increase in the number of accessible hydroxyl groups, equilibrium adsorption of arylamides and of free alkali should increase. Furthermore, due to the swelling action of sodium hydroxide in the mercerizing liquor or to the more opened-out structure in case of regenerated fibers, as indicated by the pore radius in different cellulosic fibers (*viz.*, 16 Å for standard

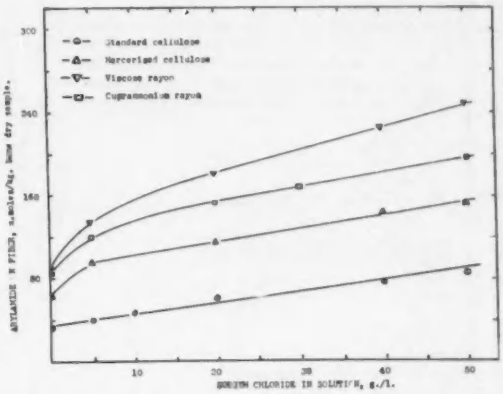

Fig. 9. Effect of sodium chloride in solution on equilibrium adsorption of phenylamide of 2-hydroxy-3-naphthoic acid on different cellulosic fibers.

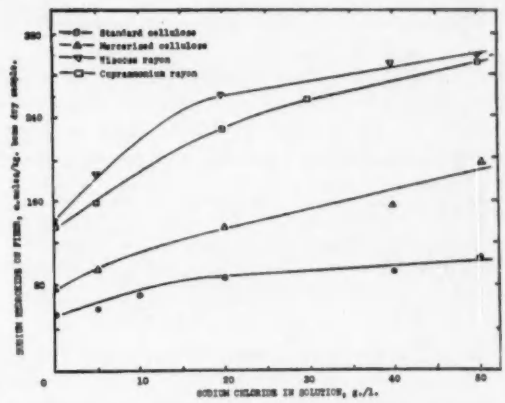

Fig. 10. Effect of sodium chloride in solution on equilibruim adsorption of sodium hydroxide on different cellulosic fibers with phenylamide of 2-hydroxy-3-naphthoic acid.

cellulose, 20 Å for alkali swollen cellulose, and 30 Å for regenerated rayons [11, 14]), entry of molecules of azoic coupling component inside the fiber substance is much easier, with the result that rate of adsorption increases.

Variation in equilibrium adsorption of arylamides on different substances for a specific increase of sodium chloride in the treating solution can to some extent be explained in terms of potential barrier which the anion of azoic coupling component has to overcome. During mercerization as well as during regeneration there is likelihood of oxidation of some hydroxyl groups to the carboxyl groups, as indicated by carboxyl content values of the fiber samples used in the present work (0.78, 0.93, 1.85, and 3.15

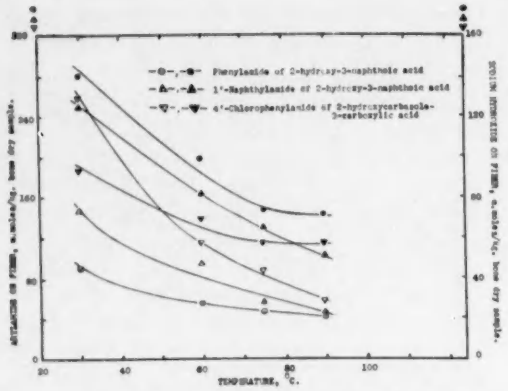

Fig. 11. Effect of temperature on equilibrium adsorption of arylamides and of excess sodium hydroxide by viscose rayon.

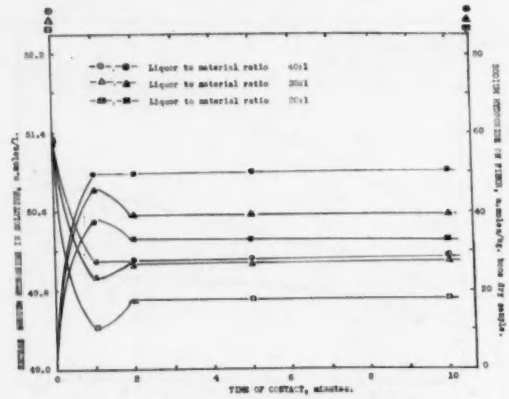

Fig. 12. Changes in sodium hydroxide concentration in solution and on fiber during treatment of standard cellulose with alkaline solution of 1'-naphthylamide of 2-hydroxy-3-naphthoic acid at different liquor : material ratios.

meq./100 g. for standard cellulose, mercerized cellulose, cuprammonium rayon, and viscose rayon respectively), with the result that mercerized cellulose and regenerated fibers are likely to show higher negative surface potential than cellulose. Thus, the effect of electrolyte in reducing the surface potential will be more pronounced with regenerated cellulose fibers, less so with mercerized cellulose, and not so appreciable in case of standard cellulose.

Effect of Temperature

Temperature dependence of the adsorption characteristics of arylamides (1, 4, and 10) was studied at the same alkali concentration (moles of alkali : moles of arylamide 4 : 1) and varying the temperature of impregnating solution from 30 to 90° C. The liquor : material ratio was kept constant at 40 : 1; the fiber substance used was standard cellulose. Results indicate that with an increase in temperature of the impregnating solution, the amount of arylamide and free sodium hydroxide adsorbed at equilibrium diminishes appreciably (Figure 11). However, in all cases the rate of uptake is increased considerably and equilibrium conditions are obtained within 1 min. of the treatment.

Adsorption of arylamides on cellulosic fibers is an exothermic reaction, as indicated by negative values of the heats of reaction (Table VI); therefore, increase in temperature is bound to bring about a decrease in equilibrium adsorption. The same argument applies to the adsorption of free alkali which is adsorbed on the same sites as those for the arylamides—accessible hydroxyl groups in the noncrystalline regions in the fiber substance. Increase in the rate of adsorption is due to the additional energy of activation supplied by the thermal energy which facilitates the entry of the molecules of both the coupling component and of free alkali inside the fine structure of cellulose. The effect of rise in temperature is more marked between 30 and 60° C. than between 60 and 90° C. and also in case of arylamides of higher substantivity (Figure 11).

Simultaneous Adsorption of Free Sodium Hydroxide and Arylamide on Cellulosic Fibers from Aqueous Alkaline Solutions of These Compounds

One of the most interesting observations recorded in the present work is that in the initial stages of impregnation of cellulosic fibers with aqueous alkaline solutions of arylamide, decrease in concentration of free alkali in the bath is appreciable, while the reduction in the concentration of the arylamide is moderate. After a specific time, the concentration of free alkali in the solution increases, while that of arylamide decreases continuously till the final conditions of equilibrium are attained. This behavior is more marked at lower material : liquor ratio and higher concentration of sodium chloride in the impregnating solution with arylamides of higher substantivity and when regenerated rayons are used as fiber substances (Figures 12 and 13).

The active sites for adsorption of both the arylamide anions and the hydroxyl anions from sodium hydroxide are the accessible hydroxyl groups in the

cellulose fiber substance. The hydroxyl anions, being small, diffuse through the fine structure of cellulose rapidly in the initial stages and occupy some of the hydroxyl groups in cellulose. The anions of the arylamide, by virtue of their larger size, take a longer time to diffuse, but when they have entered the fiber structure, because of their higher affinity for cellulose they are capable of displacing the hydroxyl ions of sodium hydroxide from accessible hydroxyl groups. As a result reversal of alkali in the impregnating solution takes place. The higher the concentration of arylamide in the impregnating solution and the greater the amount of electrolyte in the impregnating solution, the more marked is this reversal effect because in these cases both the free hydroxyl ions and arylamide ions can approach the fiber surface more readily than otherwise.

Furthermore, when the arylamides have higher affinity for the fiber, they will be in a better position to displace the hydroxyl ions of alkali than when arylamides of lower substantivity are present. Similar observations have also been recorded by Elöd [6] during the studies in dyeing of wool from a hydrochloric acid bath containing an acid dye and sodium chloride where the dye by virtue of its higher affinity for the fiber has been shown to be capable of displacing chloride ions which have occupied the positively charged basic groups in the fiber substance during initial stages of dyeing.

Affinities, Heats of Reaction, and Entropy Changes During Application of Different Arylamides of 2-Hydroxy-3-Naphthoic Acid to Different Cellulosic Fibers

Although the mechanism of dyeing of cellulosic fibers with direct cotton and leuco vat dyes based on thermodynamic fundamentals has been studied by several workers [7, 15, 25], similar treatment in case of azoic coupling components have been given only by Dunn [5], Modena [18], and Moryganov and Mel'nikov [19]. Dunn during his investigations showed that when Peters and Vickerstaff's [26] theory for calculation of affinities and heats of reaction was applied to four different azoic coupling components, the slopes of the plots correlating logarithm of ionic products in the fiber with the logarithm of ionic products in solution did not have a theoretical value of unity; thus he doubted the validity of the theory in the adsorption of arylamides. Moryganov and Mel'nikov [19] determined heats of reactions

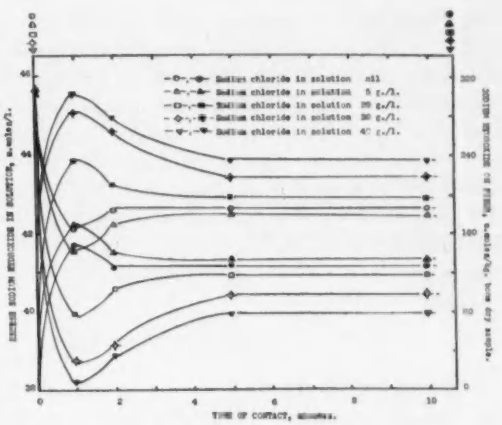

Fig. 13. Changes in sodium hydroxide concentration in solution and on fiber during treatment of viscose with alkaline solution of 1′-naphthylamide of 2-hydroxy-3-naphthoic acid under different conditions of sodium chloride concentration.

for eight different azoic coupling components from affinity values calculated on the basis of the treatment of Marshall and Peters [15].

If it is assumed that the arylamide Na_2Ar, being a strong electrolyte, is completely dissociated both in the solution and in the fiber phase and the arylamide anion, by virtue of its spatial configuration, is specifically adsorbed on cellulose while the sodium ions are present in the fiber to maintain electrical neutrality, the standard change in free energy ΔG^0, which is also termed the affinity, is given by the equation

$$-\Delta G^0 = RT \ln \frac{A_f}{A_s} \qquad (1)$$

where A_f and A_s are the activities of the arylamide in the fiber and in solution respectively, R the gas constant, and T the absolute temperature. The activity of the arylamide in solution is given by

$$A_s = (Na_s)^z \cdot (Ar_s) \qquad (2)$$

assuming the activity coefficient to be unity. In the fiber, activity of the arylamide, A_f, will be given by

$$A_f = \frac{(Na_f)^z \cdot (Ar_f)}{V^{z+1}} \qquad (3)$$

where (Na_f) and (Na_s) are the concentrations of the sodium ions in the fiber and in the bath expressed in terms of gram ions per kilogram of dry

fiber and gram ions per liter of the solution respectively, (Ar_f) and (Ar_s) are the ionic concentrations of the arylamides in the fiber and in the solution expressed in terms of gram ions arylamide per kilogram dry fiber and gram ions arylamide per liter respectively, z is the basicity of arylamide, and V is the effective volume of cellulose phase expressed in liters per kilogram dry cellulose. Substituting the values of A_s and A_f in Equation 1

$$-\frac{\Delta G^0}{RT} = \ln (Ar_f)\cdot(Na_f)^z - \ln (Ar_s)\cdot(Na_s)^z - (z+1)\ln V \quad (4)$$

When the values of (Na_f) are calculated, utilizing the Donnan membrane equilibrium maintained between Na ions and the OH ions in the fiber and in external solution (a treatment similar to that employed by Marshall and Peters [15] for direct cotton dyes and by Fowler, Michie, and Vickerstaff [7] for leuco vat dyes using volume term V as 0.3 l./kg. dry fiber), the plot of log A_f against log A_s gave straight lines with slopes much less than unity (Table II). If the technique developed in the present work of estimating the concentration of arylamide and free alkali in the fiber is employed, the values of (Na_f) can be calculated directly from experimental data. When these values of (Na_f) are considered, the plots correlating log A_s against log A_f using $V = 0.3$ l./kg. dry fiber are shown in Figure 14 and the values of slopes for six different arylamides studied are given in Table II; they show that the slopes in this case are nearer unity.

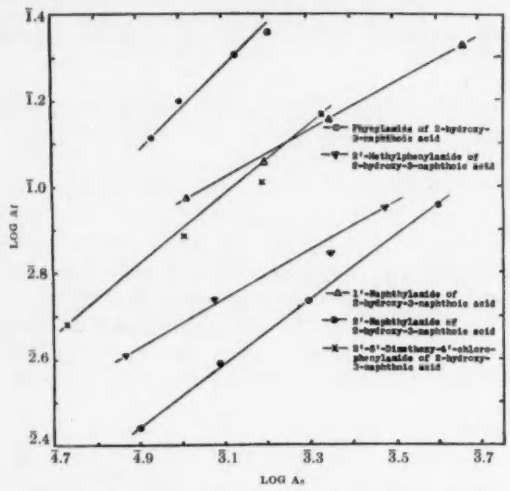

Fig. 14. Adsorption of arylamides on standard cellulose; plot of log of ionic products in the fiber and in solution.

When affinity values for different arylamides studied have been calculated based on Na_f values from the Donnan membrane equilibrium, the affinity values of arylamides vary considerably at different concentrations of sodium hydroxide in the bath, while when the experimentally determined values of Na_f are substituted, affinity values obtained are nearer each other. Even then the affinity values of the same arylamide on different cellulosic fibers using $V = 0.30$, 0.50, 0.45, and 0.65 l./kg. for cotton, mercerized cellulose, viscose rayon, and cuprammonium rayon respectively (as used by Marshall and Peters [15]) show considerable deviation. It appears that this deviation in the values of ΔG^0 for the same arylamide for different cellulosic fibers is due to inappropriateness of the values of the volume term V used by Marshall and Peters for different cellulosic fibers based on adsorption of Chrysophenine G.

However, when the values obtained from moisture adsorption data (0.22, 0.26, 0.46, and 0.37 l./kg. for

TABLE II. Slopes of Ionic Product Plots for Different Arylamides

Arylamide	Slope of ionic product plot: Na_f calculated from Marshall and Peters equation	Slope of ionic product plot: Na_f as experimentally determined
Phenylamide of 2-hydroxy-3-naphthoic acid	0.56	0.76
2'-Naphthylamide of 2-hydroxy-3-naphthoic acid	0.33	1.02
4'-Chlorophenylamide of 2-hydroxycarbazole-3-carboxylic acid	0.18	0.70
2'-Methyl-4'-chlorophenylamide of 2-hydroxy-3-naphthoic acid	0.28	—
2'–5'-Dimethoxy-4'-chlorophenylamide of 2-hydroxy-3-naphthoic acid	—	0.81
4'-Methoxyphenylamide of 2-hydroxy-3-naphthoic acid	—	0.66
2'-Methyl phenylamide of 2-hydroxy-3-naphthoic acid	—	0.59
1'-Naphthylamide of 2-hydroxy-3-naphthoic acid	—	0.59

cotton, mercerized cellulose, viscose, and cuprammonium rayon respectively [33]) are utilized in the present work as the volume term V, the calculated values of ΔG^0 agree not only at different concentrations of sodium ions in the solution but also on different cellulosic fibers (Table III). To check the validity of this treatment further, the sodium ion concentration in the impregnating solution was changed by keeping the total alkali constant, varying the concentration of arylamide, and then calculating the values of ΔG^0 using experimentally determined values of (Na_f). Results are shown in Table IV, where standard cellulose was used as fiber substance.

Thus it appears that, because of specific adsorption of OH ions of sodium hydroxide on the same sites as those responsible for the adsorption of arylamide ions, as observed in the experimental part of the present work, sodium ion concentration in the fiber (Na_f) should be actually determined in the calculation of affinity values. The concentration calculated from Donnan membrane equilibrium should not be used.

Peters and Simons [25] also observed that with increasing concentration of alkali in the vat dye bath the proportion of the leuco vat dye ions adsorbed at equilibrium on cellulosic fiber substance decreases. In their treatment they have assumed that the hydroxyl ions and the dye ions are adsorbed independently, but in the present investigation it was found that the arylamide ions were capable of displacing already adsorbed hydroxyl ions of alkali from the accessible sites. Furthermore, the volume term as used by Marshall and Peters for different cellulosic fibers does not fit well in the present case, where the affinity of arylamides is calculated on different cellulosic fibers.

It has been reported that the volume phase changes not only with different dyes but also with temperature. In the present work, the values of volume phase for different cellulosic fibers as determined by Urquhart and Eckersall [33] from moisture regain seems to fit well. It can be observed that at very high concentration of sodium hydroxide in the impregnating solution, the calculated values of the affinities decrease (Table III).

It is very likely that at high alkali concentration the sodium hydroxide can act as an electrolyte and can bring about aggregation of the arylamide in the solution, with the result that such a solution will deviate from ideal behavior and the assumption of

TABLE III. Affinity Values Calculated Using Urquhart and Eckersall's Values for Moisture Adsorption as the Effective Volumes for Cellulose Phases

Arylamide	Cotton			Mercerized cotton				Cuprammonium rayon				Viscose rayon			
	Moles arylamide: moles total sodium hydroxide	Na_f determined experimentally, g. ions/kg. dry fiber	Affinity $-\Delta G^0$ cal./mole	Mean affinity $-\Delta G^0$ cal./mole	Moles arylamide: moles total sodium hydroxide	Na_f determined experimentally, g. ions/kg. dry fiber	Affinity $-\Delta G^0$ cal./mole	Mean affinity $-\Delta G^0$ cal./mole	Moles arylamide: moles total sodium hydroxide	Na_f determined experimentally, g. ions/kg. dry fiber	Affinity $-\Delta G^0$ cal./mole	Mean affinity $-\Delta G^0$ cal./mole	Moles arylamide: moles total sodium hydroxide	Na_f determined experimentally, g. ions/kg. dry fiber	Affinity $-\Delta G^0$ cal./mole	Mean affinity $-\Delta G^0$ cal./mole
Phenylamide of 2-hydroxy-3-naphthoic acid	1:2.4	0.0786	2,518	2,479	1:2.3	0.1020	2,920	2,834	1:2.5	0.2447	2,900	2,893	1:2.3	0.1641	2,826	2,753
	1:3.5	0.0985	2,568		1:4.1	0.1424	2,831		1:3.9	0.2847	2,906		1:3.8	0.2314	2,732	
	1:6.0	0.1338	2,353		1:6.7	0.1687	2,752		1:4.9	0.2975	2,872		1:4.6	0.2723	2,702	
	1:12.0	0.2264	2,249		1:10.0	0.1958	2,527		1:7.4	0.3129	2,811		1:7.0	0.3614	2,638	
1'-Naphthylamide of 2-hydroxy-3-naphthoic acid	1:2.6	0.1032	3,284	3,101	1:2.2	0.1136	3,414	3,338	1:2.5	0.1555	3,680	3,593	1:2.9	0.1039	3,295	3,301
	1:4.2	0.1180	3,079		1:3.9	0.1617	3,284		1:4.4	0.2244	3,607		1:4.4	0.2740	3,320	
	1:7.1	0.1488	2,942		1:4.2	0.1754	3,316		1:5.1	0.2628	3,494		1:5.5	0.3128	3,290	
	1:10.0	0.1784	2,847		1:7.2	0.2403	3,168		1:8.5	0.3511	3,434		1:8.2	0.4088	3,190	
4'-Chlorophenylamide of 2-hydroxycarbazole-3-carboxylic acid	1:2.9	0.1164	3,724	3,485	1:2.7	0.1321	3,750	3,676	1:2.8	0.1959	4,183	4,051	1:3.0	0.2848	4,156	4,058
	1:5.7	0.1438	3,424		1:4.5	0.1815	3,677		1:4.3	0.2615	4,022		1:6.2	0.4045	3,960	
	1:8.6	0.1780	3,298		1:5.2	0.1872	3,603		1:5.0	0.2773	3,950		—	—	—	
	1:11.5	0.1846	3,137		1:7.7	0.2128	3.427		1:7.6	0.3901	3,716		1:9.2	0.4414	3,768	

an activity coefficient of unity would no longer be valid. Similar deviations have also been recorded by Marshall and Peters in their determination of the affinities of direct cotton dyes from dyebaths containing large proportions of electrolyte.

In Table V are given the calculated values of affinities of different arylamides studied by the treatment mentioned above. These affinity values generally lie between − 2,400 and − 3,500 cal./mole. The order of increasing affinities for different arylamides is more or less the same as that given by different workers for increasing substantivity arrived at in a purely arbitrary fashion [17]. The highly substantive azoic coupling components have affinity values between − 3,100 and − 3,500 cal./mole; the medium substantive ones, between − 2,800 and − 3,100 cal./mole; and those with low substantivity, between − 2,400 and − 2,700 cal./mole. Comparison of the affinity values of different arylamides (− 2,400 to − 3,500 cal./mole) with those of direct cotton dyes (− 3,500 to − 8,000 cal./mole) indicates that these values are much lower for arylamides than those for direct cotton dyes. This is because the molecule of arylamide is comparatively simple, with a single group (amido, -CONH-) capable of taking part in the hydrogen bond formation, while with direct cotton dyes the elongated dye molecule fits closely in a direction parallel to the fiber axis, with a number of suitable hydrogen bonding groups, resulting in higher values for affinities.

TABLE IV. Effect of Change in Arylamide Concentration on Affinity Values Using Standard Cellulose as Fiber Substance

Arylamide	Concentration of arylamide in the solution, m.moles/l.	Concentration of sodium hydroxide in the solution, m.moles/l.	Affinity $-\Delta G^0$ cal./mole	Mean affinity $-\Delta G^0$ cal./mole
Phenylamide of 2-hydroxy-3-naphthoic acid	9.50	93.83	2,503	2,338
	18.76	92.11	2,279	
	28.26	93.78	2,254	
	37.78	94.05	2,309	
1′-Naphthylamide of 2-hydroxy-3-naphthoic acid	8.43	93.47	2,957	2,861
	15.91	93.69	2,852	
	24.11	92.90	2,744	
	32.06	92.58	2,892	
4′-Chlorophenylamide of 2-hydroxycarbazole-3-carboxylic acid	7.50	95.78	3,302	3,340
	15.26	93.80	3,451	
	22.51	93.80	3,341	
	30.26	94.04	3,368	

TABLE V. Affinity Values of Different Arylamides Obtained in Present Work and Those Recorded by Other Workers

Arylamide	Mean affinity $-\Delta G^0$ cal./mole obtained in present work	Affinity as recorded by Dunn $-\Delta G^0$ cal./mole	Affinity as recorded by Modena $-\Delta G^0$ cal./mole
Phenylamide of 2-hydroxy-3-naphthoic acid	2,479	3,100	2,270
2′-Methylphenylamide of 2-hydroxy-3-naphthoic acid	2,616	3,240	—
2′-Methyl-4′-chlorophenylamide of 2-hydroxy-3-naphthoic acid	2,655	—	—
4′-Methoxyphenylamide of 2-hydroxy-3-naphthoic acid	2,837	3,490	2,520
4′-Chlorophenylamide of 2-hydroxy-3-naphthoic acid	2,905	—	2,940
2′–5′-Dimethoxy-4′-chlorophenylamide of 2-hydroxy-3-naphthoic acid	2,969	—	—
2′–4′-Dimethoxy-5′-chlorophenylamide of 2-hydroxy-3-naphthoic acid	3,046	—	—
1′-Naphthylamide of 2-hydroxy-3-naphthoic acid	3,101	—	—
2′-Naphthylamide of 2-hydroxy-3-naphthoic acid	3,419	—	—
4′-Chlorophenylamide of 2-hydroxycarbazole-3-carboxylic acid	3,488	—	—

If ΔG_1 and ΔG_2 are the affinities of an arylamide at temperature T_1 and T_2 respectively, the heat of adsorption ΔH^0 can be evaluated from

$$\Delta H^0 = \frac{\left(\frac{\Delta G_1}{T_1} - \frac{\Delta G_2}{T_2}\right)}{\left(\frac{1}{T_1} - \frac{1}{T_2}\right)}$$

If ΔH^0 is constant, the plot of $\Delta G^0/T$ against $1/T$ should give a straight line of slope ΔH^0. The plots of $\Delta G^0/T$ against $1/T$ for three different arylamides at four different temperatures using viscose as fiber substance (Figure 15) are fairly linear; the values of ΔH^0 calculated from their slopes are given in Table VI. Entropy changes (ΔS) during the reaction for three different arylamides on viscose rayon at 30° C. were calculated by making use of the equation $\Delta G^0 = \Delta H^0 - T\ \Delta S$; values obtained are given in Table VI. These results show that the entropy of reaction increases with an increase in heat of reaction for the three arylamides studied on viscose rayon.

Values of heats of adsorption calculated represent to a certain extent the energy of association between the arylamide and the fiber substance. However, these values cannot be taken as an absolute measure of the bond strength in the absence of further data on cellulose–water, arylamide–water, and arylamide–arylamide interaction. The heats of adsorption of the three arylamides studied vary between $-7{,}000$ and $-11{,}000$ cal./mole (Table VI) and are lower than the heats of dyeing of direct cotton dyes, which lie between $-11{,}000$ and $-31{,}000$ cal./mole for different dyes depending on their chemical constitution [15].

This is natural because in the arylamide molecule the main contribution for the arylamide–fiber combination is due to hydrogen bond formation between the amide (-CONH-) group and the hydroxyl (-OH) group in the fiber substance. The energy of association of arylamide and fiber will vary to some extent depending on the specific substituents at suitable positions in the arylamide molecule, whereas in the case of direct cotton dyes the number of hydrogen bond forming groups are many; also, the conjugated system of double bonds capable of contributing to secondary valency forces for dye–fiber attachment is so long that the energy of association is much higher and more widely varying, depending on the structure of the dye.

The significance of the entropy of reaction is at present rather obscure; it can be considered in general terms as a measure of the degree of orientation or restraint achieved by the adsorption of the arylamide on the fiber as compared with that in solution. Thus, an arylamide showing a greater entropy change is more rigidly attached or more precisely orientated on the fiber as compared with that in which entropy changes are of lesser order. This is substantiated by the fact that increase in heats of reaction and increase in entropy changes run parallel (Table VI).

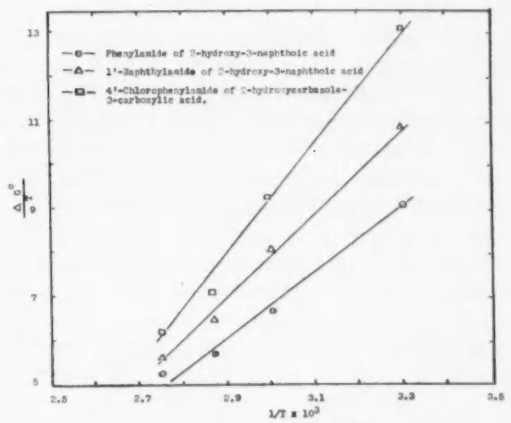

Fig. 15. Effect of temperature on affinity of arylamides for viscose.

TABLE VI. Affinities, Heats of Adsorption, and Entropy Changes for Three Different Arylamides

Arylamide	Affinity at 30° C. $-\Delta G^0$, cal./mole	Heat of reaction $-\Delta H^0$, cal./mole	Entropy at 30° C. $-\Delta S$, cal./deg./mole
Phenylamide of 2-hydroxy-3-naphthoic acid	2,753	7,650	16.16
1′-Naphthylamide of 2-hydroxy-3-naphthoic acid	3,301	9,750	21.28
4′-Chlorophenylamide of 2-hydroxycarbazole-3-carboxylic acid	4,058	11,520	24.62

Chemical Constitution and Affinity

Previous workers such as Krzikalla and Eistert [12] and Ruggli [29] attributed substantivity to presence of an acid amide group in the molecule of an azoic coupling component, while Schirm [30] was of the opinion that substantivity was mainly due to the residual valency forces from a conjugated system of double bonds present in the molecule. Venkataraman [34] indicated that substantivity could be increased by the introduction of halogen, methoxyl, or nitro groups in the benzene ring of the arylamide molecule and that transition from anilide to naphthanalide of 2-hydroxy-3-naphthoic acid caused considerable increase in substantivity. Spiegler [31], from the study of the atomic models of arylamides, concluded that the most important criteria for an arylamide to be substantive to cotton were linear configuration, coplanarity, and presence of hydrogen bond forming groups situated at 10 Å in the molecule.

In the present work, no detailed study has been made of the effect of chemical constitution on substantivity, but it is possible to compare substantivity of arylamides from the calculated affinity values. It can be seen from Table V that the order of increasing affinity is the same in the present work and in the work of Dunn [5] and of Modena [18], although the values in these three cases are different because of the fact that the treatments given by Dunn, Modena, and the present workers are not identical.

For an arylamide to have high substantivity for cellulosic fibers, in addition to being planar it must contain a long conjugated chain of double bonds. This is possible only if the following structure of the arylamide of 2-hydroxy-3-naphthoic acid is accepted:

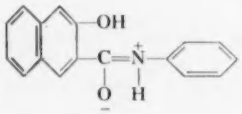

This view is supported by the fact that if the amide group is acetylated or if a methylene group is interposed between the naphthalene ring and the carbonyl group, continuity of the system of a conjugated chain of double bonds is disrupted and substantivity is lost [12]. Thus, differences in the affinities of the arylamides studied can be explained on the basis of specific electron interaction of the substituents in the benzene nucleus with the amide group. This is supported by the fact that substitution of CH_3, OCH_3, or Cl either in ortho or in para position to the amide group in the benzene nucleus increases the electron density at the aromatic amide substituted carbon and stabilizes the negative charge on the carbonyl oxygen, resulting in greater tendency for hydrogen bond formation with the hydroxyl of cellulose.

This substitution also stabilizes the double bond between the amide carbon and nitrogen atoms, thereby increasing the effective length of conjugation. This effect will be more marked on purely theoretical grounds as the hydrogen in the benzene nucleus in the ortho or in the para position is replaced by CH_3, OCH_3, or Cl respectively; this is actually found to be true, as observed by the fact that affinity of phenylamide of 2-hydroxy-3-naphthoic acid is − 2,479 cal./mole, that of 2′-methyl phenylamide of 2-hydroxy-3-naphthoic acid is − 2,616 cal./mole, and that of 4′-methoxyphenylamide of 2-hydroxy-3-naphthoic acid is − 2,837 cal./mole, while that of 4′-chlorophenylamide of 2-hydroxy-3-naphthoic acid is − 2,905 cal./mole. When two of these groups are in ortho or in para position to the amide in the benzene nucleus, affinity is increased still further; affinity values of 2′-5′-dimethoxy-4′-chlorophenylamide of 2-hydroxy-3-naphthoic acid and of 2′-4′-dimethoxy-5′-chlorophenylamide of 2-hydroxy-3-naphthoic acid are −2,969 and − 3,046 cal./mole respectively.

It can, however, be seen that in case of these compounds the affinity values are not very high due to the presence of an additional group in the meta position which has the effect of reducing the negative charge on carbonyl oxygen and thereby diminishing the substantivity to a certain extent. This is in agreement with the fact that meta-substituted arylamides have little or no substantivity for cellulosic fibers. Substitution of benzene by a naphthalene nucleus increases the length of chromophore area and should lead to enhanced substantivity. This is actually found in the present work, where affinity of 1′-naphthylamide of 2-hydroxy-3-naphthoic acid is − 3,101 cal./mole and that of 2′-naphthylamide is − 3,419 cal./mole.

However, when comparison is made between these two arylamides, it is observed that 2′-naphthylamide shows higher affinity than 1′-naphthylamide. It is well known that electron density in the β-position is lower than in the α-position; therefore these differ-

ences cannot be explained on the basis of electron density alone. The higher affinity of the β-derivative can be explained on steric grounds. It has been shown from atomic models of α- and β-derivatives that there are considerable differences between the linear configuration in these two cases. The β-derivative is quite linear, therefore can fit readily parallel to cellulose chain molecules, while in the case of the α-derivative the configuration is angular; close fit with the cellulose chain molecule therefore is not possible [31]. When the anilide of naphthoic acid is replaced by an anilide of carbazole carboxylic acid, the length of the chromophore is increased further without any change in linearity of configuration. Therefore increased chromophore area should give rise to further increase in secondary valency forces, resulting in increased affinity. This is observed in the present results, where affinity of 4′-chlorophenylamide of 2-hydroxycarbazole-3-carboxlyic acid is of the order of − 3,500 cal./mole.

Thus, affinity values obtained in the present work can be conveniently taken as suitable means of expressing substantivity of different azoic coupling components under different conditions of alkali or arylamide concentration in the bath and on different fibers at a definite temperature. The values obtained are in conformity with theoretical considerations which are likely to favor the substantivity of these compounds for cellulosic fibers.

The main conclusion to be drawn from these thermodynamic treatments is that the mode of attachment of azoic coupling components to different cellulosic fibers is the same, as indicated by the fact that the same value of affinity is obtained for a particular arylamide during application. Application with such compounds consists in molecular attraction between the arylamide molecule and cellulose chain molecule. The energy changes on adsorption are mainly dependent on molecular structure of the arylamides rather than on the physical structure of the fiber. The differences in the adsorption behavior of different cellulosic fibers are solely due to differences in the physical structure of the fibers, which in turn influence the effective volumes of cellulose phase for the adsorbed ions.

Summary

With all cellulosic fibers studied, increase in concentration of free sodium hydroxide in the impregnating solution makes only a slight difference in equilibrium adsorption of different arylamides, but the equilibrium adsorption of free sodium hydroxide shows a progressive increase.

Additions of different amounts of sodium chloride to the bath brings about a marked increase in the rate of adsorption and also in the amount adsorbed at equilibrium of the azoic coupling components as well as of free alkali. This effect is more marked with azoic coupling components of medium and high substantivity.

In a majority of cases, concentration of free alkali in the bath decreases in the first minute and then increases as the time of impregnation is continued. This reversal effect is more prominent with increasing amounts of sodium chloride in the solution at lower liquor : material ratio with azoic coupling components of high substantivity and when regenerated fibers are used as substrate.

Increasing the temperature of treatment results in a decrease of adsorption of azoic coupling components as well as of free alkali by viscose, but the rate of adsorption by the fiber substance increases rapidly.

Under identical conditions of application the equilibrium adsorption as well as rate of adsorption of a coupling component from the impregnating solution increases in the order standard cellulose < mercerized cellulose < viscose or cuprammonium rayon.

Affinity values calculated for different azoic coupling components lie between − 2,400 and − 3,500 cal./mole while the heats of adsorption vary between − 7,000 and − 11,000 cal./mole.

Mechanism of application of an azoic coupling component to different cellulosic fibers is similar to the dyeing of cellulosic substances with a direct cotton dye except that for calculation of affinity values consideration must be given to the adsorption of hydroxyl ions from free sodium hydroxide in the bath by the hydroxyl groups in the substrate which are also the sites for adsorption of arylamide ions.

Acknowledgment

The authors are indebted to Professor G. M. Nabar for valuable suggestions and keen interest throughout the progress of this work.

Literature Cited

1. Bhat, R. V., Forster, R. B., and Venkataraman, K., *J. Soc. Dyers Colourists* **56**, 166 (1940).

2. Clibbens, D. A. and Geake, A., *J. Textile Inst.* **19**, T77 (1928).
3. Coward, H. F., Spencer, L., and Wood, F. C., *J. Textile Inst.* **14**, T529 (1923).
4. Daruwalla, E. H. and Desai, N. F., *Anal. Chem.* **29**, 116 (1957).
5. Dunn, A. S., *Disc. Faraday Soc.* **16**, 230 (1954).
6. Elöd, E., *Trans. Faraday Soc.* **29**, 327 (1933).
7. Fowler, J. A., Michie, A. G. H., and Vickerstaff, T., *Melliand Textilber.* **32**, 296 (1951).
8. Giles, C. H., *J. Soc. Dyers Colourists* **60**, 280 (1944).
9. Heyes, T. F., *J. Soc. Chem. Ind.* **47**, T90 (1928).
10. Heyn, A. N. J., TEXTILE RESEARCH JOURNAL **19**, 163 (1949).
11. Hunt, C. M., Blaine, R. L., and Rowen, J. W., TEXTILE RESEARCH JOURNAL **20**, 43 (1950).
12. Krzikalla, H. and Eistert, B., *J. prakt. Chem.* **143**, 50 (1935); *vide C. A.* **29**, 5659 (1935).
13. Leighton, A., *J. Phys. Chem.* **20**, 32 (1916); *vide C. A.* **10**, 824 (1916).
14. Madras, S., McIntosh, R. L., and Mason, S. G., *Can. J. Res.* **B27**, 764 (1949).
15. Marshall, W. J. and Peters, R. H., *J. Soc. Dyers Colourists* **63**, 446 (1947).
16. Marsson, R. W., *Am. Dyestuff Reptr.* **20**, 43 (1931).
17. Maynard, Jr., *vide* Lubs, H. A., "The Chemistry of Synthetic Dyes and Pigments," New York, Reinhold, 184 (1955).
18. Modena, G., *Ricerca. Sci.* **26**, 1451 (1956); *vide C. A.* **50**, 16, 111 (1956).
19. Moryganov, P. V. and Mel'nikov, B. N., *Tekstil Prom.* **17**, 41 (1957); *vide J. Soc. Dyers Colourists* **73**, 347 (1957).
20. Moryganov, P. V. and Rostovtsev, V. E., *Trans. Inst. Chem. Tech. Ivanovo* (U.S.S.R.) No. 2, 102 (1939); *vide C. A.* **33**, 8995 (1939).
21. Nabar, G. M. and Padmanabhan, C. V., *Proc. Ind. Acad. Sci.* **31**, 371 (1950).
22. Nabar, J. A., Barve, P. M., Patel, A. M., and Desai, B. N., *Proc. Ind. Acad. Sci.* **10**, A344 (1939).
23. Neale, S. M., *J. Textile Inst.* **21**, T225 (1930).
24. Neuenstein, W. V., *Kolloid Z.* **43**, 241 (1927); *vide J. Soc. Dyers Colourists* **44**, 90 (1928).
25. Peters, R. H. and Simons, J., *J. Soc. Dyers Colourists* **70**, 557 (1954).
26. Peters, R. H. and Vickerstaff, T., *Proc. Roy. Soc.* **A192**, 292 (1948).
27. Rath, J., *J. Soc. Dyers Colourists* **39**, 334 (1923).
28. Rath, J., *J. Soc. Dyers Colourists* **44**, 10 (1928).
29. Ruggli, P., *J. Soc. Dyers Colourists*, (Jubilee Issue) 77 (1934).
30. Schirm, E., *J. prakt. Chem.* **144**, 69 (1935); *vide C. A.* **30**, 2009 (1936).
31. Spiegler, L., *J. Org. Chem.* **18**, 1292 (1953).
32. Subramanian, P., M.Sc. (Tech.) Thesis, University of Bombay (1957).
33. Urquhart, A. R. and Eckersall, N., *J. Textile Inst.* **23**, T163 (1932).
34. Venkataraman, K., Presidential Address, 32nd Indian Science Congress, 1945.

Manuscript received January 20, 1959.

Mechanics of Elastic Performance of Textile Materials

Part XIV: Some Aspects of Bending Rigidity of Singles Yarns[1]

Milton M. Platt, William G. Klein, and Walter J. Hamburger

Fabric Research Laboratories, Inc., 1000 Providence Highway, Dedham, Massachusetts

Abstract

Theoretical analyses are given of the effects of fiber properties and yarn structure on singles yarn bending rigidity, assuming the fibers to be elastically isotropic and to exhibit linear stress–strain behavior. The two extreme cases of complete freedom and no freedom of relative fiber motion are analyzed.

The effects on yarn rigidity of fiber dimensions, fiber stiffness, torsional to bending rigidity ratio, yarn density, size, twist, fiber clustering, and prior relaxation treatments are analytically investigated.

1. Where freedom of fiber motion prevails, yarn rigidity is equal to the sum of fiber bending rigidities geometrically modified by yarn twist in a manner such that twist increases produce decreases in yarn rigidity.
2. For most practical yarns, residual torsional stresses produce only a minor influence (increase) in yarn rigidity.
3. Relaxation of twisting stresses prior to yarn bending alters very slightly the effects of yarn twist on rigidity. Consequently only changes in fiber modulus produced by relaxation are of significance.
4. Fiber clustering, i.e., the aggregate action of groups of fibers, produces marked increases in yarn rigidity, roughly proportional to the number of fibers per cluster.
5. The extreme case of fiber clustering, i.e., no freedom of relative fiber motion, results in rigidity of the order of the number of fibers in the yarn divided by the yarn packing factor times the rigidity obtained when freedom of motion prevails.

The rigidity of blended yarns is discussed, and the interaction of gross yarn structure, properties of the fibers being blended, and their spatial distributions qualitatively analyzed.

1. For a uniform blend distribution, total rigidity is determined from the summative rigidities of the fibers, modified by yarn twist to the same proportionate extent as is a self-fiber yarn.
2. Location of fibers in a nonuniform blend determines not only the yarn rigidity but also its variation with twist. Generally, when stiffer fibers predominate in the core of the yarn, less rapid decreases in rigidity with twist increases take place than in a uniform blend; the converse is true when the stiffer fibers are present in the yarn sheath.
3. Changes in fiber location resulting from twist or blend changes can significantly affect yarn rigidity.

Introduction

A variety of practical end-use considerations of textile structures are associated with the bending rigidity of the yarns comprising the structure. The association may be obvious or subtle, and in either case, the magnitude of the interrelationship may be large or small. Examples of obvious associations are flexural rigidity or drapeability of fabrics and fabric crease resistance or resilience in bending. Examples of more subtle associations are curl and skew or shape instability of knit and woven goods. Although it would be expected that fabric stiffness generally must reflect yarn stiffness, it would not necessarily be expected that differences in the flexural rigidities of yarns are perfectly translated into differences in fabric rigidity, particularly since the

[1] Part of a study jointly supported by the Office of Naval Research and the Bureau of Supplies and Accounts, U. S. Navy.

mode of fiber and yarn bending in a fabric could be different from that of a freely bending yarn. Thus, where the multifilamentous character of a yarn is maintained, increases in filament denier (or diameter) at constant yarn denier could result in increases in yarn bending rigidity. However, if the construction of the fabric is sufficiently tight to prevent the multifilamentous character of the yarn from being evidenced, little or no difference in fabric rigidity might be experienced from changes in filament denier.

In any event, it is clear that an understanding of the influence of yarn structure and fiber properties on yarn bending rigidity is of significance in the understanding of many important fabric properties. It is the purpose of this work to present theoretical analyses of the response of yarns to a bending deformation, the final formulations of which indicate the principal influencing factors. The analyses are based primarily on the fiber strains and curvatures in bent yarns as formulated by Backer [1] and the idealized geometry of the bent yarn as developed in his rigorous analysis of the problem. The two extreme conditions, as delineated by Backer [1] and also Hamburger et al. [6], of complete freedom of relative fiber motion and no freedom of relative fiber motion are analyzed independently, since they each yield entirely different results, although some factors of construction and fiber properties are common to both.

In order to develop theoretical relations of yarn bending rigidity, which are a reflection of fiber forces, from fiber strains compatible with the geometry of the bent yarn state, assumptions must be made or *a priori* knowledge available as to the relation between fiber stress and strain. For purposes of the present work, linear isotropic elasticity will be assumed, since this permits the derivation of a general solution to the problem. For very high bending strains, such an assumption generally will not be valid for purposes of precise results. However, most textile fibers exhibit a fairly constant modulus over the low strain region; thus, for radii of curvature large enough, it is believed that only small errors would be introduced. For the case of complete freedom of fiber motion, radii of curvature of the fiber central axis large compared to the fiber radius are assumed. For the case of no freedom of fiber motion, radii of curvature of the central axis of the yarn large compared to the yarn radius are assumed, in order that linear elasticity be a valid approximation.

It should be emphasized that the relations derived in this work are based upon an idealization of the yarn geometry. As has many times been stated, actual textile structural geometry oftentimes significantly departs from the idealized forms assumed. Nonetheless, the value of such idealized models has been sufficiently well established so that their use is justified [1, 2, 3, 6, 7, 10, 11].

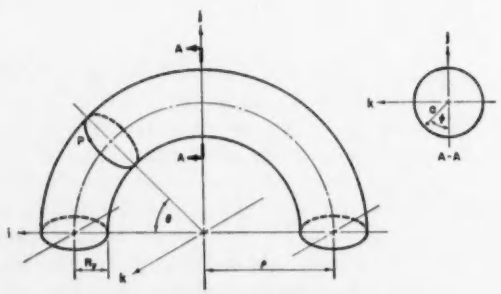

Fig. 1. Coordinates for idealized bent yarn.

Response of Yarns with Complete Freedom of Relative Fiber Motion

Review of Basic Fiber Geometry in Bent Yarn

A complete picture of the geometrical relations for fibers in bent twisted yarns can be obtained by study of the work of Backer [1]. The condition of yarn bending is shown in Figure 1. The yarn radius is R_y, radius of curvature of the center line of the bent yarn is ρ, original yarn twist in turns per unit length is T_0, angle θ specifies any cross section of the bent yarn, and radius to any point in the yarn cross section from the yarn center is a. The angle φ shown in the enlarged cross section represents the angular coordinate to any point in the yarn cross section, with the origin of φ being at the inside of the bend for all cross sections. As Backer has shown, there is a relation between the angles θ and φ such that[2]

$$\varphi = \lambda\theta \tag{1}$$

where

$$\lambda = \frac{\rho}{a}\tan Q_0 \tag{2}$$

and Q_0 is the original (before bending) helix angle of the yarn at radius a.

[2] Equations 1 and 2 can be derived by assuming plane sections of the yarn remain plane after bending.

Because of the symmetry of the bent form, total or resultant bending conditions are the same for all values of θ, although different fibers will generally be located, for a given value of a and φ, at one cross section, θ, than at another. Thus, all final calculations will be made with $\theta = \pi/2$ (for computational convenience), although in the derivation of equations for curvature and helix angle, θ must be considered as a variable.

By analysis of the geometry consistent with the foregoing, Backer has shown that the coordinates $\bar{Y}$ of any point P on the center line of any fiber when the yarn is bent may be represented by the vector equation

$$\bar{Y} = i[\rho \cos\theta + a \cos\varphi(-\cos\theta)] + j[\rho \sin\theta + a \cos\varphi(-\sin\theta)] + k[a \sin\varphi] \quad (3)$$

where i, j, and k are unit vectors in the directions shown in Figure 1, the origin of coordinates being at the center of curvature of the bent yarn.

Under conditions of complete freedom of relative fiber motion while the yarn is bent, two physical phenomena deducible from Equation 3 take place. The first of these is the change in helix angle from that before bending. The second is the change in fiber curvature from that present before the yarn is bent.

With respect to helix angle changes, prior to yarn bending the local helix angle Q_0 is determinable from

$$\tan Q_0 = 2\pi T_0 a \quad (4)$$

where T_0 is the original yarn twist before bending.

After yarn bending, the local helix angle at any radius a in the yarn can be determined from the new local yarn twist T, where

$$T = \frac{T_0}{1 + e_y} \quad (5)$$

and e_y is the local yarn strain corresponding to the bent state. From elementary mechanics of bending, when plane sections remain plane

$$e_y = -\frac{a \cos\varphi}{\rho} \quad (6)$$

Thus the local helix angle after bending, α, is found from Equations 5 and 6 to be

$$\tan\alpha = \frac{2\pi T_0 a}{1 - \frac{a}{\rho}\cos\varphi} = \frac{\tan Q_0}{1 - \frac{a}{\rho}\cos\varphi} \quad (7)$$

Equation 7 above checks Backer's Equation 33, deduced from the i component of the unit tangent vector to fiber axis in the bent yarn at $\theta = \pi/2$. For those fibers above the neutral axis of the yarn, $\cos\varphi$ is negative, hence helix angles are reduced below those present prior to bending. Similarly, the helix angles of fibers below the neutral axis are increased as a result of yarn bending.

For purposes of determination of fiber curvatures and components thereof, the unit tangent vector to any fiber in the bent yarn is required. This is given by Backer's Equation 31b

$$\bar{T}_{ijk} = \frac{d\bar{Y}_{ijk}}{d\theta} \frac{1}{\sqrt{\sum_{m=i}^{k} \frac{d\bar{Y}_m}{d\theta}\frac{d\bar{Y}_m}{d\theta}}} \quad (8)$$

which, after calculation of the respective derivatives from Equation 3 is found to be

$$\bar{T} = i[-\rho + a\cos\varphi]/\sqrt{u} + j[\rho \tan Q_0 \sin\varphi]/\sqrt{u} + k[\rho \tan Q_0 \cos\varphi]/\sqrt{u} \quad (9)$$

where

$$u = (\rho - a\cos\varphi)^2 + \rho^2 \tan^2 Q_0 \quad (10)$$

Equation 9 for the unit tangent vector to any fiber in the bent yarn is obtained from the more general Equation 8 for the value $\theta = \pi/2$, for the reasons previously discussed.

For space curves, of which the fiber in the bent twisted yarn is an example, total curvature is best represented by the vector defining it for both magnitude and direction. Following Backer

$$\bar{K} = \frac{1}{u^2}\left[u\frac{d^2\bar{Y}}{d\theta^2} + \frac{d\bar{Y}}{d\theta}(a\cos\varphi - \rho) \times (\rho \tan Q_0 \sin\varphi)\right] \quad (11)$$

The derivatives required in Equation 11 are obtained from Equation 3, and after substitution and simplification there results

$$\bar{K} = \frac{i}{u^2}\{u(-2a\lambda\sin\varphi) + (a\cos\varphi - \rho)^2(a\lambda\sin\varphi)\} + \frac{j}{u^2}\{u[-\rho + a(1+\lambda^2)\cos\varphi] + (a\cos\varphi - \rho)(a\lambda\sin\varphi)^2\} + \frac{k}{u^2}\{u(-a\lambda^2\sin\varphi) + (a\cos\varphi - \rho)(a\lambda\sin\varphi)(a\lambda\cos\varphi)\} \quad (12)$$

where $\bar{K}$ is the *resultant* curvature vector on any fiber in the bent yarn, and all terms are as previously defined. Equation 12 is found from Equation 11 following substitution of $\theta = \pi/2$ after the indicated differentiations are performed.

By the term resultant curvature is meant the final curvature of any fiber after the yarn is bent. In the case of zero twist yarns, the resultant curvature of fibers is merely that introduced by the bending of the yarn. In the case of a twisted yarn, as has been shown [1, 11], each fiber possesses a curvature prior to yarn bending. Imposition of a bend to the yarn changes the fiber curvature. Thus, Equation 12 represents the final curvature of the fiber after the yarn is bent, hence is its total curvature, including that introduced by the twisting operation.

Analysis of Fiber Bending Moments

For an isotropically elastic rod bent to a large radius of curvature (large with respect to its cross-sectional dimensions), the bending moment required for elastic equilibrium is

$$M_B = EI/\rho = EIK \tag{13}$$

where ρ is the radius of curvature in the bent state and K is the curvature in the bent state. E is the modulus of elasticity, assumed constant with strain, tension, and compression, and I is the cross-sectional moment of inertia about the neutral axis in the plane of bending. Equation 13 will be assumed applicable to the case of fibers comprising a bent yarn. Note that this assumes radii of curvature large compared to fiber cross-sectional dimensions.

Figure 2 illustrates the classical bending defined by Equation 13. M_B is the external bending moment applied to the rod whose cross-sectional flexural rigidity is EI, producing an equilibrium radius of curvature ρ or a curvature $K = 1/\rho$. The internal bending moment required for equilibrium is also M_B. For ease in computation, the vector representing M_B is also shown in Figure 2. This vector is always perpendicular to the plane defined by the tangent vector to the elastically bent curve and the principal normal to the curve. Its sense is defined by the right hand screw rule for rotation of the tangent to the curve into the curvature vector though an angle less than 180°. Thus, it is in the direction of the binormal [9] to the elastically bent curve, and of magnitude equal to $EI/\rho = EIK$ where K is the magnitude of the curvature. In more general terms

$$\bar{M}_B = \bar{T} \times EI\bar{K} \tag{14}$$

where $\bar{T}$ is the unit tangent vector to the elastically bent curve, $\bar{K}$ is the resultant curvature vector, and EI, assumed to be a scalar quantity, is the cross-sectional rigidity of the bent element. Since in Equation 14 $\bar{T}$ is a vector of unit magnitude which by definition is perpendicular to the curvature vector $\bar{K}$, the magnitude of the cross-product given in Equation 14 is

$$\begin{aligned} |M_B| = |\bar{T} \times EI\bar{K}| &= EI|\bar{T}||\bar{K}| \sin\gamma \\ &= EI|\bar{K}| \\ &= EI/\rho \end{aligned} \tag{15}$$

where $\gamma = \pi/2$ is the angle between $\bar{T}$ and $\bar{K}$.

For cases where bending takes place in a single plane, as is the usual case for most structural materials, Equation 13 is sufficient for analysis and design purposes. However, in dealing with the geometrical distortions which occur in the case of a bent twisted yarn, Equation 14 is the more powerful for general use, particularly since it makes unnecessary the difficulty of attempting solutions by visualization of highly complex three-dimensional geometric states.

The bending moment vector defined by Equation 14 has, in general, components along the i, j, and k axes defined in Figure 1. The bending moment acting on the yarn at the cross section corresponding to the plane $\theta = \pi/2$ of Figure 1 is simply given by the k component of $\bar{M}_B$ defined by Equation 14. The remaining components of $\bar{M}_B$ at $\theta = \pi/2$ may give rise to couples about the i and j axes, and will be made use of in future publications. For the present purpose of defining twisted yarn bending rigidity, only the k component of $\bar{M}_B$ will be considered. In general, for the unit vector directions defined by Figure 1, if

$$\begin{aligned} \bar{T} &= T_1 i + T_2 j + T_3 k \\ \bar{K} &= K_1 i + K_2 j + K_3 k \end{aligned}$$

then

$$\bar{T} \times \bar{K} = -i\begin{vmatrix} T_2 T_3 \\ K_2 K_3 \end{vmatrix} + j\begin{vmatrix} T_1 T_3 \\ K_1 K_3 \end{vmatrix} - k\begin{vmatrix} T_1 T_2 \\ K_1 K_2 \end{vmatrix} \tag{16}$$

For the unit vector system of Figure 1, $j \times k = -i$; $i \times k = j$; $i \times j = -k$. Thus, the k component of $\bar{M}_B$ is given by

$$\frac{(\bar{M}_B)_k}{EI} = (\bar{T} \times \bar{K})_k = \bar{T}_{ij} \times \bar{K}_{ij} \qquad (17)$$

where the subscript ij refers only to the i and j components of each of the vectors $\bar{T}$ and $\bar{K}$.

Performing the cross product indicated by Equation 17 on Equations 9 and 12 there results, after simplification

$$\frac{(\bar{M}_B)_k}{EI} = -k \times \left[\frac{(a\cos\varphi-\rho)^2+a^2\lambda^2(1+\sin^2\varphi)-a\rho\lambda^2\cos\varphi}{u^{3/2}}\right] \qquad (18)$$

where

$$u = (a\cos\varphi - \rho)^2 + \rho^2\tan^2 Q_0$$
$$\lambda = \rho/a[\tan Q_0] \qquad (19)$$

Each fiber in the bent yarn cross section, at the plane $\theta = \pi/2$, contributes a bending moment to the yarn the magnitude of which is given by $(\bar{M}_B)_k$ defined by Equation 18, where EI is average of the fiber rigidities $= E_f I_f$. The value of ρ is constant for all fibers, while (a, φ) define the position of the fiber in the yarn cross section. For each value of a, there is also a value of Q_0, the helix angle in the unbent yarn, determined from

$$\tan Q_0 = 2\pi T_0 a \qquad (20)$$

Analysis of Yarn Bending Moment

For the assumptions made, $\bar{M}_{Bk}$ from Equation 18 represents the contribution to the yarn bending moment from any fiber for which a, φ, and Q_0 are known. The total bending moment in the yarn is then given by the sum of all such contributions, since they all act in a single direction.

The differential element of yarn cross-sectional area is given by

$$dA = a\,da\,d\varphi \qquad (21)$$

For this element of area, the total number of fibers encompassed is given by

$$dN_f = \frac{N_f}{\pi R_y^2}\,a\,da\,d\varphi\cos\alpha\left[\frac{\tan^2 Q_{0s}\cos Q_{0s}}{2(1-\cos Q_{0s})}\right] \qquad (22)$$

where all terms are as previously defined, N_f is the total number of fibers in the yarn cross section, and Q_{0s} is the original helix angle at the surface of the twisted yarn. Little difference exists in most cases whether $\cos\alpha$ or $\cos Q_0$ is used in Equation 22,

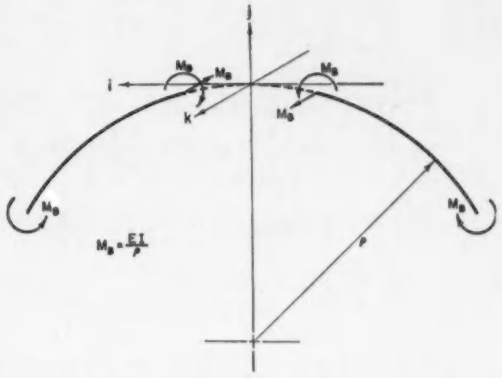

Fig. 2. Classical bending to constant radius of curvature.

particularly at large radii of curvature compared to the yarn radius. The bracketed term in Equation 22 takes into account the effect of yarn radial growth with increasing yarn twist for the close packing implicitly assumed in the analysis. Such radial growth was not taken into consideration in previous publications [11] dealing with similar problems.

The total yarn bending moment $(dM_B)_y$ supplied by all fibers in the differential element of area is then given by

$$(dM_B)_y = -\frac{E_f I_f}{u^{3/2}}[(a\cos\varphi-\rho)^2 + a^2\lambda^2(1+\sin^2\varphi) - a\rho\lambda^2\cos\varphi] \times \frac{N_f}{\pi R_y^2}\,a\,da\,d\varphi\cos\alpha \times \left[\frac{\tan^2 Q_{0s}\cos Q_{0s}}{2(1-\cos Q_{0s})}\right] \qquad (23)$$

where I_f is the number average of the fiber moments of inertia.

After substitution and simplification Equation 23 becomes

$$(dM_B)_y = -\frac{N_f E_f I_f}{\pi R_y^2\rho}\left\{\frac{1-a/\rho\cos\varphi}{[(1-a/\rho\cos\varphi)^2+\tan^2 Q_0]} + \frac{\tan^2 Q_0(1-a/\rho\cos\varphi)(\sin^2\varphi-\rho/a\cos\varphi)}{[(1-a/\rho\cos\varphi)^2+\tan^2 Q]^2}\right\} \times a\,da\,d\varphi\left[\frac{\tan^2 Q_{0s}\cos Q_{0s}}{2(1-\cos Q_{0s})}\right] \qquad (24)$$

The total yarn bending moment $(M_B)_y$ is then found by integration of Equation 24 over the entire yarn cross section.

$$(M_B)_y = -\int_{a=0}^{R_y}\int_{\varphi=0}^{2\pi}\frac{N_f E_f I_f}{\pi R_y^2 \rho} \times\left\{\frac{(1-a/\rho\cos\varphi)}{[(1-a/\rho\cos\varphi)^2+\tan^2 Q_0]} + \frac{\tan^2 Q_0(1-a/\rho\cos\varphi)(\sin^2\varphi-\rho/a\cos\varphi)}{[(1-a/\rho\cos\varphi)^2+\tan^2 Q_0]^2}\right\} \times a\,da\,d\varphi\left[\frac{\tan^2 Q_{0s}\cos Q_{0s}}{2(1-\cos Q_{0s})}\right] \quad (25)$$

In Equation 25, ρ is a constant and a and $\tan Q_0$ are constants with respect to the integration over $d\varphi$ since $\tan Q_0 = 2\pi a T_0$.

The direct integration of Equation 25 in closed form does not appear to be possible by standard means. It is, however, possible to obtain highly precise values through the expedient of expanding the denominators of each of the terms within the braces of Equation 25. Thus

$$\begin{aligned}&\frac{1}{[(1-a/\rho\cos\varphi)^2+\tan^2 Q_0]^n}\\ &=[1+\tan^2 Q_0-(2a/\rho\cos\varphi-a^2/\rho^2\cos^2\varphi)]^{-n}\\ &=[\sec^2 Q_0-(2a/\rho\cos\varphi-a^2/\rho^2\cos^2\varphi)]^{-n}\\ &=(\sec^2 Q_0)^{-n}+(-n)(\sec^2 Q_0)^{-n-1}(-1)\\ &\quad\times(2a/\rho\cos\varphi-a^2/\rho^2\cos^2\varphi)\\ &\quad+\frac{(-n)(-n-1)}{2}(\sec^2 Q_0)^{-n-2}\\ &\quad\times(2a/\rho\cos\varphi-a^2/\rho^2\cos^2\varphi)^2+++ \quad (26)\end{aligned}$$

Under the assumption that $a/\rho \ll 1$, i.e., that the yarn radius is much less than the radius of curvature of the bend, appropriate terms of the expansion of Equation 26 may be substituted into the integrand of Equation 25 and the double integration carried out. In so doing, a good many terms involving integration of odd powers of $\cos\varphi$ from 0 to 2π vanish, resulting in a higher degree of precision for the integral than that present in the series of Equation 26 itself. The result is

$$(M_B)_y = -\frac{N_f E_f I_f}{\rho}\left[f_1(Q_{0s})+\frac{R_y^2}{\rho^2}f_2(Q_{0s})+\cdots\right]\times\left[\frac{\tan^2 Q_{0s}\cos Q_{0s}}{2(1-\cos Q_{0s})}\right] \quad (27)$$

where

$$f_1(Q_{0s}) = \frac{1}{\tan^2 Q_{0s}}\times[2\ln\sec^2 Q_{0s} - 3\sin^2 Q_{0s} + (1-\cos^4 Q_{0s})] \quad (28)$$

and Q_{0s} is the *surface* helix angle of the twisted yarn before bending. The negative sign preceding Equation 27 merely represents the direction of $(M_B)_y$, which for the bending defined by Figure 1 is in the direction given in Figure 2. The term $f_2(Q_{0s})$ is of lower magnitude than $f_1(Q_{0s})$. For example, for $Q_{0s} = 0°$, $f_1(Q_{0s}) = 1$ and $f_2(Q_{0s}) = 1/4$. Thus, if $R_y/\rho \leq 1/5$, the second term in the series of Equation 27 representing the integral is equal to or less than 1% of the first term. A third term, involving $(R_y/\rho)^4$, is equal to or less than 2% of the second term for these same conditions. Similarly, for $Q_{0s} = 30°$–$35°$, the second term is only of the order of 1% of the first term for $R_y/\rho \leq 1/5$. Evidently then, the first term given in Equation 27 is a highly precise representation of the total bending moment on the yarn and consequently may be used for the range of geometries defined. Therefore

$$(M_B)_y = \frac{N_f E_f I_f}{\rho}\times\left[\frac{2\ln\sec^2 Q_{0s}-3\sin^2 Q_{0s}+(1-\cos^4 Q_{0s})}{\tan^2 Q_{0s}}\right]\times\left[\frac{\tan^2 Q_{0s}\cos Q_{0s}}{2(1-\cos Q_{0s})}\right]$$
$$0 \leq Q_{0s} \leq 35°, \quad R_y/\rho \leq 1/5 \quad (29)$$

with a direction obvious from the direction of yarn bending.

The bending rigidity of the yarn is defined as the bending moment required to produce unit curvature, or

$$(EI)_{\text{yarn}} = (M_B)_y\rho = N_f E_f I_f \times\left[\frac{2\ln\sec^2 Q_{0s}-3\sin^2 Q_{0s}+(1-\cos^4 Q_{0s})}{\tan^2 Q_{0s}}\right]\times\left[\frac{\tan^2 Q_{0s}\cos Q_{0s}}{2(1-\cos Q_{0s})}\right] \quad (30)$$

subject to the limitations given in Equation 29, for accuracy of about 1%. Note that the limitations imposed by Equation 29 apply only to the mathematical accuracy of representation of the entire bending function by a portion of a series. Physically, departure from linearity of the stress–strain relation may control accuracy. As stated previously, low strain levels, for this case, depend upon the ratio of fiber radius to radius of curvature being low.

Figure 3 dimensionlessly plots yarn bending rigidity, for the case of complete freedom of fiber

motion, versus yarn surface helix angle, Q_{0a}. Note that increases in yarn twist produce decreases in yarn rigidity, the rigidity for a zero-twist yarn being equal to the sum of the bending rigidities of the fibers, $N_f E_f I_f$.

For the particular case of circular fibers, the factor $N_f I_f$ may be analyzed as follows: $I_f = \pi R_f^4/4$ where R_f = fiber radius. The number of fibers in the yarn, N_f, = yarn denier/fiber denier. Thus

$$N_f I_f = \frac{\text{Yarn denier}}{\text{Fiber denier}} \frac{\pi R_f^4}{4} = \frac{D_y}{D_f} A_f \frac{R_f^2}{4} \quad (31)$$

where D_y = zero twist yarn denier, D_f = fiber denier, and A_f = cross-sectional area of a fiber. Now $A_f = C_1 D_f/\sigma$ where C_1 is a constant and σ is the fiber density. Then, since $R_f^2/4 = C_2 A_f = C_3 D_f/\sigma$, where C_2 and C_3 are constants

$$N_f I_f = D_y/D_f \quad C_1 D_f/\sigma \quad C_3 D_f/\sigma = C D_y D_f/\sigma^2 \quad (32)$$

From Equation 32 it is clear that on a fiber geometry basis, yarn bending rigidity is directly proportional to the product of yarn denier by fiber denier divided by the square of the fiber density. The influence of fiber modulus is a directly proportional one.

Effect of Yarn Relaxation Prior to Bending

Equation 29 for yarn bending moment was derived from considerations of the resultant curvatures of all fibers in the bent twisted yarn, including curvatures imposed by the original twisting process. Implicit in the analysis then is the assumption of retention of twisting stresses.

In many cases, fiber bending stresses corresponding to the twisted yarn state are relaxed, i.e., reduced to zero, either as the result of a controlled relaxation treatment or as the result of time alone. In either case, the final bending moment on a fiber would not be given by Equations 13 or 14, but instead would be determined from the *change* in curvature of the fiber between the twisted (relaxed) state and the twisted bent yarn state. Again, it is assumed that radii of curvature are large compared to the fiber radius, thus permitting both linear elasticity to be assumed and also the neglect of original fiber curvature in controlling location of the neutral axis of the fiber [12].

Prior to yarn bending, as has been shown in a previous publication [11], components of fiber

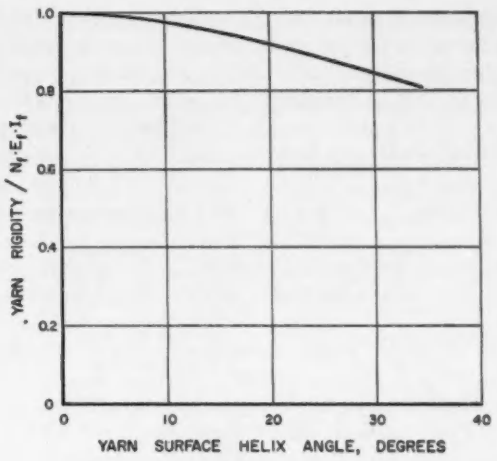

Fig. 3. Effects of twist on yarn rigidity; complete freedom of motion.

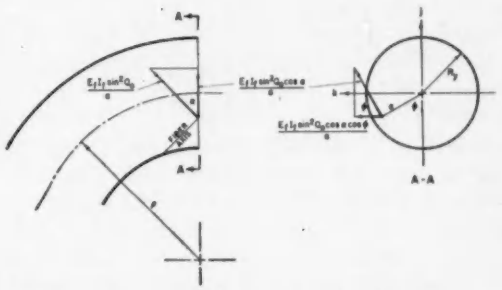

Fig. 4. Components of original fiber bending moment.

bending moments corresponding to their curvatures in the twisted yarn by symmetry produce a zero resultant, insofar as yarn bending moments are concerned. Thus, except for possible fiber modulus changes produced as a result of relaxation of fiber stresses, it would be anticipated that yarn bending rigidity would be only slightly affected by yarn relaxation.

In formal terms, the bending moment on the yarn for the case of complete relaxation of bending stresses induced by twisting would be

$$(M_B)_y' = \frac{N_f E_f' I_f}{\pi R_y^2} \int_{a=0}^{R_y} \int_{\varphi=0}^{2\pi} \bar{T}_{ij} \times [\bar{K}_{ij} - (\bar{K}_{ij})_0] a da d\varphi \cos\alpha \times \left[\frac{\tan^2 Q_{0a} \cos Q_{0a}}{2(1 - \cos Q_{0a})}\right] \quad (33)$$

wherein all terms are as previously defined, $(\bar{K}_{ij})_0$ represents the pertinent components of the original fiber curvature, i.e., due to the twisting process alone, and E_f' represents the relaxed fiber modulus of elasticity, assumed alike for all fibers in the yarn. Equation 33 may be rewritten as

$$(M_B)_y' = \frac{N_f E_f' I_f}{\pi R_y^2} \int_{a=0}^{R_y} \int_{\varphi=0}^{2\pi} (\bar{T}_{ij} \times \bar{K}_{ij}) a da d\varphi \cos\alpha \times \frac{\tan^2 Q_{0s} \cos Q_{0s}}{2(1-\cos Q_{0s})} - \frac{N_f E_f' I_f}{\pi R_y^2} \int_{a=0}^{R_y} \int_{\varphi=0}^{2\pi} \bar{T}_{ij} \times (\bar{K}_{ij})_0 a da d\varphi \cos\alpha \frac{\tan^2 Q_{0s} \cos Q_{0s}}{2(1-\cos Q_{0s})} \quad (34)$$

The first integral in Equation 34 duplicates the bending moment which would be found without relaxation with E_f replaced by E_f', the relaxed fiber modulus. As regards the second integral, note that

$$\frac{N_f E_f' I_f}{\pi R_y^2} \int_{a=0}^{R_y} \int_{\varphi=0}^{2\pi} [(\bar{T}_{ij})_0 \times (\bar{K}_{ij})_0 a da d\varphi \cos Q_0] \times \left[\frac{\tan^2 Q_{0s} \cos Q_{0s}}{2(1-\cos Q_{0s})}\right] = 0 \quad (35)$$

where $(\bar{T}_{ij})_0$ is the unit tangent vector to the fiber axis in the twisted but unbent state. The only difference between the second integral in Equation 34 and that of Equation 35 is that induced by the change in helix angle as a result of bending, since this change is responsible for the differences between $\bar{T}_{ij}$ and $(\bar{T}_{ij})_0$ on the one hand and $\cos\alpha$ and $\cos Q_0$ on the other. If the change in helix angle is small $(a/\rho \cos\varphi \ll 1)$, then the second integral of Equation 34 is negligible. In any case, this second integral merely represents the sum of the k components of the *original* fiber bending moments, displaced from their original directions to those corresponding to the bent yarn state. Let M_0' equal the second integral of Equation 34. Then, from what has been discussed

$$M_0' = \frac{N_f E_f' I_f}{\pi R_y^2} \int_{a=0}^{R_y} \int_{\varphi=0}^{2\pi} \frac{\sin^2 Q_0}{a} \times (\cos\alpha)(\cos\varphi) a da d\varphi \cos\alpha \times \frac{\tan^2 Q_{0s} \cos Q_{0s}}{2(1-\cos Q_{0s})} \quad (36)$$

In Equation 36, $\sin^2 Q_0/a$ is the original fiber curvature. When this is multiplied by $\cos\alpha$, the result gives the component of the bending moment vector in the plane of the yarn cross section. Multiplication then by $\cos\varphi$ gives the k component of the fiber bending moment corresponding to its original curvature. These components are shown in Figure 4.

TABLE I. Effect of Yarn Relaxation on Yarn Rigidity

Q_{0s}, Yarn surface helix angle, °	$(M_{By})^*/N_f E_f' I_f$	$M_0'\dagger/N_f E_f' I_f$	$M_0'/(M_B)_y \times 100$, %
0	1.000	0.000	0
11.3	0.971	0.00025	0.025
21.8	0.908	0.006	0.7
26.6	0.870	0.0127	1.5
30	0.847	0.0204	2.4
35	0.822	0.0352	4.3

* From Equation 29.
† From Equation 38.

Alternatively, $\bar{T}_{ij}$ is given by the first two terms of Equation 9. The vector $(\bar{K}_{ij})_0$ is given by $\sin^2 Q_0/a[(j \cos\varphi - k \sin\varphi)]$. Thus

$$\bar{T}_{ij} \times (\bar{K}_{ij})_0 = -k \left[\frac{\sin^2 Q_0}{a} \cos\varphi\right] \times \left[\frac{a\cos\varphi - \rho}{\sqrt{(\rho - a\cos\varphi)^2 + \rho^2 \tan^2 Q_0}}\right] \quad (37)$$

From Backer [1] or from Equation 7, the second term in brackets of Equation 37 is $-\cos\alpha$, showing the equivalence of Equation 36 and the second integral of Equation 34.

The value of M_0' may now be determined from Equation 36, following substitution of the pertinent geometric quantities. The result is again most easily found by series expansion of the complex denominator terms. In this case, neglecting terms of order $(R_y/\rho)^2$ and higher, there results

$$M_0' = -\frac{N_f E_f' I_f}{\rho} \times \left[\frac{\ln \sec^2 Q_{0s} - 2\sin^2 Q_{0s} + 1/2(1-\cos^4 Q_{0s})}{\tan^2 Q_{0s}}\right] \times \left[\frac{\tan^2 Q_{0s} \cos Q_{0s}}{2(1-\cos Q_{0s})}\right] \quad (38)$$

The negative sign in Equation 38 indicates M_0' to be in the same direction as $(M_B)_y$.

As anticipated, the first bracketed term of Equation 38 is very small compared to the corresponding term given by Equation 29, the influence of twist on bending moment. This is shown by the calculated results given in Table I.

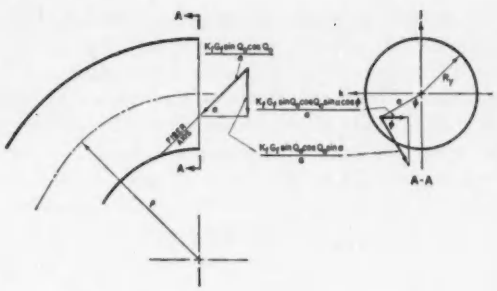

Fig. 5. Components of original fiber torque.

Aside from its possible effect on changing fiber modulus, relaxation of fiber bending stresses imposed during yarn twisting diminishes yarn bending rigidity. The effect is slight, ranging from no effect at zero twist to 4.3% at a surface helix angle of 35°.

The influence of twist on yarn bending rigidity is essentially unaffected by the process of relaxation. With prior relaxation, twist causes a slightly greater rate of decrease of yarn bending rigidity than without relaxation.

The foregoing assumes no interaction between original twist (strains induced by twisting) and the effects of relaxation on modulus. This appears reasonable in light of the small fiber strains involved when $a/\rho \cos \varphi \ll 1$. For example, Morgan [8] has shown that over a very broad range of strains, moduli following relaxation are essentially constant for selected keratinous fibers. Clearly, if the fiber modulus does not change, prior relaxation produces essentially no change in yarn rigidity.

Effect of Residual Fiber Torsional Stresses on Yarn Bending Rigidity

For the assumed case of complete freedom of fiber motion, the process of yarn bending does not induce any net change in fiber torque. Theoretically, as Backer [1] has indicated, the increased torsional strains required in portions of the fiber length on one side of the neutral axis of the yarn is provided by the decrease in torsional strain required on the other side of the neutral axis. Under such circumstances, the torsion present in fibers resulting from the original twisting operation represents the total fiber torsion in the bent yarn state. Obviously, then, prior relaxation could completely eliminate fiber torsional effects insofar as yarn bending rigidity is concerned. The following analysis shows the magnitude of fiber torsional effects on yarn rigidity, assuming no relaxation and complete freedom of fiber motion.

As has been shown by Platt et al. [11], fiber torsion resulting from yarn twisting produces yarn torque, but because of symmetry, no resultant *yarn* bending moment results when the axis of the yarn is straight. In the bent yarn state, fiber torques equivalent to those originally present exist (for the foregoing assumptions), but their directions are changed, due to helix angle changes, and symmetry no longer exists. Thus, the original fiber torques can effect the yarn bending moment.

Again, linear elasticity is assumed. Then, the fiber torque present in the bent state is given by

$$M_T = K_f G_f \frac{\sin Q_0 \cos Q_0}{a} \tag{39}$$

where $K_f G_f$ is the torsional rigidity of the fiber cross section.

The derivation of Equation 39 is given earlier [11]. As is the case for bending moments, torques can be represented by vectors, in this case the direction of the vector coinciding with the fiber tangent, and in the sense governed by the right hand screw rule for fiber twist. This is illustrated in Figure 5, for a bent yarn with an S twist. As will be evident, twist direction plays no part in either the magnitude or the direction of the effect being characterized.

The component of M_T in the plane of the bent yarn cross section at $\theta = \pi/2$ is $M_T \sin \alpha$. The component of $M_T \sin \alpha$ in the k axis direction is $-M_T \sin \alpha \cos \varphi$. Thus, the contribution of original fiber torsion to bent yarn bending moment is

$$(M_T)_B = -K_f G_f \frac{\sin Q_0 \cos Q_0}{a} \sin \alpha \cos \varphi \tag{40}$$

The negative sign in Equation 40 indicates the increment of yarn bending moment to be in the direction of the $-k$ axis.

When one follows the standard procedures previously used herein, it is clear that the total bending moment on the yarn due to all fiber torques is given by

$$M_T' = \frac{N_f K_f G_f}{\pi R_y^2} \int_{a=0}^{R_y} \int_{\varphi=0}^{2\pi} \frac{\sin Q_0 \cos Q_0}{a} \times \sin \alpha \cos \varphi a da d\varphi \cos \alpha \times \frac{\tan^2 Q_{0a} \cos Q_{0a}}{2(1 - \cos Q_{0a})} \tag{41}$$

Following substitution for $\sin\alpha$ and $\cos\alpha$ into Equation 41, there results

$$M_T' = \frac{N_f K_f G_f}{\rho} \times \left[\frac{\sin^2 Q_{0s}(2 - \cos^2 Q_{0s}) - \ln \sec^2 Q_{0s}}{2 \tan^2 Q_{0s}}\right] \times \left[\frac{\tan^2 Q_{0s} \cos Q_{0s}}{2(1 - \cos Q_{0s})}\right] \quad (42)$$

as the first order term found by neglecting terms of order $(R_y/\rho)^2$ and higher. The direction of M_T' is such that it increases the total bending moment on the yarn, thereby effectively increasing the bending rigidity. Although the mathematical accuracy of Equation 42 is not as great as the other cases analyzed herein, i.e., less rapid convergence of the series expansion then previously found, the magnitude of M_T' is sufficiently low so that a greater error can be tolerated without significant consequences.

Thus, for no prior yarn relaxation

$$(EI)_{yarn} = (M_B)_y\rho + M_T'\rho = N_f E_f I_f \left[\frac{2 \ln \sec^2 Q_{0s} - 3 \sin^2 Q_{0s} + (1 - \cos^4 Q_{0s})}{\tan^2 Q_{0s}}\right] \times \left[\frac{\tan^2 Q_{0s} \cos Q_{0s}}{2(1 - \cos Q_{0s})}\right] + N_f K_f G_f \left[\frac{\sin^2 Q_{0s}(2 - \cos^2 Q_{0s}) - \ln \sec^2 Q_{0s}}{2 \tan^2 Q_{0s}}\right] \times \left[\frac{\tan^2 Q_{0s} \cos Q_{0s}}{2(1 - \cos Q_{0s})}\right] \quad (43)$$

The trigonometric portion of M_T' is considerably less than that of $(M_B)_y$. Thus, for torsional rigidity equal to or less than bending rigidity, the effect of fiber torque on bending rigidity is relatively small. This is illustrated by Table II.

From Table II it can be seen that residual fiber torque increases yarn bending rigidity, the effect, however, being slight for helix angles below 35°.

TABLE II. Effect of Fiber Torque on Yarn Rigidity

Q_{0s}, °	$(M_B)_y\rho / N_f E_f I_f$	$M_T'\rho / N_f K_f G_f$	Percent increase in rigidity: $K_f G_f / E_f I_f =$ 1.00	$K_f G_f / E_f I_f =$ 1/2
0	1.00	0.00	0	0
11.3	0.971	0.009	<1	<1
16.7	0.941	0.018	1.9	<1
26.6	0.870	0.036	4.1	2
30	0.847	0.040	4.7	2.4
35	0.822	0.043	5.3	2.7

The magnitude of the effect is functional with the ratio of fiber torsional stiffness to bending stiffness; the higher the ratio the greater the increase in yarn stiffness. However, for most materials [11] the ratio $K_f G_f / E_f I_f$ is of the order of 1/5–1/3 except for wool (0.70) and nondrawn synthetics. Under such circumstances, the effect of fiber torsion can safely be neglected. Moreover, in no case does it change the trend of decreasing yarn stiffness with increasing yarn twist, even for the extreme case of $K_f G_f = E_f I_f$.

Effect of Fiber "Clustering" on Yarn Rigidity

Clustering, as used herein, is defined as the joint action of groups of fibers acting thereby as single fibers. Thus far the analysis has considered all fibers to be acting independently, i.e., complete freedom of relative motion among all the fibers, so that there are no net tension or compression forces acting on any of their cross sections. The opposite case, that of complete restriction to freedom of fiber motion, will be subsequently discussed. There is little doubt that the action of real yarns lies somewhere between the limits imposed by these extremes, being influenced, for example, by yarn twist. Consideration of the effects of fiber clustering will be illustrative of intermediate stages between these extremes.

Consider, for example, a yarn comprised of N_f total fibers acting independently. For convenience, consider these fibers to be circular. For a yarn surface helix angle Q_{0s}, the bending rigidity of the yarn would be given by

$$(EI) = N_f E_f I_f \times \left[\frac{2 \ln \sec^2 Q_{0s} - 3 \sin^2 Q_{0s} + (1 - \cos^4 Q_{0s})}{\tan^2 Q_{0s}}\right] \times \left[\frac{\tan^2 Q_{0s} \cos Q_{0s}}{2(1 - \cos Q_{0s})}\right] \quad (44)$$

where I_f, the fiber moment of inertia, $= \pi R_f^4/4$, R_f = fiber radius.

Now let it be assumed that fibers act in pairs, i.e., that any two adjacent fibers are intimately bonded only to each other with no relative motion possible between them. There will then be $N/2$ such groups of two fibers each comprising the yarn. The assumption is also made that each group of two fibers acts independently of any other group. If N_f is large, $N_f/2$ is also large. In this case, the bending rigidity for the yarns will be

TABLE III. Effects of Fiber Clustering on Yarn Rigidity

Fibers per cluster	Groups of clusters	Moment of inertia of cluster: $I_f = \pi R_f^4/4$	Clusters × (inertia/cluster)
1	N_f	I_f	$N_f I_f$
2	$N_f/2$	$6\ I_f$	$3\ N_f I_f$
4	$N_f/4$	$20\ I_f$	$5\ N_f I_f$
9	$N_f/9$	$105\ I_f$	$11\frac{2}{3}\ N_f I_f$
16	$N_f/16$	$336\ I_f$	$21\ N_f I_f$

$$(EI)_2 = \frac{N_f}{2} E_f I_f' \times \left[\frac{2 \ln \sec^2 Q_{0s} - 3 \sin^2 Q_{0s} + (1 - \cos^4 Q_{0s})}{\tan^2 Q_{0s}}\right] \times \left[\frac{\tan^2 Q_{0s} \cos Q_{0s}}{2(1 - \cos Q_{0s})}\right] \quad (45)$$

I_f' is now the moment of inertia of two contiguous circular cross sections. The moment of inertia of such a group is dependent upon its orientation with respect to the plane of bending of the group. As a rough guide, assume such orientation to be random, that is, equally likely to be at any angle to the plane of bending. Figure 6 gives the values of moment of inertia for a variety of positions of the group with respect to an axis of bending through its center of gravity. Since either the x–x or y–y axis is an axis of symmetry, the product of inertia of the cross section is zero [5]. The average value of the moment of inertia would be given by

$$\bar{I}_f' = \frac{1}{2\pi} \int_{\beta=0}^{2\pi} (I_{xx} \cos^2 \beta + I_{yy} \sin^2 \beta) d\beta = \frac{1}{2\pi} [10\ I_f \pi + 2\ I_f \pi] = 6\ I_f \quad (46)$$

Therefore, the average moment of inertia of two contiguous fibers of circular cross section is six times that of a single fiber. Equation 45 now becomes

$$(EI)_2 = \frac{N_f}{2} E_f (6\ I_f) \times \left[\frac{2 \ln \sec^2 Q_{0s} - 3 \sin^2 Q_{0s} + (1 - \cos^4 Q_{0s})}{\tan^2 Q_{0s}}\right] \times \left[\frac{\tan^2 Q_{0s} \cos Q_{0s}}{2(1 - \cos Q_{0s})}\right] \quad (47)$$

Thus, the average bending rigidity of a yarn consisting of groups of two circular fibers is three times that of a yarn in which all fibers act independently.

Other groupings may be taken; for example, groups of 4, 9, or 16 fibers acting together. Each of these cases is geometrically symmetrical about two axes, with equal principal moments of inertia, and thus orientation plays no part in determining moments of inertia. Table III tabulates results for such cases.

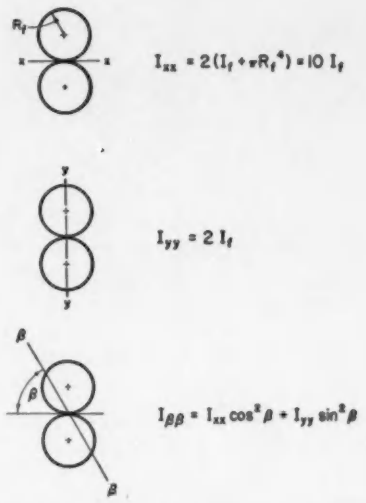

Fig. 6. Moments of inertia of two contiguous circular cross sections.

The last column of Table III gives the relative rigidity of yarns having the same surface helix angles Q_{0s} and shows the marked effect of clustering on rigidity.

As will subsequently be shown, the rigidity of a circular yarn with complete lack of freedom of motion among any of its fibers is approximately N_f/p times that for complete freedom of motion among all fibers, where p is the packing factor of the yarn. It can easily be seen from Table I that for x number of fibers in a cluster, the rigidity is approximately x/p times the rigidity obtained for one fiber in a cluster. The value of p for the cases given in Table I is constant at $\pi R_f^2/4\ R_f^2 = \pi/4 = 0.785$. The case of complete lack of freedom of motion among all fibers would be similar to a yarn consisting of a single cluster containing all N_f fibers.

Response of Yarns With No Freedom of Relative Fiber Motion

The analyses thus far presented have considered all individual fibers or, in the case of the previous section on clustering, groups of fibers, to be free to

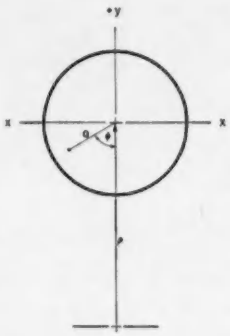

Fig. 7. Cross section of a bent yarn.

move with respect to each other. Such movements involve relative motions of surfaces of adjacent fibers which may be in contact with each other. In the case of a twisted yarn, this motion permits the extra length required for portions of a fiber above the neutral axis of the yarn to be supplied by the extra length made available by segments of this same fiber which lie beneath the yarn neutral axis. Under such circumstances, no resultant tensions or compression will be developed across any fiber cross section. Backer [1] has indicated the results of an analysis by Chow [3] which shows that for $\rho/a \geq 5/2$ any finite yarn twist at all satisfies the length balance implied above, although it would appear that a yarn length sufficiently great so that approximately one turn of twist would be encompassed in the bend would be required for lengths to balance.

Under the extreme condition of no freedom of relative fiber motion, comparatively high fiber strains are developed as a result of bending. From elementary beam theory, maximum tensile and compressive strains of the order of R_y/ρ will be developed, whereas for complete freedom, strains of the order of the ratio of fiber radius to radius of curvature of the fiber axis will result. For a very large number of fibers in the yarn cross section, strains in the latter case will be much smaller than in the former. Thus, for linear elasticity to be evidenced, higher radii of curvature are required for the case of no freedom of motion than when freedom prevails. Assuming, for example, a maximum permissible strain of say, 5%, then $R_y/\rho \leq 1/20$ is required for the case of no freedom of relative fiber motion.

The step-wise analysis of the effects of fiber clustering on yarn bending rigidity has, to an extent, afforded a preview of the limiting case of complete lack of freedom of motion. A more direct analysis which gives the effect of twist explicitly follows. The analysis, with some minor modifications, is very similar to one independently performed by Backer [2].

Under the assumption that plane sections remain plane, axial strain on the yarn following bending is given by

$$e_y = y/\rho \tag{48}$$

where y is the distance *above* the neutral axis, as shown in Figure 7. In terms of previously defined quantities

$$y = -a\cos\varphi$$
$$e_y = -\frac{a\cos\varphi}{\rho} \tag{49}$$

If one assumes the helix radius of any fiber to be invariant with strain, then, as Platt [10] has shown

$$e_f = \sqrt{\frac{(1+e_y)^2 + \tan^2 Q_0}{1+\tan^2 Q_0}} - 1 \tag{50}$$

where e_f is the fiber strain. Thus, for a given yarn strain e_y the strain on a fiber whose helix angle before yarn bending is Q_0 is determinable from Equation 50. For yarn strains e_y much less than 1.00, Equation 50 may be approximated by the binominal series expansion of the square root term. This yields

$$e_f = e_y \cos^2 Q_0 \tag{51}$$

As shown [10], the approximation of Equation 50 by 51 is extremely precise for values of $e_y \leq 20\%$ and $Q_0 \leq 35°$, which is more than adequate for present purposes of defining bending rigidity. Equation 50 with e_y substituted from Equation 49 duplicates Backer's corresponding result for local fiber strains derived by analysis of the differential geometry of the bent helix. By combination of Equations 49 and 51, the fiber strain resulting from bending the yarn to a radius of curvature ρ is

$$e_f = \frac{-a}{\rho}\cos\varphi\cos^2 Q_0 \tag{52}$$

If the fiber has a constant modulus E_f in tension or compression, the axial fiber stress following bending is

$$f = E_f e_f = -E_f a/\rho\cos\varphi\cos^2 Q_0 \tag{53}$$

and if the fiber cross-sectionalarea is A_f, the total axial force on the fiber F_f is

$$F_f = fA_f = -E_f A_f a/\rho \cos\varphi \cos^2 Q_0 \quad (54)$$

The component of the force F_f parallel to the yarn axis is

$$(F_f)_a = F_f \cos\alpha \quad (55)$$

The moment exerted by the force F_f about the neutral axis of the yarn is

$$\begin{aligned} M_f &= F_f \cos\alpha y \\ &= E_f A_f a^2/\rho \cos^2 Q_0 \cos^2\phi \cos\alpha \end{aligned} \quad (56)$$

where α is the local helix angle after bending. For large radii of curvature

$$\cos\alpha = \cos Q_0(1 - a/\rho \cos\varphi \sin^2 Q_0 + \cdots) \quad (57)$$

In a differential element of yarn cross-sectional area, the number of fibers encompassed is

$$dN_f = (N_f/\pi R_y^2) a da d\varphi \cos\alpha \left[\frac{\tan^2 Q_{0s} \cos Q_{0s}}{2(1-\cos Q_{0s})}\right] \quad (58)$$

Thus, from this element of area, there would be a yarn bending moment, dM_{By}, given by

$$\begin{aligned} dM_{By} &= M_f dN_f \\ &= \frac{N_f E_f A_f}{\pi R_y^2}\left[\frac{a^3}{\rho}\cos^2 Q_0 \cos^2\alpha \cos^2\varphi da d\varphi \right. \\ &\quad \left. \times \frac{\tan^2 Q_{0s} \cos Q_{0s}}{2(1-\cos Q_{0s})}\right] \end{aligned} \quad (59)$$

The total yarn bending moment is then

$$\begin{aligned} M_{By} &= \frac{N_f E_f A_f}{\pi R_y^2}\int_{a=0}^{R_y}\int_{\varphi=0}^{2\pi} \\ &\quad \times \left[(a^3/\rho)\cos^2 Q_0 \cos^2\alpha da d\varphi \cos^2\varphi \right. \\ &\quad \left. \times \frac{\tan^2 Q_{0s} \cos Q_{0s}}{2(1-\cos Q_{0s})}\right] \end{aligned} \quad (60)$$

In Equation 60 a and Q_0 are independent of φ but $\cos\alpha$ is given by

$$\cos\alpha = \frac{1 - a/\rho \cos\varphi}{\left[\left(1 - \frac{a}{\rho}\cos\varphi\right)^2 + \tan^2 Q_0\right]^{1/2}} \quad (61)$$

Equation 61 is substituted into Equation 60, followed by expansion of the denominator into the binominal series previously described. Actually, consistency demands that Equation 57 be used for $\cos\alpha$ rather than Equation 61, since previous use of $e_y \cos^2 Q_0$ to represent fiber strain assumed large values of ρ/R_y. In any event, neglect of powers of $(R_y/\rho)^2$ following the integration called for in Equation 60 results in

$$\begin{aligned} M_{By} = \frac{N_f E_f A_f}{\rho} R_y^2 &\left[\frac{\ln \sec^2 Q_{0s} - \sin^2 Q_{0s}}{2\tan^4 Q_{0s}}\right] \\ &\times \left[\frac{\tan^2 Q_{0s} \cos Q_{0s}}{2(1 - \cos Q_{0s})}\right] \end{aligned} \quad (62)$$

Additional terms neglected through the use of the limited series are of the form given by Equation 62 but multiplied by $(R_y/\rho)^2$, $(R_y/\rho)^4$, etc., resulting in rapid convergence when $R_y/\rho \ll 1$. Note that in the derivation of Equation 62, helix radii were assumed constant and the influence of transverse forces negligible, both of which assumptions are believed reasonable for bending involving helix angles less than 35° for the following reasons.

1. Calculations of the physically unreal but extrème case of constant volume distortion [10] to relate helix radii to fiber strain yield only a slight decrease in rigidity from that given by Equation 62. In any real case of bending, helix radii could not change to the degree implied by such a constant volume distortion, due to the marked variance of bending strains with position in the yarn cross section as compared to the more uniform strain distribution for yarn tension.

2. Hearle [7] has shown a relatively slight influence of transverse stresses on twisted yarn tensile modulus for helix angles less than 35°. When bending is considered, transverse stresses less than those encountered for yarn tension would probably develop since the incremental increase of transverse pressure is much greater for tensile load as the yarn center is approached than for yarn bending as the neutral axis is approached. In addition, such transverse stresses are zero at the external boundary of the yarn for both tension and bending. Thus it would be expected that both transverse pressures and also their influence on axial fiber stresses, hence yarn rigidity, would be small for yarn bending to large radii of curvature. Moreover, the moments about the yarn neutral axis both of such transverse forces and any altered fiber stresses would be slight, even if the relative magnitude of transverse forces did increase, as the neutral axis were approached, to the same extent as it does in the case for tensile loads.

A more rigorous analysis much more complex than the foregoing would be required for a numerical estimate of the effect of transverse forces on yarn bending rigidity, although it is anticipated

that its effects are of second order of magnitude for large radii of curvature of bending. For small radii of curvature, where the direction of fiber bending, for fibers below the yarn neutral axis, may be reversed from that which existed in the unbent yarn, transverse force effects will be greater.

The bending rigidity of the yarn, for the case of no freedom of fiber motion and neglecting transverse forces, is then given by

$$(EI)_y = M_{By}\rho = N_f E_f A_f R_y^2 \times \left[\frac{\ln \sec^2 Q_{0s} - \sin^2 Q_{0s}}{2 \tan^4 Q_{0s}}\right] \times \left[\frac{\tan^2 Q_{0s} \cos Q_{0s}}{2(1 - \cos Q_{0s})}\right] \quad (63)$$

Figure 8 dimensionlessly plots yarn bending rigidity for this case versus surface helix angle Q_{0s}. Note that increase in twist produces decreases in rigidity, the effect being of the same general sort described by Figure 3 for the case of complete freedom of motion. However, with no freedom of motion, twist is somewhat more effective in reducing rigidity.

The term $N_f A_f R_y^2$ preceding Equation 63 is worthy of general examination. $N_f A_f$ is the solid area of the yarn cross section $= \pi R_s^2$, where R_s is the equivalent solid radius of the yarn. R_y, on the other hand, is the bulk radius of the yarn (i.e., $\pi R_s^2/p = \pi R_y^2$), where p here is defined as the average yarn packing factor. Thus

$$N_f A_f R_y^2 = \frac{\pi R_s^4}{p} \quad (64)$$

From Equation 64 we conclude that bending rigidity is not proportional to the fourth power of the yarn radius but to the fourth power of the solid radius of the yarn divided by the packing factor. As the yarn density decreases, the packing factor decreases, and hence the rigidity rises, but only in inverse proportion to the packing factor. Increases in yarn twist which presumably increase the yarn packing factor would, if lack of freedom of motion prevailed, cause decreases in yarn rigidity.

For comparison with the case of complete freedom of fiber motion, the term $N_f A_f R_y^2$ may be roughly analyzed for circular fibers as follows.

$$\begin{aligned} N_f A_f R_y^2 &= N_f \pi R_f^2 R_s^2/p \\ &= N_f \pi R_f^2 N_f R_f^2/p \\ &= N_f^2 \pi R_f^4/p \\ &= N_f^2 4\, I_f/p \\ &= 4\, N_f^2 I_f/p \end{aligned} \quad (65)$$

The value of the yarn rigidity is then given by

$$(EI)_{\text{no freedom}} = \frac{4\, N_f^2 E_f I_f}{p} f_2(Q_{0s}) \quad (66)$$

where the magnitude of $f_2(Q_{0s})$ is given by the ordinate to Figure 8. For the case of complete freedom of fiber motion

$$(EI)_{\text{freedom}} = N_f E_f I_f f_1(Q_{0s}) \quad (67)$$

where $f_1(Q_{0s})$ is given by the ordinate to Figure 3. The ratio of the rigidities for the two extreme cases is

$$4\, N_f/p[f_2(Q_{0s})/f_1(Q_{0s})] \quad (68)$$

From Figures 3 and 8 $[f_2(Q_{0s})/f_1(Q_{0s})]$ is approximately constant, ranging from 1/4 to 1/5 over the range of Q_{0s} from 0° to 35°. Thus, from Equation 68

$$\frac{(EI)_{\text{no freedom}}}{(EI)_{\text{freedom}}} \approx \frac{N_f}{p} \quad (69)$$

Equation 69, derived from comparison of the two extreme cases, expresses the same result as given in the previous section on clustering. Obviously, yarn rigidity for no freedom of fiber motion greatly exceeds that when freedom of motion is present, by a factor of roughly the number of fibers in the yarn. It should be noted, however, the limited experimental evidence available indicates that in practical yarns there is little inhibition to complete freedom of motion. For example, in a research on the bending rigidity of singles cotton yarns, the rigidity of yarns encompassing a broad range of cotton counts and twists was found to be inversely proportional to the count, i.e., directly proportional to the average number of fibers in the yarn cross section. This is consistent with freedom of motion. For no freedom of motion, yarn rigidity would be roughly directly proportional to the square of the number of fibers in the yarn.

A factor of theoretical and possibly practical significance arises from the analysis of bending of twisted yarns with no freedom of relative fiber motion. Those fibers or portions of fiber length which lie above the yarn neutral axis are under tension, while those below are under compression. The yarn bending rigidity was derived from the moments about the yarn neutral axis of the components of such fiber axial forces parallel to the yarn central axis. The remaining component for any fiber lies in the plane of the cross section of the yarn and is perpendicular to the radius vector of

the fiber center from the yarn center; this is shown in Figure 9. For illustrative purposes, fibers at $\varphi = 0$ and $\varphi = \pi$ (inside and outside of the bend respectively) are shown in Figure 9a. The fiber forces are F_c (compression) at $\varphi = 0$ and F_T (tension) at $\varphi = \pi$, with the magnitude of F_c equal to the magnitude of F_T. As can be seen from Figure 9a or 9b, F_c and F_T both have components $F_c \sin \alpha_c$ and $F_T \sin \alpha_T$ which are in the same direction across the yarn cross section. Similarly, other fibers in the yarn cross section have components of their tensile or compressive axial stress which act in the same direction; these are designated as F_c' and F_T' in Figure 9b. Thus, bending of a yarn with no freedom of relative fiber motion produces a net transverse shear force across the yarn section F_R in the direction of the binormal to the bent yarn axis. Such yarn transverse shear forces will be modified in magnitude, probably to a greater extent than is the yarn bending rigidity, by any transverse fiber forces which are present as result of the yarn bending; nonetheless a resultant yarn transverse shear must exist for the assumptions made. Such transverse shear forces require twisting moments in two planes as well as forces at the bent yarn ends for static equilibrium, and unless the yarn is so loaded at its ends, instability of the bent yarn form may result. The practical significance of this result must await experimental verification of both its existence and magnitude, as well as further analytic and experimental work on modifications, if any, introduced by transverse fiber forces. In essence, the effect of bending on the creation of the transverse yarn shear force described by Figure 9 is very similar to the development of rotational torque, in an otherwise balanced singles yarn, due to tensile loading.

The comparison of relative rigidities given by Equation 69 obviously indicates the likelihood of increasing yarn rigidity with increasing yarn twist, under the assumption that such increases in twist produce restraints against freedom of motion. Without such restraints imposed by twist increases, bending rigidity of yarns would decrease as twist increases. For whenever freedom of motion is maintained, Figure 3 indicates the mechanical effect of twist increases to produce a decreased yarn rigidity. Similarly, from Equation 66 and Figure 8, where no freedom of motion exists, twist increases will decrease yarn rigidity on the basis of helix angle increases. If such twist increases caused yarn densification (increased yarn packing factor), rigidity would be further decreased. For very high twists, where fiber fit becomes difficult because of the oblique fiber area in the plane of the yarn cross section, twist increases could cause some lowering of yarn packing factor, hence slight increases in rigidity, although it is believed that the mechanical effect of helix angle increases on lowering rigidity would dominate.

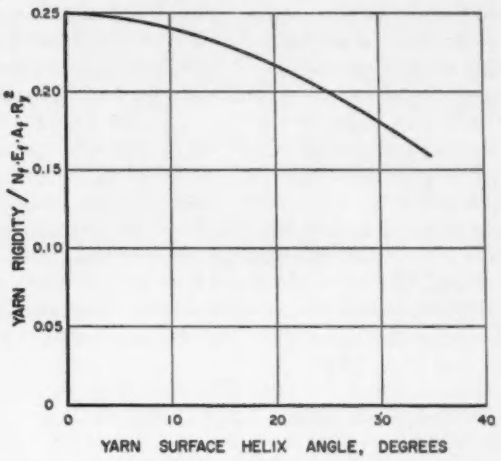

Fig. 8. Effects of twist on yarn rigidity; no freedom of motion.

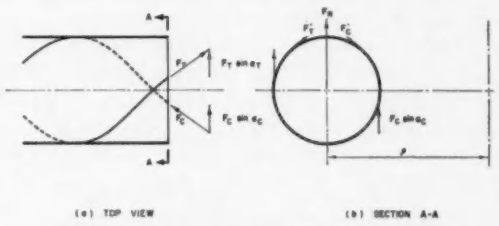

Fig. 9. Yarn shear created by yarn bending.

General Comments on Rigidity of Blended Yarns

Throughout the preceding analyses, self-fiber yarns of uniform fiber diameter were assumed. Thus, E_f, I_f, and N_f were constant. When blended yarns are considered, no special difficulties are encountered so long as the idealized yarn geometry is maintained and the spatial distribution of the blending fibers specified. For any assumed yarn organization, the methods of analysis herein employed could be applied to determine relative rigidities. In a physical sense, blends are more complex

than self-fiber yarns, since in blends there is a greater likelihood of varying degrees and locations of restraints to freedom of fiber motion, of a presently unpredictable sort, than is the case for self-fiber yarns. Because of this and the variety of blending states which could exist, any attempt to quantify in detail the rigidity of blends appears impractical at this time. Consequently, only a few possibly interesting relations between the results of analyses made for self-fiber yarns and the bending rigidity of blended yarns will be qualitatively discussed. Future publications will deal with the experimental study of the bending rigidity of blended yarns [4].

Consider first the case of a yarn wherein complete freedom of motion exists among all elements. The effect of twist on the bending rigidity of the self-fiber yarn is shown as Curve *a* of Figure 10. Assume now that a yarn of the same weight as that of *a* but consisting of an intimate uniform blend with *a* of stiffer fibers is made. A uniform blend is defined as one in which the blend distribution is constant for all elements of cross-sectional area. The bending rigidity, at zero twist, of such a yarn would obviously exceed that of the self-fiber yarn. The rigidity, in this case, would be

$$(EI)_{\text{Blend}} = N_{fa}E_{fa}I_{fa} + N_{fb}E_{fb}I_{fb}$$

where subscripts *a* and *b* refer to the original fiber and stiffer blending fiber, respectively. The restriction of constant yarn weight is

$$N_{fa}A_{fa}\sigma_a + N_{fb}A_{fb}\sigma_b = \text{Original (self-fiber) yarn weight}$$

where σ is the fiber density. For such a uniform blend, twist increases would cause the same proportional reduction of rigidity as was the case for the self-fiber blend, i.e.

$$(EI)_{\text{Blended yarn}} = (N_{fa}E_{fa}I_{fa} + N_{fb}E_{fb}I_{fb})[f_1(Q_{0e})]$$

where $f_1(Q_{0e})$ is defined by Equation 28. This is shown as Curve *b* in Figure 10.

Consider the effects of a nonuniform distribution of the stiffer blending fiber across the yarn cross section. Two extremes are considered: when the stiffer fibers form the core of the blended yarn and when the stiffer fiber forms the outer sheath. At zero twist, no effect of blend cross-sectional distributions would be experienced for large radii of curvature. However, with twist increases, it is clear that when the stiffer fibers form the sheath of the yarn, more rapid decreases in rigidity will result than when the stiffer fiber forms the core. The precise difference will depend on the blend proportions and also the relative stiffness of the

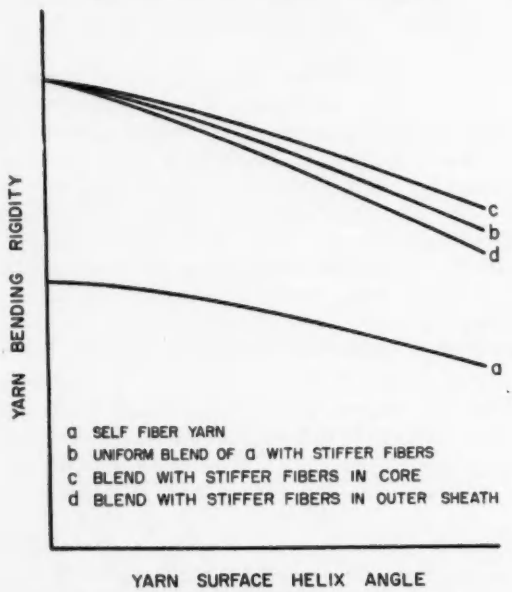

Fig. 10. Effects of twist on blended yarn rigidity; complete freedom of fiber motion.

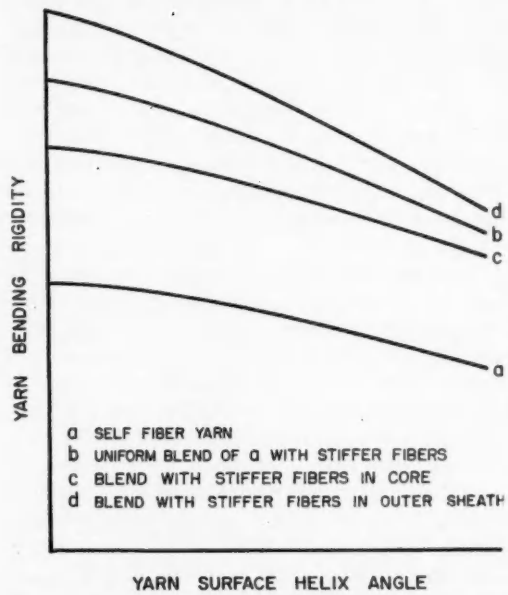

Fig. 11. Effects of twist on blended yarn rigidity; no freedom of fiber motion.

blending fiber to the original fiber. This effect is shown in Figure 10, Curve *c* for the stiff fiber forming the core and Curve *d* for the stiff fiber forming the outer sheath. Obviously, where there is a vast difference between the diameters of the blending fibers, the effects of fiber fit in yarn cross section on yarn surface helix angles at prescribed twists must be taken into account.

For the case of complete lack of freedom of motion among the fibers, similar considerations apply. When the blend distribution is uniform, the effects of twist increases on yarn bending rigidity are proportionally the same as for a self-fiber yarn. This is shown in Curves *a* and *b* of Figure 11, where *b* represents the uniform blend of stiffer fibers (in tension and compression) with *a*. For a zero twist yarn, blend distribution can have a highly significant effect when there is no freedom of motion. Thus, at zero twist, location of the stiffer fiber in the blended yarn core will produce a yarn rigidity lower than the uniform blend. This is shown as Curve *c* in Figure 11. Conversely, where the stiffer blending fiber forms the yarn sheath, a much stiffer yarn than the uniformly distributed blend will result; this is indicated in Figure 11, Curve *d*. As twist increases, more rapid loss in rigidity will take place for the yarn with the stiff fiber in the sheath than for the yarn with the stiff fiber in the core; Figure 11, Curves *c* and *d*. The magnitude of the rate difference will depend upon blend distribution and the relative axial load stiffness of the stiffer and original fibers. Thus, uniformity of blend distribution influences yarn rigidity differently for the two cases of complete freedom of fiber motion and no freedom of fiber motion. Moreover, as can be seen from Figure 11, if twist changes influence fiber location in the blended yarn cross section, then at least theoretically it would be anticipated that rigidity could either rise or fall over a twist range in a complex manner predictable only from a knowledge of the actual blend distribution.

Acknowledgment

The authors wish to acknowledge the many helpful and fruitful suggestions made by Myron J. Coplan and Henry M. Morgan during the course of this work. In addition, they wish to thank Prof. S. Backer of Massachusetts Institute of Technology for his many valuable comments relating to certain of the analyses covered.

Literature Cited

1. Backer, S., Textile Research Journal **22**, 668 (1952).
2. Backer, S., unpublished Doctoral Thesis, Massachusetts Institute of Technology (1952).
3. Chow, T., unpublished Master's Thesis, Massachusetts Institute of Technology (1948).
4. Coplan et al., ONR Technical Report, "Rigidity of Blended Woolen Yarns," part of a series "A Study of Blended Woolen Yarns (in preparation).
5. Fuller, C. E. and Johnston, W. A., "Applied Mechanics," Vol. I, London, Stanhope Press, 151 *et seq.* (1913).
6. Hamburger, W. J., Platt, M. M., and Morgan, H. M., Textile Research Journal **22**, 695 (1952).
7. Hearle, J. W. S., *J. Textile Inst.* **49**, T389 (1958).
8. Morgan, H. M., private communication.
9. Phillips, H. B., "Calculus," Part II, Cambridge, Addison-Wesley Press, 388 (1941).
10. Platt, M. M., Textile Research Journal **25**, 132 (1954).
11. Platt, M. M., Klein, W. G., and Hamburger, W. J., Textile Research Journal **28**, 1 (1958).
12. Roark, R. J., "Formulas for Stress-Strain," New York, McGraw-Hill, 143 (1943).

Manuscript received April 2, 1959.

An Application of a Sequential Type Analysis to Field Tests

H. R. Rush

QM R&E Field Evaluation Agency, Fort Lee, Virginia

Abstract

A unique situation is encountered in determining the durability of fabrics under field test situations; i.e., the data can be analyzed at any point in time in the test. This suggests that the sensitivity of the test can be determined at any point by utilizing the well-known concept of the power of the analysis of variance test. With this information, a decision can be made to stop or continue the test as in the usual sequential procedures. The results of the application of this method to an actual test is presented.

Introduction

The present paper concerns an adaptation of the concept of sequential type analysis for use with accelerated wear field tests of fabric durability. The term sequential analysis is used here in its broader sense and does not refer to the sampling procedure developed by Wald [16] and applied by many investigators in various fields [2, 4, 5, 6, 8, 11, 14]. The important distinction between the field test situation and those circumstances which have thus far proved amenable to sequential analysis concerns the sampling or observation procedure. In the more typical sequential analyses a series of independent observations are made on items subjected to a given test, and the hypothesis is accepted, rejected, or a decision made to sample additional independent items subjected to the same test. In field tests, the sample size usually is established prior to the initiation of the test, and testing is cyclical in nature, producing cumulative wear and degradation. In these instances, additional observations represent one more test cycle for the entire fixed sample rather than one more sample subjected to a predetermined amount of testing.

Methods

The pitfalls that beset an intuitive approach to the problem of treating fixed sample size tests in a sequential manner have been pointed out by Anscombe [1]. When an experiment has progressed to some logical stopping point, a practical experimenter frequently will apply appropriate statistical tests to determine to what extent observed differences may be attributable to chance. If the observed differences are not statistically significant at the desired level, he may examine the data carefully for trends, inconsistencies, etc. and then decide that the experiment should be continued because a few more cases, assuming comparable results, will provide the desired probability level or that the experiment should be stopped because the erratic results thus far make it improbable that significant differences would be obtained even with a large increase in the number of observations. Obviously some decision criteria other than intuition is needed—some method of determining the sensitivity of the test in a manner analogous to the orthodox sequential procedures. Given the necessary information, Neyman et al. [13] have shown how the sensitivity of the randomized block test for two treatments is determined, and Tang [15] has formulated a general solution for the case of t treatments. For both cases this sensitivity is determined after the test is completed. For the type of field test investigated here, however, as will be apparent later on, the sensitivity can be determined as the test progresses. This being true, a decision can be made to either stop or continue the test at any point as in the ordinary sequential procedure.

Since the question to be posed in this investigation is whether, at any given time in the test, any two adjacent ranked treatment means differ significantly from each other, the case considered by Neyman is applicable here. Since the exact calculation of this probability is rather complicated, an adequate approximate solution can be obtained from the following equation

$$\delta = \sqrt{\frac{2}{r}}\,\sigma(t_1 + t_2)$$

(the notation is that used in Cochran and Cox [7]) where δ = specified true difference desired to detect; σ = true standard error per unit; t_1 = value of t, with appropriate degrees of freedom, from the ordinary t-table corresponding to a fixed risk α, of rejecting the null hypothesis when it is true; r = number of replications per treatment; and δ and σ are expressed as a percent of the mean of the experiment. Solving for t_2, find P_2, the probability corresponding to t_2 in the ordinary t-table. Since the ordinary t-table gives probabilities that a value lies outside the limits $\pm t_2$, the required probability P is $1-\frac{1}{2}P_2$. In applying such a procedure, the assumption is made that σ, the true standard error, is no longer a random variable, but has been uniquely determined as far as the test under consideration is concerned. A further assumption, that the relationship between the test items will remain relatively unchanged, is implicit.

The value of P can be calculated at any interval during the test and used as the basis for a decision to stop testing or to continue testing until the next interval. The criterion value of P can be set arbitrarily depending on the purpose of the investigator and the nature of the particular testing situation. Figure 1 shows the P values associated with some values of r, δ, and σ encountered in field tests.

The utility of such a procedure was evaluated by applying it to data obtained from several tests previously conducted on the Field Evaluation Agency's Fabric Courses. The data from these field tests become available in time sequence, and a large number of test subjects are required for protracted periods of time. Thus, such tests are typical of those which appear amenable to sequential procedures and from which maximum benefits in efficiency might be expected.

The Field Evaluation Agency's Fabric Courses are designed to enable comparative evaluation of fabrics in terms of durability under conditions approximating accelerated normal wear. The courses consist of a series of obstacles which when traversed by subjects wearing test garments produce types and amounts of wear similar to that observed in garments salvaged from normal use. The complete course is used for testing cotton fabrics, and a modified version is used for wool fabrics. One pair of trousers made from each test fabric is assigned to each man

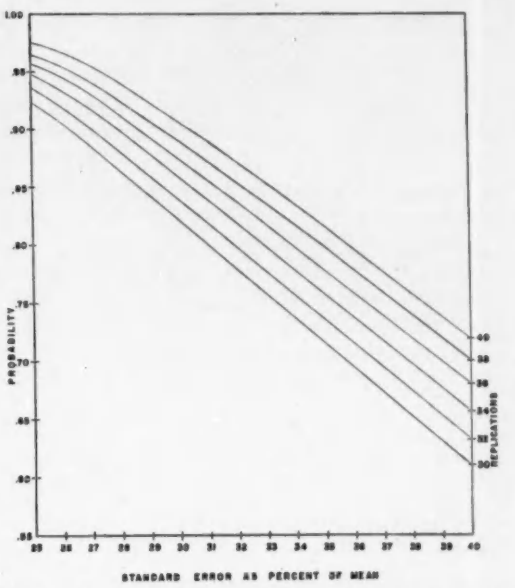

Fig. 1. Probability of detecting true differences for specified values of r and σ for $\delta = 20\%$.

participating in the test. The garments are worn through a preplanned number of cycles with a cycle consisting of two traversals of the fabric course and one laundering. The trousers are examined after each cycle; failures are charted and scored by means of a weighted scoring system developed by the Field Evaluation Agency. A statistical analysis is made at the end of the number of cycles designated in the test plan to determine if differences in average wear scores of fabric types are significant. The experimental design used is that of randomized blocks, where each test subject is a "block." The order of wear of the fabric type is randomized, with each fabric type being represented during each wear cycle.

The scoring system used is one based on visual inspection of the garments. Obviously considerable wear will have occurred before it can be detected by this means. For this reason little would be gained by an analysis at a cycle before reliable detectable trends have developed. Data available from a large number of past tests suggest that such trends have become established when wear scores approximate values of 40 for cotton fabrics and 25 for wool serge and similar wool blend fabrics.

The point at which analysis of this data would start having been determined, the familiar analysis of variance would be performed and an appropriate

TABLE I. Analysis of Cotton Fabric Test Data ($r = 37$)

Cycle of wear	Results of analysis of variance: F-value	Multiple comparison test*	Std.† error	Value of P ($\delta = 20\%$; $\alpha = .05$)
7	27.86	CS 38.5 KR 46.5 K 62.8 CW 81.2	38	0.73
8	26.80	CS 45.5 KR 53.4 K 72.5 CW 91.6	37	—
9	25.46	CS 55.0 KR 63.0 K 83.7 CW 101.0	33	—
10	22.21	CS 65.9 KR 76.6 K 94.8 CW 112.6	30	—

* Duncan's Multiple Range Test. Means *not* underscored by the same line are significantly different at 5% level.

† As percent of over-all mean. CS—9 oz. Combed Sateen, Cotton, Std.; CW—8.5 oz. Carded Sateen, Cotton, Std.; KR—9 oz. Carded Sateen, 75% Cotton, 25% Black Pigmented Rayon; K—9 oz. Carded Sateen, Cotton.

test for comparing means, such as Duncan's Multiple range test [9], employed. The investigation would end in the unlikely event that all difference obtained between adjacent ranked means exceeded $\sqrt{2}s_{\bar{x}}t_{.05}$. Normally, though some of the fabric means may be found to differ significantly, other means will be grouped in such a manner that the decision to accept the null hypothesis or to continue the test is surrounded by uncertainty. These are the means of concern and to which the criteria for termination are applied. It is at this point that a value of P would be computed, utilizing the sample variance as an estimate of σ^2 and setting δ at any value of interest to the experimenter. For the fabric course, with α fixed at 0.05 and considering the values of r and σ^2 encountered, a value of $\delta = 20\%$ was selected as a critical one. In other situations values of δ lower than this might be appropriate, depending, of course, on α, r, and σ. The computed value of P is then evaluated against some predetermined level. For the fabric course a P of 0.80 was selected as giving reasonable protection levels against committing a type II error.

Results

The results of the application of this type of sequential analysis to a test of cotton fabrics [12] can be seen from Table I. In this test four different cotton fabrics were run for 10 cycles on the fabric course. Using the usual procedure, only that analysis shown in the last row of Table I would be made. However, examination of the mean wear scores by cycle indicated that a statistical analysis might profitably be made after cycle 7 where the lowest average wear score, 38.5, was an adequate approximation of the minimum wear score required for establishment of reliable trends. Analysis of the data at this cycle allowed definitive statements to be made with respect to types K and CW. The maximum difference between adjacent ranked means for the remaining fabrics, in this instance CS and KR, expressed as a percent of the general mean, was 14%.

The standard error expressed as a percent of the over-all mean was found to be 38%. Since the test of significance is to be a one-tailed test at the 5% level, the value for t would be the 10% value in the ordinary t-table corresponding to 108 degrees of freedom, the number available for estimating σ^2. By interpolation in the t-table [10], this value was found to be 1.660. By substitution of the above values of t_1 and σ, with $\delta = 20\%$ and $r = 37$, in the formula and rearrangement, the terms become

$$t_2 = \frac{\delta - \sqrt{\frac{2}{r}}\,\sigma t_1}{\sqrt{\frac{2}{r}}\,\sigma} = \frac{20 - \sqrt{\frac{2}{37}}\,(38)\,(1.660)}{\sqrt{\frac{2}{37}}\,(38)} = 0.604$$

From the t-table we find the probability (P_2) associated with this value of t to be approximately 0.54. Then the desired probability of detecting a difference of as much as 20% is $1-\frac{1}{2}\,P_2 = 0.73$.

Applying the stipulated decision criteria, the test would be terminated at this point. Comparison of these results with those obtained at the end of 10 cycles showed that the same conclusions would be drawn with the same level of confidence. The seemingly desirable inverse relationship between the number of cycles and the magnitude of the standard error as seen in Table I can be misleading, since it is accompanied by decreasing proportional differences between fabric wear scores as maximum wear is attained by all fabric types, as attested by decreasing F-values.

In a similar manner, the foregoing procedure was applied to an additional two cotton fabric and three wool fabric tests. It was found that the proposed procedure worked quite well for cotton tests, allowing a reduction in the test period of from two to three cycles. The same conclusions with respect to fabric comparisons would be made after the proposed

shortened test period as were made at the original end of the test. Applying the same criterion, that of conformance of results, to the three woolen tests, some discrepancies in conclusion were noted. In these instances, however, it was felt that the shortened test period gave a truer evaluation of fabric differences.

Discussion

The efficacy of such a procedure for fabric course testing and other comparable testing situations would certainly be worthwhile. Speaking only of the realm of field testing, it might profitably be applied to durability testing of many items, particularly to the testing of footwear, socks, gloves, and other clothing items. It would be feasible also in other fields of experimentation where the data can be examined at any given time sequence in the test.

A recent article by Bechofer [3] presents a multiple decision procedure for selecting the best one of several normal population means with a common unknown variance and, as pointed out in the article, the problem of selecting and ordering the t populations with the largest population means also can be treated within the same general theoretical framework. However, the sampling procedure, which is the orthodox sequential one, could be unworkable for the type of experiment discussed here. Consider a test of five treatments (fabrics). It would require each test subject approximately four weeks to complete 10 cycles of the fabric course for this number of treatments. In other words, four weeks would be required to obtain a single observation, and an additional four weeks for each observation thereafter. It is apparent that the tests would take several months to run under this sampling procedure, even if sampling in groups were resorted to.

Summary

A sequential type approach to analysis of data obtained from accelerated wear field tests is devised through adaptation of the statistical concept of the power of a test. The method requires that the experiment be cyclical in nature and that the data become available in time sequence. From a knowledge of the magnitude of the differences it is desired to detect in the experiment and an estimate of the population variance, the probability of detecting such a difference at a given significance level is determined. This probability is used after each cyclical analysis in making a decision to continue or to terminate testing. Application of this procedure to a number of accelerated wear fabric tests conducted on the Fabric Course demonstrated a potential savings of 20–33% in test personnel man hours without loss of meaningful information. The adaptation of such methods to other field tests appears highly feasible.

Literature Cited

1. Anscombe, F. J., *Biometrics* **10**, 89–100 (1954).
2. Armitage, P., *Quart. Journ. Med.* **23**, 255–274 (1954).
3. Bechofer, Robert E., *Biometrics* **14**, 408–429 (1958).
4. Bradley, Ralph A., *Biometrics* **9**, 22–28 (1953).
5. Bross, I. D. J., *Biometrics* **8**, 183–187 (1952).
6. Brownlee, K. A. et al., *J. Am. Stat. Assoc.* **48**, 262–277 (1953).
7. Cochran, W. G. and Cox, Gertrude, "Experimental Design," 2nd Ed., Wiley, New York (1957).
8. Dixon, W. J. and Mood, A. M., *J. Am. Stat. Assoc.* **43**, 109–126 (1948).
9. Duncan, D. B., *Biometrics* **11**, 1–42 (1955).
10. Fisher, Ronald A. and Yates, Frank, "Statistical Tables For Biological, Agricultural and Medical Research," 3rd Ed., Hafner (1949).
11. Fiske, D. W. and Jones, L. V., *Psychol. Bull.* **51**, 264–276 (1954).
12. Matthews, J. M., FEA 53095, *Wear Resistance of 9 oz. Cotton Sateen Blended with Rayon*, QM R&E Field Evaluation Agency, Ft. Lee, Va. (1954).
13. Neyman, J., Iwaszkiewicz, K., and Koldziejczyke, St., *Suppl, J. Roy. Stat. Soc.* **2**, 107–154 (1935).
14. Radkins, Andrew P., *Food Research* **23**, 225–234 (1958).
15. Tang, P. C., *Stat. Res. Mem.* **2**, 126–149 (1938).
16. Wald, A., "Sequential Analysis," Wiley, New York (1947).

Manuscript received March 11, 1959.

A Study of Blended Woolen Structures

Part V: Methods of Within-Section Blend Analysis[1]

Myron J. Coplan and William G. Klein

Fabric Research Laboratories, Inc., 1000 Providence Highway, Dedham, Massachusetts

Abstract

Statistical implications of the index of blend irregularity have been elaborated, with consequent improved utility of this measure.

A more complete characterization of within-section blend distribution is now possible by two new techniques developed.

Some new light is shed on the characteristics of fiber clustering and blend irregularity within the sections of woolen wool-nylon yarn.

Introduction

Earlier parts of this series [1, 4] dealt at some length with the statistical assessment of blend distribution from section to section along the length of a strand. An index of blend irregularity was derived which characterizes this longitudinal distribution. Brief mention was also made of a similar calculation for assessing blend distribution *within* strand cross sections [1], leading to what was called the rotational I.B.I.

The rational determination of whether fibers at each section are randomly intermingled is probably of equal importance with the determination of blend distribution longitudinally. The subject has been treated by several workers [6, 9] employing various statistical tests for the lateral mixing of fibers. When properly applied, the I.B.I. for within-section distribution should also be a useful measure.

In our previous discussion of the I.B.I., no mention was made of the confidence limits that might be assigned to computed values. Walker [10] has pointed out that the calculation of I.B.I. is related to a chi-square test. Viewed in that light, the numerical values take on additional meaning, and it is possible to assign confidence limits to them. In addition, it can now also be shown that the Index for the ideal random blend, formerly given as 1.0, has a finite range which depends only upon the degrees of freedom involved in the test.

[1] Work conducted with the support of United States Navy, Office of Naval Research, and Bureau of Supplies and Accounts.

The object of this report is to define the reliability in terms of confidence limits for I.B.I. either for longitudinal or within-section analysis and to describe some appropriate methods of determining within-section distribution of blend.

The I.B.I. as a Chi-Square Test

The longitudinal I.B.I. has previously been defined as

$$\text{I.B.I.} = \sqrt{\frac{1}{n}\sum_{1}^{n}\frac{(W_i - pT_i)^2}{T_i pq}}$$

In principle, this measure is a test of goodness of fit for the hypothesis that a series of n sections were random samplings from a random mixture. The proviso has been made that to use this formulation n should be reasonably large, say 25 or more. Rigorous treatment would require summing over n sections, but dividing under the radical by ν, the degrees of freedom, rather than n. For longitudinal I.B.I. the degrees of freedom would be $n - 1$ so that the possible error in I.B.I. is negligibly small (i.e., 2% for $n = 25$). Where n/ν is sensibly larger than 1, however, as in one of the methods of within-section analysis to be described, the error in the foregoing formulation becomes significant. Strictly speaking in the general use, the appropriate form is

$$\text{I.B.I.} = \sqrt{\frac{1}{\nu}\sum_{1}^{n}\frac{(W_i - pT_i)^2}{T_i pq}} \qquad (1)$$

In computing this index one determines experimentally a set of n values of T_i and W_i, which automatically provides a set of values of N_i, and

the ratios p and q (see list of symbols). These same numerics are all that would be required to calculate a value of chi-square for the distribution of wools and nylons.

$$\chi^2 = \sum_{i=1}^{n} \frac{(W_i - pT_i)^2}{pT_i} + \sum_{i=1}^{n} \frac{(N_i - qT_i)^2}{qT_i} \quad (2)$$

But, by virtue of the defined relationships, $W_i + N_i = T_i$ and $p + q = 1$; then we have

$$\chi^2 = \sum_{i=1}^{n} \frac{p(W_i - pT_i)^2 + q(W_i - pT_i)^2}{T_i pq}$$

$$= \sum_{i=1}^{n} \frac{(W_i - pT_i)^2}{T_i pq}$$

which from Equations 1 and 2 leads to

$$(\text{I.B.I.})^2 = \frac{\chi^2}{\nu} \quad (3)$$

Calculation of I.B.I., then, is seen to be the equivalent of a χ^2 test computed in a short-cut fashion appropriate and peculiar to the present type of problem. The numerical value of I.B.I. is related to χ^2 through ν. The restrictions imposed on I.B.I. are the same as for any χ^2 test, and, in general, the principal requirement is that pT_i (the expected number of fibers of the minor constituent of the blend) shall be at least 5. Recognition of the relationship of I.B.I. and χ^2 is important in that the characteristics of the latter statistic have been well described and therefore the range of applicability of the former is now more precisely definable. As a result, the utility of the I.B.I. as a statistic is extended.

Symbols

T_i = Total number of fibers at a given section.
W_i = Total number of wools at a given section.
N_i = Total number of nylons at a given section.
$\bar{T}, \bar{W}, \bar{N}$ = Average values across all sections.
T_{L_i} = Total of all fibers on the left of an arbitrary meridian of a given section.
W_{L_i} = Number of wools on the left.
N_{L_i} = Number of nylons on the left.
$T_{R_i}, W_{R_i}, N_{R_i}$ = Fibers on the right of the arbitrary meridian.
$p = \bar{W}/\bar{T}$
$q = 1 - p$
$p_i = W_i/T_i$
$q_i = 1 - p_i$
n = Number of sections or subsections to be summed in a test.
ν = Degrees of freedom in a test.
Q_i = Total number of groups of both sorts of fiber in a linear array for a given section.
Q_{i_∞} = Expected number of groups in a random linear array of the fibers from a given section.

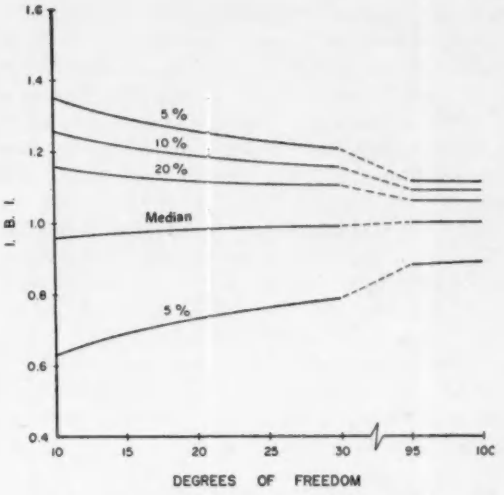

Fig. 1. I.B.I.'s significant at various confidence levels and degrees of freedom.

An important example of this is the ability to establish confidence limits for I.B.I. Employing the relationship of Equation 3 and a table of χ^2, one may calculate the expected value and upper and lower limits at particular probability levels for the I.B.I. of the random blend (see Figure 1).

Previous reference to a lower limit of I.B.I. = 1.0 for the ideal random blend is now seen to be subject to interpretation. While the *median value* is very close to 1 for degrees of freedom of 25 or more, it is apparent that in actual practice values of I.B.I. may be found both above and below 1.0 for the ideal random blend. For example, from Figure 1, where testing 25 cross sections, the chances are one in five that an I.B.I. of 1.10 or more will be found for even the ideal random blend.

For $n > 25$, the confidence limits for the I.B.I. of a random blend will be very closely approximated by

$$\text{I.B.I.} = 1 \pm \sqrt{\frac{t}{2\nu}}$$

where t is the familiar unit variance statistic.

A second important consequence of recognizing the equivalence of I.B.I. and χ^2 is in the analysis of the statistical significance of the difference between two values of I.B.I. While it was not necessary to have proven that equivalence for this purpose, it now follows without further argument that the F test for the significance of differences of

two experimental variances applies. It is necessary simply to find the ratio of the square of the larger I.B.I. to the square of the smaller and compare the ratio with F found at the appropriate degrees of freedom in standard F tables. Figure 2 has been computed from such tables of F and gives values for the ratio of two I.B.I.'s which are significantly different at three probability levels, where the I.B.I.'s were calculated for equal degrees of freedom ($\nu_1 = \nu_2$). For example, assume the I.B.I.'s of two yarns were to be 1.2 and 1.7 for 25 specimens in each of the yarns. The I.B.I. ratio is $1.7/1.2 = 1.42$. This is just significant at the 5% level.

A third useful result of the equivalence of I.B.I. and χ^2 is the arithmetically additive nature of the statistic. A grand value of I.B.I. would be found from a series of subsamplings by

$$(\text{I.B.I.})^2(\nu_1 + \nu_2 + \cdots) = \nu_1(\text{I.B.I.}_1)^2 + \nu_2(\text{I.B.I.}_2)^2 + \cdots \quad (4)$$

Thus if, as frequently happens with small samplings, statistical significance cannot be shown at an adequate confidence level though a real difference is suspected, various data can be combined to increase the effective degrees of freedom. In this way the confidence limits are narrowed and a more definitive conclusion may be drawn from the available information.

Appropriate Methods of Within-Section Analysis

The homogeneity of fiber intermingling at each cross section is a blend characteristic of equal importance with the variation in blend from section to section. This latter variability may be determined chemically or densitometrically on short finite lengths cut from the yarn for which procedure the appropriate analytical formulations have been presented [4].

For within-section analysis however, there seems to be little hope of avoiding some form of microscopical analysis. It is necessary to embed and section the yarn, retaining the spun locations of the fibers. Thereafter, of course, visual observation of the several yarn cross sections must be made with the object of determining the regularity of fiber intermingling.

It should be emphasized that the prime purpose here is *not* to determine the randomness of blend proportions from section to section. Rather, the problem is to determine whether the fibers at each section—whatever their number ratio at that section happens to be—are randomly mixed together.

This problem has two aspects. First, there is the matter of preferential radial migration of a particular component of the blend either inward toward the yarn center or outward toward its periphery. For this purpose, the yarn section might be subdivided into concentric rings and counts made of the individual fibers in each concentric area. The evaluation of blend distribution in concentric areas by graphical [1] and numerical [8] means has been described. An adaptation of the I.B.I. might be applied here, but the problem is actually susceptible to simpler treatments, as will be shown.

The second aspect of the problem of assessing within-section mixing has previously been treated [1, 5] by sectorial subdivision of yarn cross sections. Here, the purpose was not to determine if there is preferential migration of one component to a certain specific location in the yarn, as in the radial analysis. Rather, the object was to determine whether each of several rotationally symmetrical (i.e., pie-slice) areas represented a random sampling from the particular whole cross section in which it lay. Previous reports illustrated the method of dividing yarn cross sections into octants. The deviations of blend in each octant from the blend of the whole section in which the octant lay were treated by a method similar to the longitudinal I.B.I. calculations.

Actually, when the relationship between I.B.I. and χ^2 is recognized, it is apparent that the yarn subdivisions need not be entirely symmetrical, nor is it necessary to subdivide the several cross sections into octants. In fact, merely dividing each section into halves by randomly drawing a diametrical line provides the necessary data for the analysis. It should be noted immediately, however, that the number of degrees of freedom, ν, for each cross section will be one less than the number of subdivisions. Thus if 25 cross sections are each divided in half, the analysis will entail $n = 50$ subsections, but only $\nu = 25$ degrees of freedom.

The complete formulation for χ^2 in this analysis is

$$\frac{(p_i T_{L_i} - W_{L_i})^2}{p_i T_{L_i}} + \frac{(q_i T_{L_i} - N_{L_i})^2}{q_i T_{L_i}} + \frac{(p_i T_{R_i} - W_{R_i})^2}{p_i T_{R_i}} + \frac{(q_i T_{R_i} - W_{R_i})^2}{q_i T_{R_i}} \quad (5)$$

That there is only one degree of freedom associated with these four terms is readily shown. The

values p_i and q_i are given for each section from W_i and T_i (hence also N_i) found there. The section having been divided arbitrarily into approximate halves, T_{L_i} and T_{R_i} are also specified. The only independent variant is W_{L_i}. Once this value is determined, W_{R_i}, N_{R_i}, and N_{L_i} are automatically determined from

$$W_{R_i} = W_i \text{ (given)} - W_{L_i}$$
$$N_{L_i} = T_{L_i} \text{ (specified)} - W_{L_i}$$
$$N_{R_i} = N_i \text{ (given)} - N_{L_i}$$

This is to say that once the surplus of wools is found for a given half-section, the deficit of wools in the other half-section is known. Similarly, the deficit of nylons in the first half-section is specified as well as the surplus in the second half-section. Moreover, all four numerators in Equation 5 are numerically identical, leading to

$$\chi^2 = \frac{(p_iT_{L_i} - W_{L_i})^2}{T_{L_i}p_iq_i} + \frac{(p_iT_{L_i} - W_{L_i})^2}{T_{R_i}p_iq_i} \tag{6}$$
$$= \frac{T_{R_i}(p_iT_{L_i} - W_{L_i})^2}{T_{R_i}T_{L_i}p_iq_i} + \frac{T_{L_i}(p_iT_{L_i} - W_{L_i})^2}{T_{R_i}T_{L_i}p_iq_i}$$
$$= \frac{(p_iT_{L_i} - W_{L_i})^2(T_{R_i} + T_{L_i})}{T_{R_i}T_{L_i}p_iq_i}$$

But $T_{R_i} + T_{L_i} = T_i$; hence

$$\chi^2 = \frac{(p_iT_{L_i} - W_{L_i})^2}{T_{L_i}p_iq_i} \times \frac{T_i}{T_{R_i}} \tag{7}$$

$$\text{I.B.I. (within)} = \sqrt{\frac{1}{\nu}\sum_{n=1}^{n}\frac{(p_iT_i - W_{L_i})^2}{T_{L_i}p_iq_i} \times \frac{T_i}{T_{R_i}}} \tag{8}$$

It may be desired to perform a within-section analysis of blend randomness which simultaneously takes into account the distribution of fibers both radially and rotationally. A possible solution to this problem may be found by adapting to analysis of yarn sections a statistical test similar to one that has been described by DeBarr and Walker for analyzing a monolayer ribbon of fibers emerging from drawing rolls [6]. These authors describe a function γ, which relates the actual number of groups of fibers of a given sort found in such a ribbon to the number that would be expected in a purely random mixing.

These workers have pointed out that there is a statistically most probable number of groups into which pT white fibers will be distributed in a random linear array of T total fibers. ("By a group of white fibers is meant a set of one or more adjacent white fibers with a colored fiber at each end of the set.") This most probable, or expected value for the random blend is given as

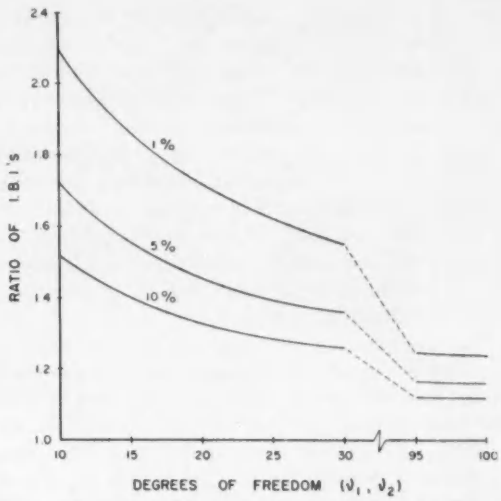

Fig. 2. Ratios of I.B.I.'s significantly different from one another at various confidence levels and degrees of freedom.

$$g_\infty = (T - 1)p(1 - p) + p \tag{9}$$

for the fiber whose number concentration in the blend is p. This reduces to

$$g_\infty = Tpq + p^2 \tag{10}$$

and, in a binary blend, the equivalent function for the other fiber is

$$g_\infty' = Tpq + q^2 \tag{11}$$

In DeBarr and Walker's procedure, the number of groups, g, of say white fibers in an essentially monolayer ribbon of fibers is counted and compared with g_∞ to yield an index

$$\gamma = g/g_\infty \tag{12}$$

For proper application of this statistic to our own procedure, to be developed, it will be necessary to take account of the number of groups of both species. Moreover, it will be necessary (and, in fact, convenient) to use the local values for T, p, and q, namely T_i, p_i, and q_i found at each section. Summing Equations 10 and 11, employing appropriate local values, we therefore calculate a value

$$Q_{i\infty} = 2T_ip_iq_i + p_i^2 + q_i^2 \tag{13}$$

For almost any practical yarn, $2T_ip_iq_i$ will always exceed 10 and $p_i^2 + q_i^2$ will range from 0.5 to 0.8.

Since $2T_ip_iq_i$ is rarely a whole number, it is entirely reasonable to use $2T_ip_iq_i$ rounded to the next higher whole number as the expected total number of groups, $Q_{i\infty}$, in a given random linear array of fibers.

Obviously, a yarn cross section does not present a linear array against which to apply the described criterion for randomness. It is desired, therefore, to reorient into a line the fiber cross sections found at each yarn section. If one were to select the fibers at random from the section, the result would be a random array, irrespective of any within-section tendency to aggregate.

Assume, however, that any fiber may be assigned coordinates, say $\rho\theta$, in the plane of the cross section. In the case of random intermingling, any selection of fibers systematically ordered with respect to the coordinates will yield a random array. However, if there is a tendency for nonrandom distribution of the fibers of a given species, the probability of a fiber at, say, ρ_1, θ_1 being like its neighbor at ρ_1, θ_2 will differ from that determined purely by chance. Thus, if one selects fibers in a sequence ordered with respect to a coordinate system, the resulting linear array will exhibit characteristics different from that of the random sequential array. It is desirable that each fiber selected and laid down in this linear array be bounded by its original neighbors in the yarn. This might be accomplished in alternative ways, but for convenience the following procedure has been adopted.

After embeddment and cross-sectioning, each section of yarn is projected onto a sheet of paper and the fiber outlines drawn as in Figure 3, identifying the fiber species appropriately. After selection of some one fiber at the center of the yarn image, a continuous line is drawn in a near spiral encompassing one (or nearly one) layer of fibers throughout its length.

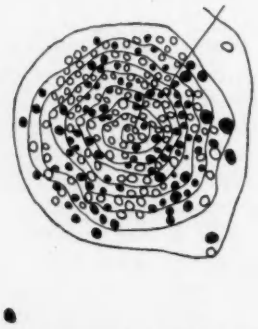

Fig. 3. Illustration of method of spiral subdivision of a typical yarn cross section.

A radial line (not necessarily straight) is then drawn from the central fiber outward to the periphery, intersecting the spiral line only between fiber groups. This is illustrated also on Figure 3. This line is merely a convenient mark for aid in tabulation.

A tally is next made of the sequential fiber arrangement, following around the spiral from the inside to the outside. It has been found most convenient to conduct this tally with the aid of a typewriter. Two adjacent letters on the keyboard are adopted to represent the two fiber species. As the operator ticks off each fiber on the diagram with a pencil in one hand, he hits the appropriate letter with a finger of the other hand. At the end of each turn around the spiral (i.e., at each intersection of the radial line), the carriage is returned. The resulting tally is typified in Table I, where the appropriate data developed from it are also tabulated.

While this procedure may seem to be tedious, it should be pointed out that whatever procedure is employed for cross-section analysis, it is necessary to complete some kind of count of the number of fibers of each sort involved in the blend. In fact, the procedure just described compares very favorably for speed and simplicity with several other techniques that have been applied. Moreover, the data that results are immediately useful in several ways besides the original intended purpose.

First, of course, the total number of blacks and whites found at each of several sections is determined. These values are required for the calculation of longitudinal I.B.I. via Equation 1.

Second, the data organized in concentric spiral rings provide a direct and simple means of assessing radial blend distribution. One might adopt the Migration Index procedure of Hamilton, published recently [8]. The basic approach of this method is, however, not without certain limitations, and the form of the data acquired by the spiral analysis lends itself to a variety of simpler treatments.

The annular blend arrangement is readily found from a set of tallies such as that illustrated. One can find the average inner-half and outer-half blends and apply to these radial subdivisions exactly the same form of within-section I.B.I. test described for the diametrical subdivision (Equation 8). Obviously, radial subdivisions into parcels smaller than inner and outer halves are also easily made. Data

TABLE I. Typewriter Method of Tallying for Spiral Analysis

Tally, by concentric spirals (i = nylon, o = wool)	Groups	Wools	Nylons	Total (cum.)
5 10 15 20 25 30 35				
iiiio	2	1	4	5
iiiiiioiii	3	2	9	16
oiioiiiioooiiiii	6	6	11	33
oiioioioioioioiioo	13	13	8	54
iooioiioioiiioooiioiiioioooooo	16	17	14	85
iiiiooioiiioioiioooiiiioooooiioio	16	15	18	118
iioiiiooiiiiiiiiioooiioiiioooooioioiio	16	17	23	158
ioioioiiiiiooiiioioooiiooiiioioo	18	17	18	193
iiiioioiiiooiiooooioio	12	11	12	216
	102	99	117	

from such subdivisions are readily treated graphically or statistically.

Aside from these purposes, however, the data provide the basis for evaluation of randomness via Equation 13. For each section, or each portion of a section under evaluation, the expected number of groups is found. These expected values are summed for all sections. The actual found number of groups in all the sections or subsections are summed, and the quotient

$$\gamma = \frac{\sum Q_i}{\sum Q_{i\infty}} \tag{14}$$

calculated, yielding an index identical with DeBarr and Walker's γ. The index may also be calculated for any reasonable subportion of the spiral array of each section, taking account, however, of the instantaneous values of T_i, p_i, and q_i for the respective subportions.

The statistical reliability of this index as a measure of the departure of the yarn from randomness may also be evaluated. One simple way uses

$$\frac{(\sum Q_i - \sum Q_{i\infty})^2}{\sum Q_{i\infty}} = \chi^2$$

with $\nu = 1$ as a measure of significance. This can be shown to be equivalent to a "t" test for significance of difference of the found Q_i and the expected $Q_{i\infty}$.

It should be pointed out that the spiral method not only organizes the fiber data conveniently for radial analysis, but that the value of γ found by the group-number test is directly influenced by any form of radial maldistribution, as well as the simple tendency to aggregate. Thus, if by the spiral analysis one fails to demonstrate a statistically reliable departure from randomness it is extremely unlikely that there is a significant degree of radial maldistribution. However, if γ is found significantly lower than 1, either of the two types of faults may exist alone or in combination.

If a radial blend gradient exists without clustering, tests for γ on any subdivision of the spiral should lead to values more nearly approaching 1 than would be found for the whole spiral. If, on the other hand, clustering is the sole cause for γ being less than 1 in the whole spiral, testing shorter lengths can lead to either no change in γ, if clustering is the same throughout the yarn cross section; or a decrease in γ for one region accompanied by an increase in γ for the remainder of the spiral, representing a preferential radial arrangement of the clusters in the whole yarn section.

The hypothesis here is that, in calculating $Q_{i\infty}$, the values T_i were not true measures of the number of units free to be distributed. Rather, a tendency to aggregate reduced the value to T_i/c, so that

$$\frac{Q_i}{Q_{i\infty}} \times c = 1 \quad \text{or} \quad \frac{1}{\gamma} = c$$

The coefficient of clustering, c, found in this way is bound to be smaller than the clustering coefficient determined by I.B.I. [1]. It will be realized that in developing the linear spiral array from the actual planar array, it was possible to arrange any one fiber so that it had adjacent in the line only *two* of its nearest neighbors in the plane. The tendency to cluster in the line, then, can represent only a component of the actual tendency to cluster in the yarn section.

Experimental Evaluation of a 50% Wool-Nylon Yarn

A 3-run (900 denier) woolen spun 50% wool-nylon yarn at high twist was tested by several of

the described methods. Cross sections (25) were taken at intervals exceeding one fiber length and the images of these sections projected onto suitable target sheets [1]. A count was made of the fibers of each sort in the whole section, in radial subdivisions and to each side of an arbitrary diametrical line through each section.

Linear arrays were compiled for each section by the method of spiral subdivision, described above. A count was made of the fibers and groups in each whole array, in each inner and outer half, and in each inner and outer third.

The foregoing experimental data were employed in the calculation of the following.

1. Whole yarn average blend composition, by number of fibers.
2. Average fiber blend composition by number for inner and outer halves and thirds.
3. Index of Blend Irregularity longitudinally; i.e., from section to section.
4. Within-section I.B.I., comparing left and right halves of each section to individual whole-section blend.
5. Within-section left-right I.B.I., for the inner $\frac{1}{3}$ separately and the outer $\frac{2}{3}$ separately of the several sectons.
6. Within-section I.B.I. comparing inner and outer halves of each section to individual whole-section blend.
7. Ratio of found to expected number of groups, γ, using entire linear array from each section.
8. Ratio, γ, using inner and outer halves separately.
9. Ratio, γ, using innermost and outermost thirds, separately.
10. Tests for significance of departure from randomness for 3 through 9, and departure from average blend composition for 2, above.

The results of these several calculations are shown in Table II; they provide some interesting features for comment. First, of course, the top five lines indicate a tendency for disproportionate distribution of nylons toward the center and wool toward the outside of the yarn. This, in itself, is not new, having been described graphically in a previous report [1]. Nor is anything new in the fact that maldistribution of blend occurs along the yarn (Line 6). This has previously been described and attributed to a probable tendency for the fibers to be distributed in clusters rather than as discrete entities.

Lines 7–9 and 11–15, however, provide a new and interesting insight into the probable modes of fiber arrangement within these yarn cross sections. Line 7 suggests, first, that within each section there is a more irregular distribution of fibers to either side of a randomly chosen diameter than would be expected from random distribution of single fibers. This tendency toward nonrandomness diminishes to the point of being only mildly significant in the inner third of the yarn (Line 8) which region is markedly lower in wool concentration. The nonrandomness, however, persists at a high level in the outer regions of the yarn (Line 9), which are more highly concentrated in wool.

The γ for the whole yarn (Line 11) indicates a strong departure from randomness which can be attributed to both localized clustering and a general blend gradient from inside to outside, which latter effect has already been demonstrated. In itself,

TABLE II. Characterization of a 900-Den. Wool-Nylon Yarn

Test	Equation	Index	Sig. level*
1. Whole yarn, no. average blend, % wool		45.2	
2. Inner half, no. average blend, % wool		42.3	These values for blend are
3. Outer half, no. average blend, % wool		47.9	all different from 45.2 at
4. Inner third, no. average blend, % wool		41.6	0.001 level or better
5. Outer third, no. average blend, % wool		48.5	
6. Longitudinal I.B.I.	1	1.5	10^{-3}
7. Whole section meridianal I.B.I.	8	1.6	10^{-2}
8. Inner third, meridianal I.B.I.	8	1.3	2×10^{-2}
9. Outer two/thirds, meridianal I.B.I.	8	1.6	10^{-3}
10. In-out I.B.I.	8	1.8	10^{-4}
11. Whole section γ	14	0.869	10^{-5}
12. Inner half γ	14	0.904	10^{-3}
13. Outer half γ	14	0.870	10^{-4}
14. Inner third γ	14	0.918	2×10^{-2}
15. Outer third γ	14	0.848	10^{-4}

* Values indicate fractional probability of randomness.

therefore, this value 0.869 for the whole yarn is not fully informative.

As one selects the regions closer to the inside of the yarn, however, the γ values (Lines 12 and 14) are seen to rise towards 1 and to diminish in statistical significance. As shorter regions of the spiral array are taken for analysis, one would expect that the effect of blend gradient on γ would diminish, leaving predominantly the local clustering influence. With γ approaching 1, toward the center of the yarn, the apparent clustering must begin to diminish. This checks out well with the inner-third meridianal I.B.I. (Line 8). Neither of these measures, however, demonstrates complete freedom from clustering.

This is quite different from the trend observed moving toward the outside of the yarn (Lines 13 and 15). Although the same increment of γ, from suppression of the general gradient of blend occasioned by selecting shorter regions, might be expected, γ stays essentially constant (0.869→0.870) at the half and actually falls to 0.848 at the outer third. One is led to conclude that the localized clustering effect becomes pronounced toward the yarn periphery.

It is now possible to propose a reasonable description of the general tendencies of fiber mixing for the subject yarn. It is likely, first, that the blending was not on a single fiber basis, but rather involved intermingling of fiber aggregations. This work, and earlier evidence, indicate that wool has a tendency to remain aggregated in larger clusters than nylon. This contributes to a more irregular distribution along the yarn than the ideal random blend.

Within yarn cross sections, the tendency for fibers to be distributed in clusters persists, but with a decided pattern appearing. Larger clusters appear to be predominantly distributed to the yarn periphery, with the clustering effect diminishing toward the yarn core. At the same time, there is a preferential distribution of wool toward the periphery.

It is probably impossible to prove unequivocally a causal relationship between blend separation and clustering. It is proposed, however, that such a relationship does exist for the woolen-spun yarn in question. Two alternatives are present. First, it is conceivable that a significant number of wool fibers are presented to any section in aggregates of such size that they tend to be physically excluded from entering the yarn core. Thus, the clustering would be the cause of partial blend separation.

Second, it is possible that for other reasons, say fiber crimp, length, surface properties, etc., some wool fibers are preferentially spun into the yarn perimeter. This tendency to migrate to peripheral locations might then be the cause for apparent clustering. In either case, the coincidence of high wool concentration and higher clustering in the yarn periphery is of some importance and bears on the question of yarn bulking properties to be discussed in the next article of this series.

Summary and Conclusions

The statistical equivalence of I.B.I. and χ^2 has been defined and enlarged upon.

The use of I.B.I. has been extended for within-section analysis.

A method of spiral subdivision of yarn cross sections has been devised and an appropriate index for randomness adapted to this method from work published elsewhere.

A 50% wool nylon yarn has been explored via the several new methods and the blend pattern more fully elucidated.

Fiber clustering seems to diminish toward the yarn core, which is disproportionately high in nylon concentration; clustering seems to be accentuated toward the yarn periphery, where wool is disproportionately high.

It is postulated the tendency for wool to cluster in large aggregates may account for its preferred distribution outside the yarn core.

Literature Cited

1. Coplan, M. J. and Klein, W. G., TEXTILE RESEARCH JOURNAL **25**, 743 (1955); see also **25**, 968.
2. Coplan, M. J. and Bloch, M. G., TEXTILE RESEARCH JOURNAL **24**, 902 (1955).
3. Coplan, M. J. and Klein, W. G., TEXTILE RESEARCH JOURNAL **26**, 914 (1956).
4. Coplan, M. J., TEXTILE RESEARCH JOURNAL **28**, 956 (1958).
5. Coplan, M. J., Lermond, C. A., and Kenney, R. A., *J. Textile Inst.* **49**, P379 (1958); see question by Ingham.
6. DeBarr, A. E. and Walker, P. G., *J. Textile Inst.* **48**, T405 (1957).
7. DeBarr, A. E. and Walker, P. G., *J. Textile Inst.* **49**, P353 (1958); see references.
8. Hamilton, J. B., *J. Textile Inst.* **49**, T411 (1958).
9. Hampson, A. G. and Onions, W. J., *J. Textile Inst.* **46**, T377 (1956).
10. Walker, P. G., *J. Textile Inst.* **48**, T133 (1957).

Manuscript received December 10, 1958.

Thermal Comfort of Clothing of Varying Fiber Content

Jane E. Werden, M. K. Fahnestock, and Ruth L. Galbraith

Departments of Home Economics and Mechanical Engineering, University of Illinois, Urbana, Illinois

Abstract

This paper reports the results of thermal comfort studies on women subjects wearing complete outfits of clothing made from fabrics of cotton, nylon, acetate, and Arnel. The conditions of temperature and humidity were controlled to create environments ranging from slightly cool to hot. Total weight loss, evaporative weight loss, weight gain of clothing, rectal temperature, time of onset of sweating, and skin temperature were the objective measures used. A subjective comfort vote was also taken.

By use of these measures, no significant differences were found among the fiber types in relation to thermal comfort of clothing. At 94° F. and 80% relative humidity the percentages of gain in clothing weight because of perspiration absorption were related to the original weights of the clothing assemblies rather than the characteristic moisture regain levels of the natural versus the man-made fibers. Environmental temperatures of 88° and 94° F. and relative humidity of 80% had decided effects on the comfort vote and total weight losses of the subjects. Evaporative weight loss was affected by relative humidity at all temperatures used in this study.

Introduction

In the minds of the general public there seems to be common acceptance of the idea that there is a difference in the comfort of clothing based on fiber content. Such comments as "I never wear nylon in the summertime; it is too hot," or "I always change to cotton slips in hot weather because they are more comfortable" bear out this idea of differences in the relative comfort of the fibers in clothing.

While there has been a large amount of work done on clothing in relation to temperature, humidity, air velocity, and the human body, most of this work has been done at extremes of environmental conditions such as those experienced in the armed services and isolated industrial situations [2, 13, 14]. Thermal comfort studies with human subjects and civilian clothing as worn by the general public under climatic conditions commonly encountered have been limited [5, 8, 12, 15, 16]. In most of these studies the emphasis was on the difference between clothed and nude people or between different amounts of clothing as defined by weight or quantity rather than on clothing of differing fiber content.

In 1953 two papers were published by Andreen et al. and Hardy et al. on clothing and thermal comfort. In the first of these [7] a laboratory method using an electrically heated surface representing the skin was devised and used in an attempt to predict thermal comfort from physical data on fabrics. It was concluded that the comfort characteristics of a given fabric could be described only under specific conditions of temperature and humidity, rate of air movement, porosity of fabric, and distance of the fabric from the skin. In the second paper [1] controlled tests were done on human beings wearing coverall garments of textiles containing different fibers. Differences between the comfort of clothing of differing fiber contents, as measured by skin temperature, degree of skin wetness, rate of sweating, total sweat, and heart rate were small. The results indicated that comfort in clothing depends largely upon the geometry of the fabric and the manner in which the fabric is worn on the body.

Since the start of the work at the University of Illinois two papers on water transport mechanisms in textile materials have been published by Hollies et al. [9, 10]. These stated that the insulating ability of textile assemblies depends on the randomness of fiber arrangement in fabrics and that fuzzy yarns with randomly arranged fibers have a low rate of water transport. A paper by Bogaty [4] showed

that fiber arrangement as well as fabric thickness determined fabric insulation.

Thus there seem to be many individual and combined factors involving fiber, yarn, and fabric characteristics and manner of applying fabric to the body which affect human thermal, physical, and psychological comfort. Many of the effects are so small that when coupled with the ability of the body to make compensating physiological adjustments they are most difficult to isolate and measure, either subjectively or objectively.

The study reported in this paper was started because of an interest in the comfort characteristics of civilian clothing worn at conditions that actually exist in the summertime. These conditions could range from hot humid environments to the environment found in air conditioned rooms. This study was also concerned with adjustments made by a person going to and from air conditioned spaces. The work was planned to test two main assumptions: that there is some difference in the thermal comfort of clothing based on fiber content and that the absorption characteristics of a fiber might be the reason for this difference.

Procedure

Women subjects between the ages of 19 and 26 were used. They had thorough physical examinations including urinalysis, electrocardiograms, and basal metabolism tests to ascertain that they were in a satisfactory state of health. Their diet was not controlled, but they were asked to eat approximately the same amount of lunch every day and at the same time. All tests were run in the afternoon on one subject in one outfit of clothing.

A complete outfit of clothing was worn by each subject during all tests. This included brassiere, pants, girdle, slip, dress, hose, and shoes. Four outfits of clothing were used at each environmental condition: all nylon, all cotton with nylon hose, acetate with nylon girdle and nylon hose, and Arnel with nylon girdle and nylon hose. All clothing was white and fitted to the individual subject. The dresses were made from a commercial pattern. The other parts of the clothing assembly were purchased commercially or made especially for the tests as in the case of Arnel. For the nylon, acetate, and Arnel assemblies, slips of tricot construction were used. For the cotton assembly a woven cotton slip was selected, as cotton slips are not made in the tricot construction. In all cases the pants used were of the same style, known as briefs, with elastic at the waist and leg openings. The brassieres were as nearly alike in construction as possible. Since it was not possible to find a girdle that contained only cotton and rubber, a two-way stretch girdle of cotton, rayon and latex was chosen for use with the cotton assembly. A girdle of nylon and rubber was used for the other three assembles. The clothing assemblies were laundered after each test. After being laundered, each assembly was always stored in the 75° F., 45% relative humidity condition in the laboratory for at least 24 hr., then weighed before being put on by the subject at the start of a test. The fabrics used in making the dresses were tested for weave, weight, thread count, thickness, and air permeability [3].

Rectal temperature and skin temperatures at 20 places on the body were measured by thermocouples assembled in a harness. The number and location of the thermocouples for measuring the regional skin temperatures and for determining the weighted mean skin temperature were based on the work of Hardy and DuBois [6].

In this paper, the term "laboratory" refers to the outer room which was conditioned at 75° ± 1.0° F. and 45 ± 2% relative humidity at all times, and both subjects and clothing were equilibrated to those conditions prior to all tests. The term "control room" refers to a smaller room within this laboratory in which the temperature and humidity could be varied over a wide range and controlled to ± 1.0° F. and to ± 2% relative humidity at each preselected level with an air velocity of 25 ft./min. or less.

The subject always entered the laboratory about 1:00 p.m. She undressed, was weighed in the nude on a Buffalo platform scale which weighed to 0.01 lb., put on the thermocouple harness, and then dressed in the appropriate outfit of clothing. After the subject's rectal temperature had become essentially constant (20 to 40 min.), an initial resting oxygen consumption and pulse rate were recorded.

The subject could read, write, or study during the test periods. Corrections were made for changes in weights of any materials used for these purposes during the test periods in determining the total weight loss of the subject.

Periodically during the test, the observer recorded the weight change and the comfort vote of the subject using a scale developed by Houghten and Yag-

TABLE I. Experimental Routines

Preliminary steps: Recorded nude weights. Subjects put on thermocouple and test clothing. Recorded rectal temperature, oxygen consumption, and pulse rate.

Series I	Series II
Temperatures used: 70, 76, 88, and 94° F.	Temperatures used: See below
Relative humidity: 40 and 80%	Relative humidity: See below
Period I—Subject entered control room, remained for 155 min., seated in balance. Comfort data recorded.	Period I—Subject remained in laboratory, seated in balance, at 75° F. and 45% relative humidity for 70 min.
Final steps—Recorded oxygen consumption. Subject returned to laboratory. Recorded nude weight and weight of clothing.	Period II—Subject entered control room at 94° F. and 80% relative humidity. Remained 100 min., seated in balance. Comfort data recorded.
	Period III—Returned to laboratory. Remained for 60 min., seated in balance. Comfort data recorded.
	Final steps—Recorded nude weight and clothing weight.

Measurements taken: Evaporative weight losses, skin and rectal temperature, comfort votes, time of appearance of sweat on lip, and oxygen consumption.

TABLE II. Fabric Properties of Dresses

Fiber content	Weave	Oz./sq. yd.	Thread count		Thickness, in.	Air permeability, ft.³/min.
			Warp	Filling		
Cotton	Plain	2.3	97	84	.021	333.0
Nylon	Plain	1.6	110	99	.028	424.0
Acetate	Oxford variation	5.0	152	78	.011	66.9
Arnel	Plain	4.5	64	50	.009	8.4

lou [11]. This scale was (1) cold, (2) cool, (3) slightly cool, (4) comfortable, (5) slightly warm, (6) warm, (7) hot. The subject was instructed to vote how she felt, not how the environment felt to her.

In this study two series of tests were run. In Series I the environmental conditions were kept constant during a given test. In Series II the subject met a rapid change in environmental conditions passing from one condition to another. The routines for both series of tests are summarized in Table I.

Discussion of Data

Series I

In no case in Series I tests was it possible to prove that the fiber content of a fabric had any significant effect upon the measured variables used in this study. In other words, any effect of the fiber type is smaller than the effects of other variables such as the differences between subjects and the day-to-day variability with any one subject. The girls differed greatly in the amount they sweat and the rapidity with which they started to sweat, and this accounts for the rather large standard deviations for the mean values. Although at times large differences in total weight loss did occur while wearing the various assemblies, these differences seemed to be more directly related to the weight of the clothing assembly rather than to fiber type.

Information about the fabric in the dresses for both series is given in Table II. The thickness results for the dress fabrics were unusual in that they were not proportional to the weights of the fabric. This was because of the various finishes applied to the fabrics. The nylon, the lightest in weight of the four fabrics, had a rather deep heat set pucker which caused it to be the thickest of the four fabrics when measured at 0.1 lb./sq. in. on a Schiefer compressometer. The cotton, a plisse, also was thicker than might have been predicted from the weight because of the pucker created by the finish. The acetate was a flat woven oxford variation fabric. The Arnel was a sharkskin. The three fabrics of man-made fibers were made from filament yarns.

Since the other parts of the clothing assembly were purchased commercially, similar tests were not done on the fabric in them. However, the total effect of the layers of fabric was, no doubt, more important than the single effect of the fabric in the dresses.

Weights of the various component parts of each assembly for Size 16 are given in Table III showing that, with the exception of nylon, the dress and slip accounted for the greatest part of the weight. These weights were taken after the clothing had conditioned for at least 24 hr. at 75° F. and 45% relative humidity.

The air permeability values for the four fabrics (Table II) used in the dresses are not apt to have been very important because of the very low air movement used in these tests, since the work of Andreen et al. [1] indicated that fabric weight had more effect on the comfort rating of fabrics than did the air permeability when low rates of air movement were used.

In Table IV data about the subjects in the Series I tests are given. Both the resting oxygen consumption and heat production values for the two sets of girls used in the tests were very close. Thus the data from the different girls might well be comparable even though the girls were not the same. Table V, giving the average resting oxygen consumption for the five subjects at each condition, tends to confirm this statement.

The figure in the last column of Table IV puts the heat production data on the basis of unit of body area so that the subjects can be more readily compared. In the two groups of the Series I data there was in each case one subject with a high heat production per unit of body area when compared with the other subjects. However, the average heat productions per unit of body area were essentially the same for both groups of subjects.

The comfort votes were essentially the same at both humidities at 70° F. However, at the higher humidity the comfort votes increased more rapidly as the temperature was raised from 70° to 94° F. The comfort vote proved to be highly related to many of the objective body measurements made in these studies, as shown by the correlation coefficients given in Table VI. The correlation coefficient between comfort vote and weighted mean skin temperature was good, but those for the temperatures of the head and extremities were very high. The relationship between the comfort votes and the temperatures except those for hands and feet were linear, while the latter were curvilinear and were fitted to reciprocal curves. It is evident that the fiber content of the clothing worn by the subjects had no significant effect on the comfort votes obtained (Figure 1) since the

TABLE III. Weight in Grams of Component Parts of Clothing Assembly (Size 16) Conditioned at 75° F. and 45% Relative Humidity for 24 Hr.

Garment	Cotton	Nylon	Acetate	Arnel
Dress	207.3	153.8	390.0	394.5
Belt	16.8	16.8	21.3	20.7
Slip	132.4	93.7	132.3	101.9
Brassiere	35.8	27.0	37.0	35.0
Pants	44.0	20.9	38.7	45.3
Girdle	107.6	101.0	101.0	95.3
Stockings	12.0	12.2	12.1	13.4
Total	555.9	425.4	732.4	705.1

TABLE IV. Physical Data on Subjects Used in Series I Tests

Series	Subject	Age	Height	Weight, lb.	Resting oxygen consumption, STP cc./min.	S.D.	Heat production/hr.	
							Kg. cal.	Kg. cal./meter^2
I*	A. R.	19	5′5″	112.5	200		57.90	37.12
	M. D.	21	5′7¼″	124.3	211		61.08	36.36
	L. L.	20	5′5½″	127.0	212		61.37	36.97
	M. W.	20	5′4¾″	110.8	243		70.35	45.68
	J. G.	19	5′7½″	142.3	232		67.16	37.94
Average			5′6″	123.4	220	17.5	63.57	38.81
I†	V. P.	19	5′6¼″	132.8	215		62.24	35.98
	D. K.	19	5′3¼″	106.6	215		62.24	41.77
	J. W.	18	5′5½″	116.7	225		65.14	40.71
	L. R.	26	5′1¼″	117.9	233		67.45	44.38
	E. S.	19	5′6¼″	119.3	233		64.56	39.85
Average			5′5″	118.7	222	7.6	64.38	40.53

* These subjects wore clothing assemblies made from cotton and from nylon.
† These subjects wore clothing assemblies made from acetate and from Arnel.

mean comfort votes for all four fibers lie well within the ±2 standard deviation limits plotted on the figure.

As the temperature of the environment was increased, the weighted mean skin temperature and rectal temperature also rose (Figure 2). Both the mean skin temperature and the rectal temperatures went higher at 80% relative humidity than at 40%. As can be seen from the closeness of the data in relation to the limits of ±2 standard deviations, no significant differences in mean skin temperature or rectal temperature were caused by wearing clothing of different fiber contents.

Figure 3 shows that the average evaporative weight losses of the subjects also increased as the environ-

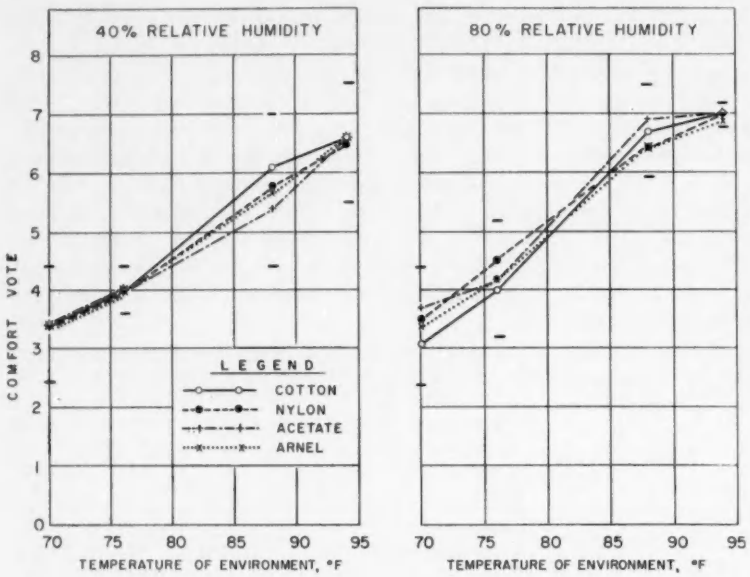

Fig. 1. Average comfort vote of five subjects dressed in cotton and nylon assemblies of clothing and five subjects dressed in acetate and Arnel assemblies of clothing for four environment temperatures and two relative humidities at each temperature (for last 120 min. of 155-min. test period).

TABLE V. Average Oxygen Consumption of Five Subjects for Series I Tests *

RH, %	Temp., °F.	Cotton Av. cc./min.	Cotton S.D.	Nylon Av. cc./min.	Nylon S.D.	Acetate Av. cc./min.	Acetate S.D.	Arnel Av. cc./min.	Arnel S.D.
40	70	227	31	223	14	231	11	220	15
	76	206	21	218	14	219	8	221	14
	88	224	27	216	23	222	6	226	18
	94	229	16	207	25	222	15	225	4
80	70	225	36	223	28	219	12	221	22
	76	221	19	230	24	219	15	219	13
	88	217	5	227	25	219	4	223	11
	94	222	28	214	21	220	11	230	8

* At four temperatures and two humidities.

TABLE VI. Correlation Coefficients Between Body Temperatures and Average Comfort Votes for Last 120 Min. of Series I Test Period

Head	Thigh	Rectal	Trunk	Legs	Arms	Mean skin	Feet*	Hands*
0.97	0.95	0.90	0.88	0.97	0.96	0.96	0.99	0.98

* Curvilinear indices of correlation fitted to reciprocal curves.

mental temperatures were increased. Again there were no significant differences caused by wearing clothing of different fiber content. When the relative humidity was 80%, the evaporative weight losses were lower at every temperature than they were at the 40% relative humidity. This was to be expected, because with the air more nearly saturated the body could not evaporate its moisture as readily. Discomfort was associated with the lower evaporative weight losses at the higher air temperatures because less body cooling took place by convection, conduction, and radiation at these temperatures. This discomfort was reflected in the higher comfort votes at the higher relative humidity at 88° and 94° F. temperatures (Figure 1). Large increases in average total weight loss (Figure 4) occurred at the higher humidities and temperatures. Differences in the amounts of weight the subjects lost while wearing the various clothing assemblies reflected the differences in the assembly weights; acetate, the heaviest assembly, caused the highest total weight loss.

Again the great increase in the total weight loss which accompanied exposure to the higher humidity coincided with more discomfort. The subjects were sweating more but were not able to evaporate the sweat so readily. Therefore additional environmental stress was being placed on the body in terms of the higher relative humidity and the body was not able to use efficiently the mechanism, sweating and evaporating this sweat, to relieve this stress.

When the gains in assembly weights from the beginning to the end of the tests made at 40% relative humidity were expressed as percentages of the original weights (Figure 5), the changes in weights were negligible for the temperature of 70°, 76°, and 88° F. and less than 5% for 94° F. No free liquid sweat was present on the body at the lower temperatures and very little, if any, at 94° F.

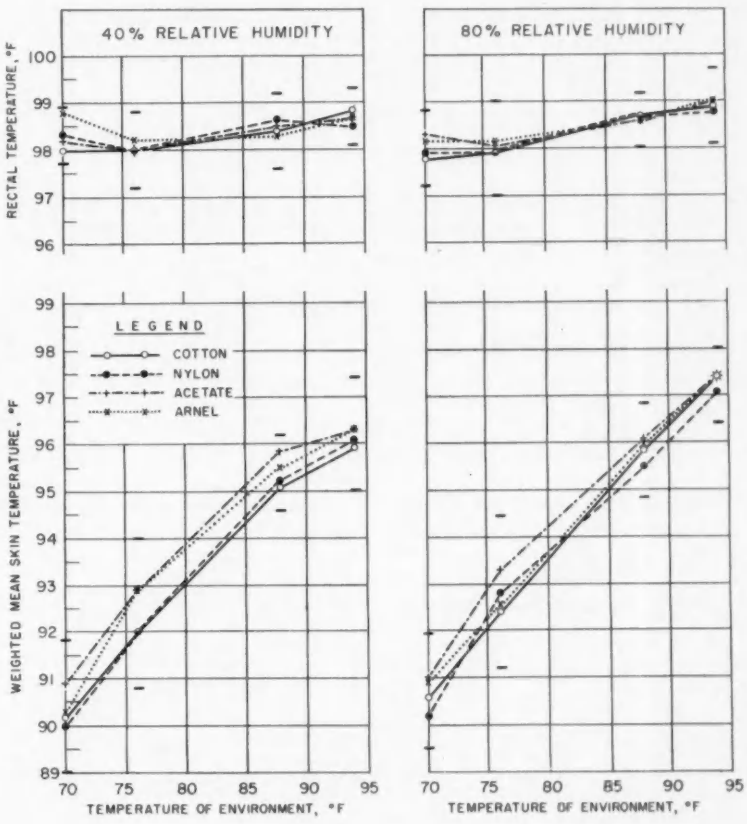

Fig. 2. Average weighted mean skin temperature and rectal temperature of five subjects dressed in cotton and nylon assemblies of clothing and five subjects dressed in acetate and Arnel assemblies of clothing for four environment temperatures and two relative humidities at each temperature (for last 120 min. of 155-min. test period).

With the 80% relative humidity conditions the percent gains in the assembly weights were less than 1.5% for the temperatures of 70° and 76° F., and again little liquid sweat was present on the surface of the skin. However, at the higher temperatures of 88° and 94° F., the subjects sweat more profusely

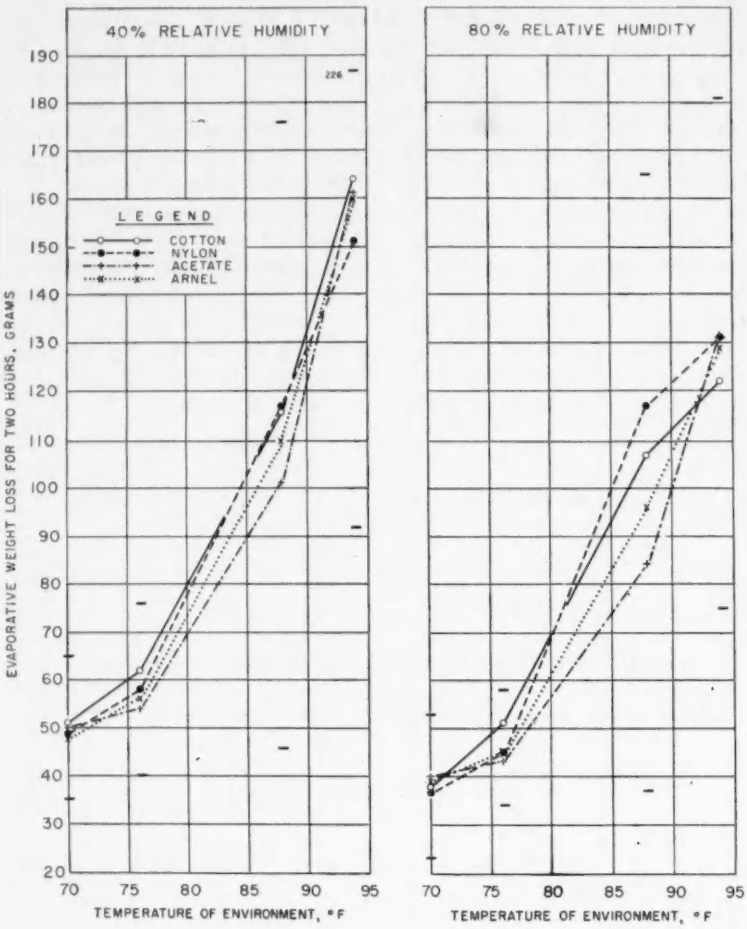

Fig. 3. Average evaporative weight loss for two hours of five subjects dressed in cotton and nylon assemblies of clothing and five subjects dressed in acetate and Arnel assemblies of clothing for four environment temperatures and two relative humidities at each temperature (for last 120 min. of 155-min. test period).

TABLE VII. Average Weight Changes in Subjects and Clothes* by Evaporation During Each Period of Series II Tests†

Test period		Conditions		Cotton		Nylon		Acetate		Arnel	
No.	Length, min.	Relative humidity, %	Temp., °F.	Wt. loss, g.	S.D.	Wt. loss, g.	S.D.	Wt. loss, g.	S.D.	Wt. loss. g.	S.D.
1	70	45	75	35.0	3.0	34.5	2.7	37.4	3.2	33.6	3.0
2	100	80	94	35.2	12.8	38.7	13.1	37.5	13.2	35.7	13.3
3	60	45	75	70.1	8.9	65.2	9.5	82.4	15.7	66.6	9.2
Total				140.3		138.4		157.3		135.9	

* These weight changes were moisture lost by the subject and did not include the evaporation of the moisture which condensed in the clothes at the beginning of Period II.

† Average of three tests for each of five subjects.

while wearing all of the assemblies of clothing; since evaporation was restricted by the high relative humidity, the sweat collected in larger amounts in the assemblies, especially at the 94° F. condition. The relative magnitude of the amounts followed the weights of the assemblies. This is in agreement with results given by Andreen et al. [1].

Series II

The results in Series II followed the same general pattern as in Series I. Again no differences in the comfort votes or body temperature measurements could be attributed to fiber content.

With the four assemblies the total evaporative weight losses that occurred during all three test periods were relatively close together (Table VII). In every case the weight change or evaporative weight loss was very high in the third period in comparison with Periods I and II. The conditions during this period were considered comfortable (75° F. and 45% relative humidity), and it is assumed that the sweat that had accumulated on the skin and in the clothing during the second period (94° F. and 80% relative humidity) had an opportunity to evaporate. The subjects clothed in the heavier acetate assembly had somewhat higher evaporative weight losses in the third period than did those dressed in the lighter fabrics. Both the total evaporative weight losses for the three periods and the high evaporative weight losses for the third period reflected the effect on the subject of the environment rather than fiber content of the fabric.

With the exception of the value obtained with the acetate clothing, the average total weight losses of the subjects during the tests (Table VIII) were relatively close, being 240, 222, 218, and 213 g. respectively for the acetate, cotton, Arnel, and nylon assemblies.

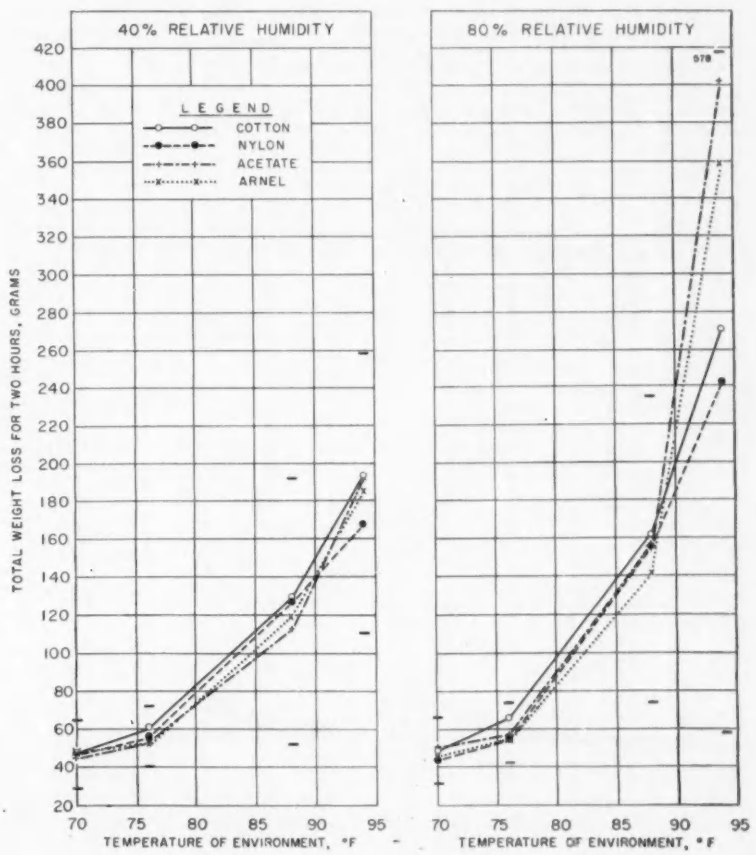

Fig. 4. Average total weight loss of five subjects dressed in cotton and nylon assemblies of clothing and five subjects dressed in acetate and Arnel assemblies of clothing for four environment temperatures and two relative humidities at each temperature (for last 120 min. of 155-min. test period).

The weight gains of the clothing assemblies (Table IX) were small when compared to those obtained in Series I at 94° F., 80% relative humidity. During the third period all the clothing assemblies had a chance to evaporate the moisture accumulated during the second period, so that changes in assembly weights were very small. While acetate was again the highest in moisture retention, the cotton assembly retained more moisture than did the Arnel in this test series. The nylon assembly still had the least amount of moisture in it at the end of the test. As shown in Table II, the total assembly weights increased in the order nylon, cotton, Arnel, and acetate.

It seems probable that differences in fabric geometry and weight plus the effects of the air spaces between the multiple layers of fabric in the clothing assemblies would tend to obscure any small differences between the warm weather comfort of clothing made from various fibers.

When the figures for the time of onset of sweating, defined as the length of time between entrance into the hot, humid conditions (94° F., 80% relative humidity) of the control room and the visual appearance of sweat on the upper lip, were averaged for all five girls for the three tests with each assembly, they were essentially the same (Table X) for the different fibers.

TABLE VIII. Average Total Weight Loss of Five Subjects During Series II Tests

Cotton		Nylon		Acetate		Arnel	
Wt. loss, g.	S.D.	Wt. loss, g.	S.D.	Wt. loss, g.	S.D.	Wt. loss, g.	S.D.
222	40.8	213	49.9	240	54.4	218	31.8

TABLE IX. Average Change in Weight of Clothing Assemblies During Series II Tests

Cotton		Nylon		Acetate		Arnel	
Average change, g.	S.D.	Average change, g.	S.D.	Average change, g.	S.D.	Average change, g.	S.D.
10.8	1.5	5.5	1.2	14.9	7.1	7.1	3.6

TABLE X. Average Time of Onset of Sweating of Five Subjects After Entering Conditions of 94° F. and 80% RH, Series II

Cotton		Nylon		Acetate		Arnel	
Time, min.	S.D.	Time, min.	S.D.	Time, min.	S.D.	Time, min.	S.D.
46	16.3	44	12.2	40	17.5	48	21.4

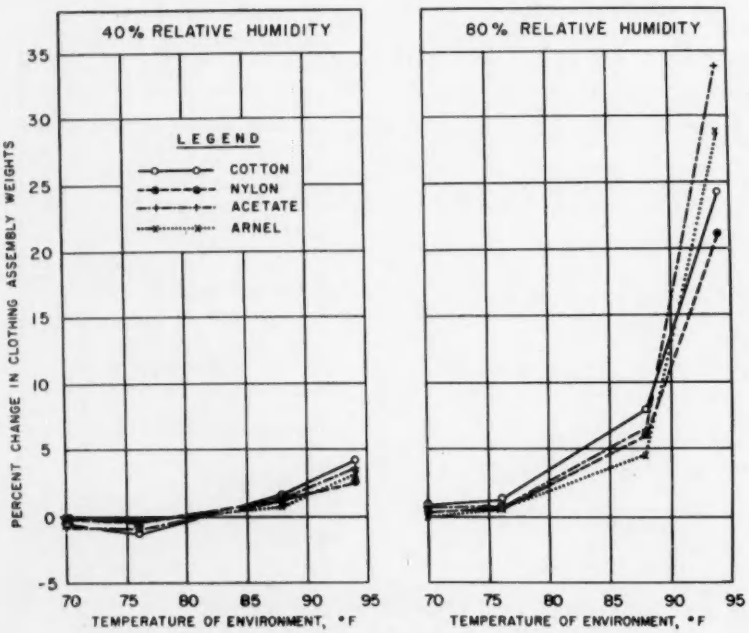

Fig. 5. Percent change in weights of clothing assemblies (average of five assemblies each of cotton, nylon, acetate, and Arnel fibers) when worn by five subjects in four environment temperatures with two relative humidities at each temperature (for entire 155-min. test period).

In Figure 6 the lowest set of data shows the rates of evaporative weight losses during the three periods of the tests. In these Series II tests the subject did not wait to start the first period of the test until she had relaxed and until her rectal temperature became about constant. Instead, she sat in the Buffalo physiological scale as soon as she had been weighed in the nude on the Buffalo platform scale, inserted the rectal thermocouple, and dressed in a given assembly of clothing. Her resting oxygen consumption was taken after 20 min. This then explains the dip in evaporative weight loss per unit of time that occurred just after the first period of the test started. The subject came into the air conditioned laboratory from temperature and humidity conditions that were usually different from those in the laboratory. She had just finished a period of activity, eating, and some walking in an environment different from 75° F. and 45% relative humidity. During the preparation period and the first portion of the first test period she was equilibrating physiologically and thermally to the sitting degree of activity and the comfortable environmental conditions.

When the subject entered the control room in the second period of the test where the temperature was 94° F. and the relative humidity 80% there was some condensation of moisture in her clothing. There was also a high absorption rate for the first few minutes. These gains account for the negative evaporative weight loss rates obtained just after the subjects entered the control room.

When the subject returned to the laboratory, 75° F. and 45% relative humidity, with large quantities of sweat in her clothes and on the skin and sat in the Buffalo physiological scale at comfortable conditions, the evaporative weight loss rates were relatively high. Although they decreased very rapidly during the first 20 min. and continued to decrease for 50 min. of the

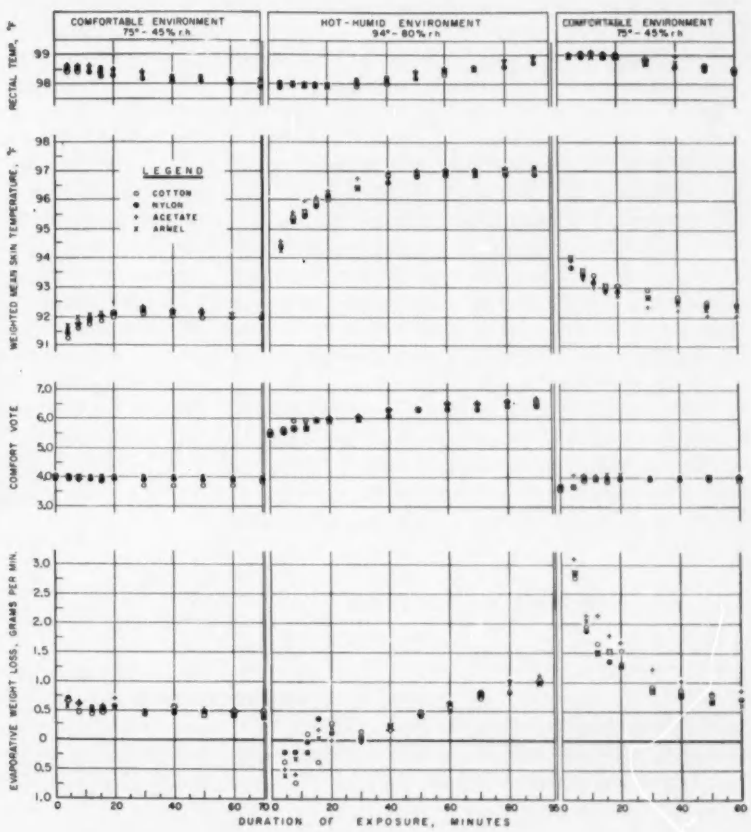

Fig. 6. Evaporative weight loss (subjects plus clothes), comfort vote and weighted mean skin and rectal temperatures in a comfortable environment, upon going from a comfortable environment into a hot-humid environment, and upon returning to the comfortable environment. Average of three tests with each of five subjects dressed in cotton, nylon, acetate, and Arnel assemblies of clothing.

60-min. period, they were still slightly higher at the end of the third period than they were at the end of the first period just before the subject entered the hot, humid conditions.

The rectal temperatures for the subjects dressed in the four assemblies were very close (Figure 6). At the end of the third period the rectal temperature had leveled off and was about the same as it was at the start of the test.

The comfort votes with the four assemblies were essentially the same during the three periods of the tests. Although there is some evidence of slight chilling during the first 8 min. of the third period, the subjects voted "comfortable" thereafter even though the evaporative weight loss rates were high on account of the excessive amounts of moisture in the clothes. This was probably because of the low air velocity, 25 ft./min. or less, in the area where the subjects were sitting in the Buffalo physiological scale. It is believed by the authors that higher air velocities would have resulted in more chilling and higher evaporative rates.

The change in the comfort vote, like that of the weighted mean skin temperature, was rapid when the subjects entered and left the hot, humid conditions. Again, as in Series I tests, the comfort vote was a reliable subjective measurement that followed closely the objective measurement of weighted mean skin temperature. The correlation coefficient (Table XI) between weighted mean skin temperature and comfort vote was 0.96 and the ones for the trunk and arms were 0.97. The rectal temperature was a poor indicator of the expected comfort vote in these tests because the changes in rectal temperatures were small and slower than the changes in skin temperature. As in Series I, the indices of correlation between the temperatures in the extremities and the comfort votes were very high, 0.99 in both cases. Again, the regression lines for the feet and hands were curvilinear, while those for the other measured areas were linear.

Summary and Conclusions

This study was made to test the commonly held assumption that the thermal comfort of clothing worn at elevated temperatures and humidities is affected by the fiber content of the fabric. Fabrics were chosen to compare natural versus man-made and high versus low moisture regain fibers.

Women in complete outfits of clothing of nylon, cotton, acetate, and Arnel were tested at temperatures from 70° to 94° F. at both medium and low humidities. The objective measures used were total weight loss, evaporative weight loss, weight gain of clothing, rectal temperature and skin temperature, and time of onset of sweating. A subjective comfort vote was also taken.

None of these indices showed significant differences among fibers in relation to the thermal comfort of clothing. The most significant effects found in any of the data were the increases in assembly weights during the tests at the 94° F., 80% relative humidity condition. These increases were proportional to the original weights of the assemblies regardless of the fiber type.

The temperature and relative humidity had a decided effect on the comfort votes and total weight losses of the subjects at 88° and 94° F. environmental temperatures. The relative humidity affected the evaporative weight losses at all four environmental temperatures.

There were large differences in the average total weight losses of the subjects in the 94° F. and 80% relative humidity environment which were related to the weights of the assemblies. In relatively still air (25 ft./min. or less) the heavier assemblies apparently caused more sweating, which resulted in greater weight losses. The subjective comfort votes were consistent and correlated well with the objective skin temperature measurements.

Similar results were obtained when the subjects were exposed to rapid changes in environment. Either with or without large quantities of sweat on the skin and in the clothing, no difference in thermal comfort as measured by comfort votes and skin temperatures could be attributed to fiber content.

Acknowledgment

The authors wish to acknowledge the cooperation of the Department of Mechanical Engineering and the Physical Environment Unit, a facility of the Graduate College. They are grateful for the cooperation and help of all the people who assisted in the performance of the tests, the various members of the textile industry who have supported the work, and to Floyd E. Boys, M.D. of the Department of Health Education for medical services and examinations of subjects.

TABLE XI. Correlation Coefficients Between Area Body Temperatures and Average Comfort Votes—Series II Tests, All Three Periods

Head	Thigh	Rectal	Trunk	Legs	Arms	Mean skin	Feet*	Hands*
0.97	0.88	−0.28	0.97	0.86	0.97	0.96	0.99	0.99

* Curvilinear indices of correlation fitted to reciprocal curves.

Literature Cited

1. Andreen, J. H. et al., TEXTILE RESEARCH JOURNAL **23**, 11 (1953).
2. American Society of Heating and Air-Conditioning Engineers, "Heating, Ventilating, Air Conditioning Guide 1958," Chapter VI.
3. American Society for Testing Materials, Committee D–13, "Standards on Textile Materials," Philadelphia, 1956.
4. Bogaty, Herman et al., TEXTILE RESEARCH JOURNAL **27**, 445 (1957).
5. Fahnestock, M. K. and Werden, J. E., *Refrigerating Engineering* **64**, 43 (February 1956).
6. Hardy, J. D. and DuBois, E. F., *J. Nutrition* **15**, 477 (1938).
7. Hardy, H. B. et al., TEXTILE RESEARCH JOURNAL **23**, 1 (1953).
8. Hick, F. K. et al., *ASHAE Transactions* **58**, 189 (1952).
9. Hollies, Norman R. S., TEXTILE RESEARCH JOURNAL **26**, 829 (1956).
10. Hollies, Norman R. S. et al., TEXTILE RESEARCH JOURNAL **27**, 8 (1957).
11. Houghten, F. C. and Yaglou, C. P., *ASHAE Transactions* **29**, 361 (1923).
12. Inouye, Tohru et al., *ASHAE Transactions* **59**, 35 (1953).
13. Newburgh, L. H., "Physiology of Heat Regulation and the Science of Clothing," W. B. Saunders Company, 291–442 (1949).
14. Winslow, C. E. A. and Herrington, L. P., "Temperature and Human Life," Princeton University Press, Chapter VI (1949).
15. Yaglou, C. P., *ASHAE Transactions* **53**, 307 (1947).
16. Yaglou, C. P., *ASHAE Transactions* **54**, 291 (1948).

Manuscript received October 27, 1958.

The Effects of Wear and Laundering on the Wrinkling of Fabrics[1]

P. R. Wilkinson and R. M. Hoffman

Textile Fibers Department, E. I. du Pont de Nemours & Co., Inc., Wilmington, Delaware

Abstract

In a garment, freedom from wrinkling depends upon the ability of the fabric to recover from bending deformations which occur during wear and laundering. During wear, the important variables are the ambient temperature and humidity and the activity of the wearer. Fabrics next to the wearer's body are exposed to temperatures of 90–95° F., to relative humidities of 60–95%, and to pressures up to 2 psi for various times. During laundering, the important conditions are temperatures of 100–140° F. while wet, pressure of 1–2 psi, and deformation times of 4–6 min. followed by temperature changes which may either *set* wrinkles in or remove them as in tumble drying.

The mechanical agitation during washing does not cause wrinkling; it actually assists the fabric to recover from wear wrinkles. Centrifugal spinning to remove water is the major cause of wrinkling in automatic washing machines.

Data and information on the above factors can be used in the design of laboratory tests which can currently predict the performance of wash-wear fabrics. Several new and modified test procedures which are being developed along these lines are described.

Introduction

This report is a continuation of others on the general subject of wash-wear from the laboratories of the Du Pont Textile Fibers Department; it covers the work being done to define the variables of wear and laundering and to study the effect of these variables on the wrinkling of fabrics. Freedom from wrinkles is one of several necessary and desirable properties of a good wash and wear garment. The visual appearance of a worn garment depends not only on the inherent ability of the fabric to recover from wrinkles but on additional factors such as the type of garment and the color, surface texture, and print pattern of the fabric. Specifically, however, the wrinkling is the result of the incomplete recovery of the fibers and yarns within a fabric from the accidental bending which occurs during wear and laundering. Fibers and fabrics vary in their inherent ability to recover from deformation. In addition, however, external factors play an important part. These are stress, strain, time, humidity, and temperature, operating in various combinations and sequences.

[1] Presented at the meeting of The Fiber Society, Clemson, S. C., May 1, 1958.

Wrinkles from Compression and Flexing During Wear

The wrinkles which occur during wear are normally confined to small areas and specific locations in a garment. The number and location of these areas vary with the type of garment. Generally speaking, a worn garment which covers one or more of the locations indicated in Figure 1 will exhibit some degree of wrinkling.

The six locations shown can be divided into a compression group, which includes those areas where the fabric is compressed between the body and some other surface, and a movement group, which includes those areas where the fabric is compressed between two parts of the body as a result of body movement. Examples of the actual wrinkling of fabrics taken from the various locations are shown in the figure.

Compression wrinkles are normally sharp and numerous, as shown by the pictures of the back of the blouse and the trouser (or skirt) seat. The direction of the formation of wrinkles depends on the location involved and the type of garment. As shown in this figure, trousers wrinkle primarily on the bias and across the warp in the seat areas, while blouses show random wrinkles on the back. The

severe wrinkles formed on a man's shirt under the belt are of the compression type.

The wrinkles in the sleeves and lap of garments are quite different in appearance from those on the seat and on the back of garments. Movement wrinkles formed at the sleeves and lap are normally long and rounded. These wrinkles are generally found to be horizontal; that is, perpendicular to the axis of bending. Therefore they are across warp yarns which run vertically up and down in most garments. Intermittent flexing of the fabric in these particular areas causes the warp yarns to be repeatedly bent in the same location. This type of wrinkle is particularly noticeable on coats, trousers, and skirts.

Fabrics which are evaluated for wrinkling in the laboratory should be wrinkled in the direction most prevalent in worn garments. This is particularly true when fabrics contain different yarns in the two directions. For example, in a man's suit or trousers most of the wrinkles are across the warp yarns and the rest are on the bias. These garments seldom contain a wrinkle which is across the filling yarns. This does not mean that the filling yarns are unimportant to the performance of trousers. On the contrary, the pressed-in creases which must be retained are across the filling yarns.

Shirts and blouses, unlike trousers, contain about an equal number of warp and filling wrinkles.

The Influence of Temperature and Humidity

The most important factors influencing the wrinkling of fabrics during wear are (1) the temperature of the fabric in contact with the body, (2) the moisture content of the fabric in contact with the body, (3) the pressure which deforms the fabric, (4) the time the fabric is deformed and the time for recovery, and (5) the number of times the fabric is bent in the same location.

Measurements were made of the fabric temperature before, during, and after deformation at the various areas in which wrinkling normally occurs. Generally, the fabric temperature reached 90–95° F. 5 min. after body contact and returned to the original temperature within 2 min. after being released from body contact. Original temperatures were variable in the range between skin temperature and room temperature.

Measurements were made of the relative humidity of the atmosphere around fabrics when they are deformed in the seat area; the apparatus is shown in Figure 2. This is a specially constructed seat, with two recesses lined with a moistureproof film. Each of these recesses contains a humidity-sensing element and a thermocouple to measure the equilibrium

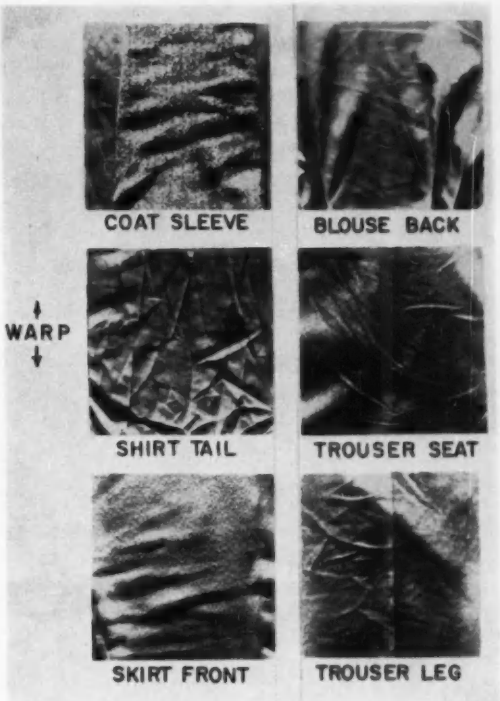

Fig. 1. Areas of wrinkling during wear. Compression wrinkles are formed at back, seat, and beltline of garments. Wrinkles due to movement are found at the sleeves, legs, and in the lap of garments.

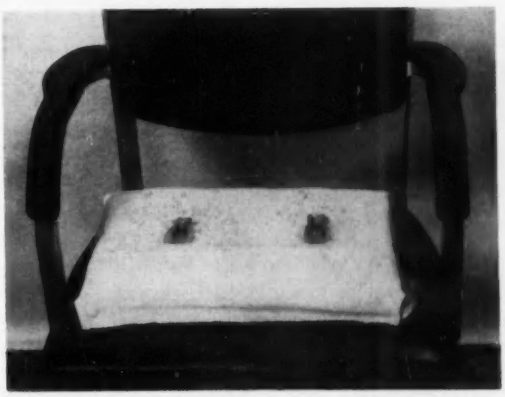

Fig. 2. Chair pad containing sensing elements for the measurement of humidity next to the body.

humidity and temperature. Data obtained with this device are shown in Table I. The relative humidity of the air in contact with the fabric depends on the prior activity of the wearer, on whether the weather or the room is comfortable or uncomfortable, and upon the time of sitting. If the ambient conditions are comfortable and if the wearer has not been engaging in physical activity such as walking, then the relative humidity in contact with the fabric is 60%. After 30 min. sitting time this rises to 75%. If the wearer has been walking prior to the test, the relative humidity rises to about 85%. If the ambient conditions are quite uncomfortable, equivalent to a hot humid day, the wearer perspires during the test and the relative humidity measured in the chair approaches 90–95%. If he has been walking or working and is perspiring more freely, the relative humidity will be very high and the fabric will be wet. These data support the conclusion that a laboratory method for simulating the formation of wear wrinkles must utilize not only a moderate humidity (65%) but also a very high one of 95% at temperatures of 90–95° F.

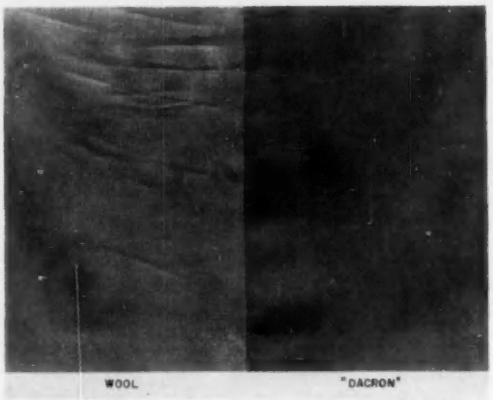

Fig. 3. Wear test skirt showing the effect of hot, humid conditions on the wrinkling of two different fabrics worn simultaneously.

Figure 3 is a photograph of a skirt, one panel made from a fabric of Dacron [2] and the other from wool. For the first ten days of wearing, no wrinkles occurred in either panel. On the eleventh day, which was hot and humid, wrinkles appeared in the wool panel and remained thereafter.

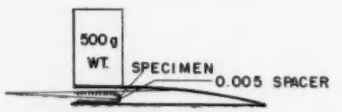

Fig. 4. The unrealistically severe deformation which occurs in the standard crease recovery test.

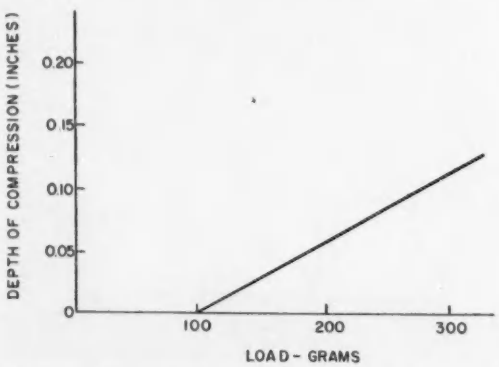

Fig. 5. Average load-compression curve for right hip of ten seated subjects.

The Effect of Pressure on Wrinkle Formation During Wear

In the crease recovery test, the load used to deform a specimen is usually 500 g., which is placed on a specimen as shown in Figure 4. The specimen is forced to bend between two hard surfaces; between the two free ends of the specimen is a metal spacer 0.005 in. thick. This is an unrealistically severe method for creasing a fabric. Unlike these metal surfaces, the human body is compressible, as are many of the other surfaces upon which people sit or lean. It is also difficult to state exactly how much pressure is being placed "per inch of bend" on the fabric because of the unknown distribution of the weight between the bend and the rest of the sample.

In order to determine what effect compressibility has on the wrinkling of fabrics, we made a chair seat of clear plastic and observed fabric loops as subjects

[2] Du Pont trademark for its polyester fiber.

TABLE I. Relative Humidity, %, of Air in Contact with Fabric When Wrinkling Occurs

	Comfortable ambient conditions		Uncomfortable ambient conditions	
Walking	85	90	95	Wet
Standing	60	75	90	95
	1	30	1	30
	Sitting time, min.		Sitting time, min.	

sat on them. We found that fabric folds are not completely collapsed into a sharp 180° fold when wrinkling takes place and that the degree of collapse varies from fabric to fabric.

We therefore made some measurements of the compressibility of the body. Subjects were asked to sit on a chair seat of clear plastic which contained an opening under the right hip. The opening was made just large enough to permit passage of a vertical strip, 1 in. wide and $\frac{1}{32}$ in. thick. Pressure was applied to the hip by raising a spring balance under the strip acting as a plunger. The curve shown in Figure 5 represents the average compression for 10 subjects. Generally, the curves of all the subjects were linear with depth of compression, but were displaced somewhat along the load axis.

The 100-g. intercept at zero depth of compression represents the load which must be applied upward through the strip in order to prevent the body from bulging into the opening. This clearly demonstrates that the pressure applied by the body is somewhat "hydraulic" in nature and is not well represented by a solid brass weight such as used in the standard crease test. The plunger height and its load is representative of the vertical height of a fabric fold under load.

Determination of the load compression curves of several folded fabrics was done with the equipment shown in Figure 6. A fabric specimen was folded between two parallel plates and held in place by double-faced adhesive tape at the ends. The direction of response of the Instron recorder was reversed so that the force of compression of the fabric fold was recorded as the head moved upward. The force required to compress the fold was converted to grams per linear inch of crease as a function of the vertical diameter of the fold. These data were then added to the plot of the compression curve of the body (Figure 5) to obtain the composite graph shown in Figure 7.

The point at which these curves cross represents the vertical height of a fabric fold compressed as it would be while being sat upon. At this point the force exerted by the body and the depth of the body compression are in balance with the resisting force and the height of the fabric loop. As stress decay occurs within the fabric fold, the height of the loop will decrease and the amount of body compression will decrease. This results in less force being applied to the fabric by the body. Therefore, we conclude that a soft material which duplicates as nearly as possible the compression of the body should be used in laboratory tests for measuring the wrinkling of fabrics.

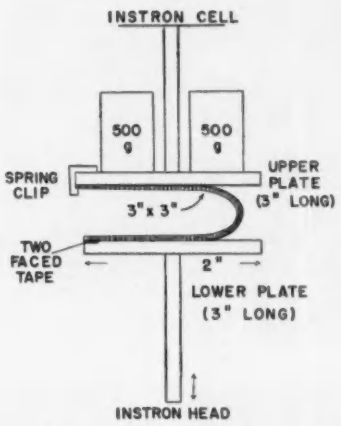

Fig. 6. Fabric loop compression apparatus.

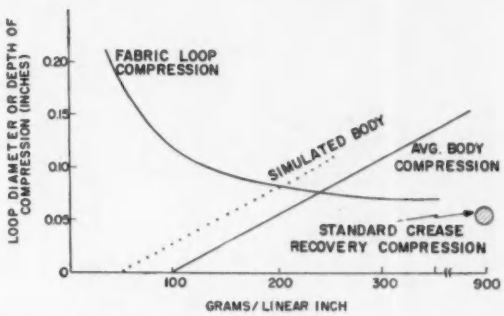

Fig. 7. Relation of fabric loop compression to body compression.

Various types of materials were examined in order to find one which could be used to simulate the amount and kind of pressure exerted by the body. The data for such a material, a 1-in. thick layer of foam rubber compressed by a dead weight of 1 lb./sq. in., are shown by the dotted line in Figure 7. The displacement between the two curves indicates that this material is not an exact duplication of the body but is close enough for the purpose.

We next compared these new pressure conditions with those generally used in the standard crease recovery test procedure. The standard $4 \times 1\frac{1}{2}$ cm. specimen was placed in the fabric fold compression apparatus (Figure 6). A metal spacer 0.005 in. in thickness was placed between the free ends as in the normal crease recovery procedure. The loop of

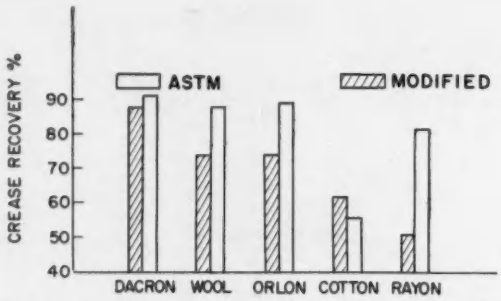

Fig. 8. Comparison of crease recovery values by standard and modified test conditions.

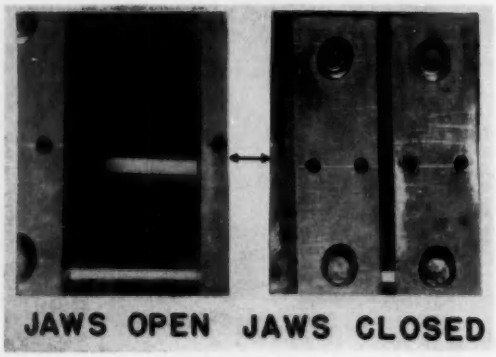

Fig. 9. Device for wrinkling fabrics by repeat flexing.

fabric was then compressed to the standard load of 500 g. In this case, the load per linear inch of crease was 900 g. and the average diameter (five fabrics) of the loop was 0.05 in. A point representing these data is shown by the circle at the lower right of Figure 7 (note scale change). It is clearly evident that the standard crease recovery test pressure produces sharper bends than would actually occur during wear and is therefore unrealistic.

Combined Effect of New Test Conditions

Figure 7 illustrates typical results using a modified crease recovery test procedure based on the proper choice of all of the variables discussed above. The creasing conditions were 90° F., 85% RH, and a 20-min. load time with the simulated body material described above. The recovery conditions were 65% RH and 70° F. These results are compared to those obtained by the standard ASTM procedure. In three cases, the new conditions cause a marked decrease and in one case (cotton) an improvement in measured crease recovery. This, then,

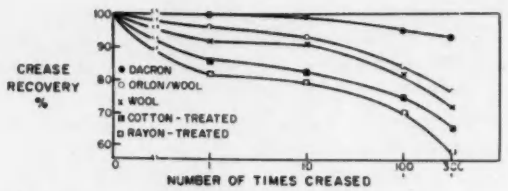

Fig. 10. Recovery of fabrics from mild creases, put in repeatedly.

is the combined result of more severe temperature, humidity, and deformation time with a less severe manner of applying pressure. The crease recovery values obtained with the new test conditions correlate much better with the actual wear test performance of these particular fabrics. This modified test has been designed so that the results are related to the wrinkles which occur during sitting. It is therefore too severe to predict the performance or the appearance of the creases that we see in the sleeves of coats or the lap of trousers.

Wrinkles from Repeated Flexing

As shown in Figure 1, sleeve wrinkles are quite rounded and appear to have been formed under conditions which are less severe than those which produce sharp wrinkles in the back or the seat of garments. We find that the inner diameter of the fold produced in these areas is 0.05 in. or larger, depending on the type of fabric which is used in the garments. Creases of these diameters do not normally produce an objectionable appearance in a fabric after a few bendings. However, we find that bad wrinkles produced in these areas are formed by repeatedly bending the same yarns in the same locations during the period of wear. With the apparatus shown in Figure 9, we have studied the effect of repeatedly bending a fabric.

A fabric specimen 4 × 1½ cm. is placed between the two jaws of the apparatus as shown. When the apparatus is started, the jaws alternately open (2 in. apart) and close (0.12 in. apart), forming a natural bend in the fabric. By means of an electronic circuit a delay feature is built into the apparatus to stop the movement for 2 min. when the jaws close. This procedure is repeated for as many times as desired; then the specimens are removed from the apparatus and placed in a standard crease recovery tester for measurement of the angle after 5 min. of recovery.

Data obtained from this procedure are shown in Figure 10. A single flexing produced mild wrinkling in some of the fabrics, particularly with rayon and cotton. Nine more cycles caused but little increase. However, when the creasing was repeated 100 or more times, some of the fabrics developed objectionable wrinkles. These wrinkles and the corresponding decreases in recovery were very pronounced for the rayon and the cotton fabrics, less pronounced for the wool fabric, and still less for the one of Orlon[3] and wool. The fabric of Dacron showed very slight wrinkling after 300 cycles.

These data agree well with the appearance of the front of trousers observed during field tests with garments made of these particular fabrics and ranked for wrinkle resistance.

In summary, there are basically two types of wrinkles which occur in wear—sharp wrinkles at the seat or back and rounded wrinkles at the sleeves and lap. The temperature and moisture environment of the fabric is often as severe as 90° F. and 85% RH for both types. The deformation pressure and the manner in which it is exerted differ widely for the two types. Both types occur in many kinds of garments and must be covered in any laboratory evaluation used to predict the wrinkle resistance of fabrics during wear.

The Removal of Wear Wrinkles During Laundering

In a strict sense the popular belief that washing produces wrinkles is not true. On the contrary, the machine agitation or washing step of laundering is primarily responsible for the removal of wrinkles which are formed in wear.

The effect of agitation on fabrics is shown in Figure 11. A shows the back of a shirt after one day of wear; B shows the garment after 15 min. of machine agitation with a full load of clothes. It is essentially free of wrinkles. In comparison, C and D show that the worn garment after only one minute of agitation or after a hand washing still contains some wrinkles even though they have been reduced in severity. Neither C nor D show any wrinkles due to washing, but both were considered as needing touch-up ironing. Fabrics from thermoplastic fibers require a warm water temperature of 95° F. or higher during agitation in addition to good mechanical action for the adequate removal of wear wrinkles. We conclude that *worn* garments should generally be used for a reliable laundering evaluation of wash-wear performance, particularly in the case of hand washing or cold water washing.

[3] Du Pont trademark for its acrylic fiber.

The Formation of Wrinkles during Spinning

The so-called wash wrinkle is not present in garments which have been agitated and hung to drip dry. The formation of wrinkles during laundering occurs during the two spinning operations and should properly be called spin wrinkles.

Figure 12 shows the movement of a typical wash and wear garment through the various operations of machine laundering and drying. The heavy double

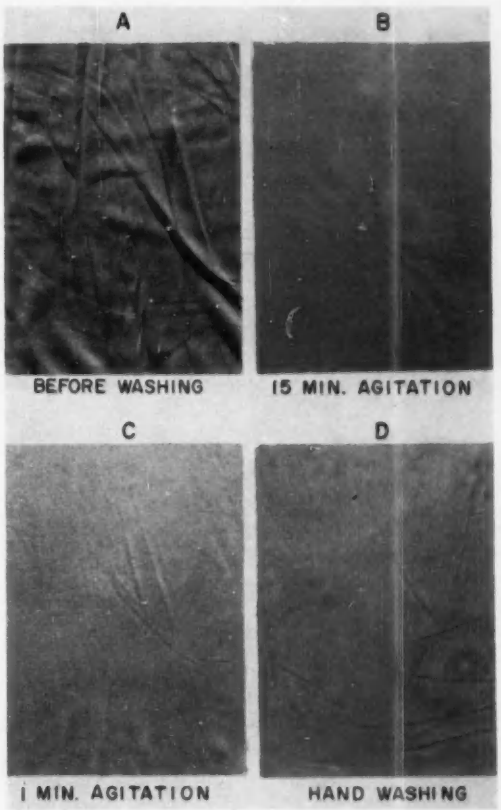

Fig. 11. The removal of wrinkles by agitation during warm water washing.

lines represent the two wrinkling operations. Agitated garments show a few insignificant wear wrinkles, but no new additional wrinkles. Rinse spinning, the operation which removed the dirty soapy water from the garments, introduces the first spin wrinkles. These are removed to some extent during the next operation, that of rinse agitation. The last operation, spin drying, wrinkles the fabrics a second time. This is undoubtedly the most severe wrinkling operation of the entire home laundering cycle.

The best appearing garments of the three drying methods are those that have been tumbled-dried. In general all fabrics appear better after tumble drying than after any other procedure involving machine laundering. Those from procedures which eliminate the final spin-dry operation are second best.

During spinning, the fabrics are subjected to cooling, loss of water, and creasing under high pressures for about 5 min. The temperature which affects the wrinkling of fabrics during laundering is that of the water which is removed from the fabrics during spinning. For fabrics which contain synthetic fibers, this temperature is 95–100° F. at the start of both rinse spinning and spin drying, when the recommended warm water setting is used. The hot water setting used for rayons and cottons results in water temperatures of 125–135° F. at the start of rinse spinning but only 95–100° F. at the start of the final spin dry. We have found that the temperature of the fabrics decreases 10–20° F. as evaporation takes place during spinning. Finally, the fabric temperature drops to below room temperature when the garment is removed from the washer and exposed to the cooler air. The chilling effect during spinning and after the fabric is removed from the washer tends to set wrinkles in fabrics, particularly those which contain thermoplastic fibers. For this reason, improved performance of thermoplastic fiber fabrics is obtained when garments are spun from cold water and chilling is eliminated.

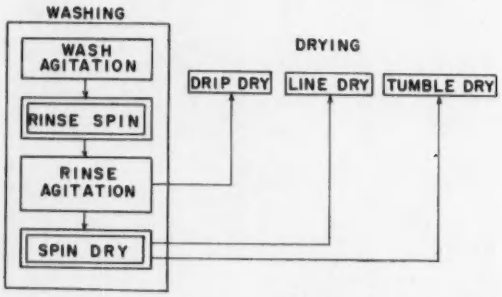

Fig. 12. The wrinkle removing steps (−) and wrinkle forming steps (=) in three methods of home laundering.

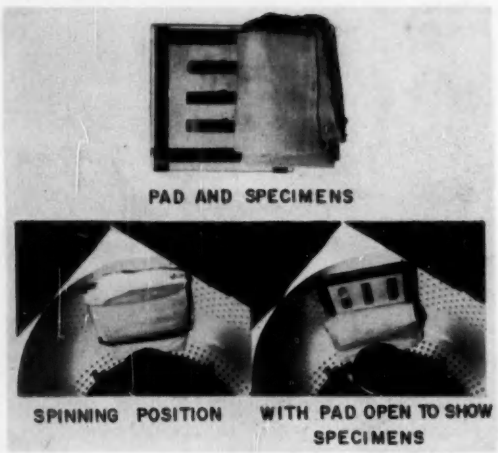

Fig. 13. Method of forming spin wrinkles in small samples of fabric.

Laboratory Test for Spin Wrinkles

We have devised a laboratory method for evaluating small fabric samples when complete garments are unavailable. This test uses the centrifugal force of the spinning drum in a washing machine to force a wet pad of fabric against a folded fabric specimen. This is an expedient way of obtaining a realistic pressure which *decreases* as water is removed while spinning proceeds.

The pad shown in Figure 13 consists of many layers of fabric attached to a base plate of plastic.

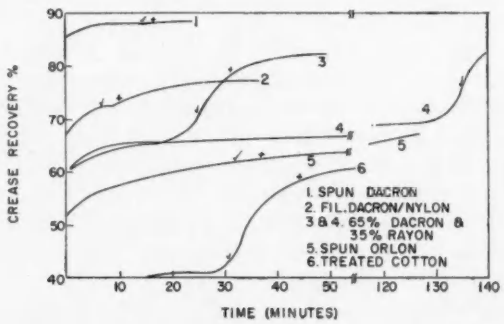

Fig. 14. Time dependence of fabric recovery from wet creasing. Water retention is shown at 5% (V) and 0% (+).

Three fabric samples of the same size as ordinary crease recovery specimens are inserted between the pad and its base, as shown. The pad is then soaked in water, placed in the washer in the spinning position, and centrifuged with the final spin dry cycle. When the machine stops spinning, the specimens are removed and placed in crease recovery testers for angle measurement. Creases obtained in this manner appear very similar in appearance to the severe spin wrinkles which occur in complete machine-washed fabrics.

Eighty layers of thin fabric are used for the pad. This number was chosen after a calculation of the pressure involved during the spin drying of shirts.

A 4-lb. load of shirts was washed in a washer having a drum diameter of 20 in. After being spun, the shirts were distributed in a thick band 6 in. high around the drum; the total area of this band was about 378 sq. in. This amounted to 5 g. dry fabric/sq. in. The fabric used in our pad required 80 layers to give this weight. When a washer which spins at 550 rpm is used for washing, the pressure decreases from about 2 psi early in the spinning operation to about 1½ psi at the end of spinning. These pressures vary with the type of garments which are being laundered, the spinning speed of the washer, and the water retention of the fabrics.

The Wrinkle Recovery of Fabrics During Drying

The recovery versus time curves from wet creases obtained by using this spinning pad procedure are shown in Figure 14. Certain fabrics undergo some initial recovery; then there is a period of inactivity followed by a rapid increase in recovery rate. The increase occurs when the water retention of the sample has dropped to about 5% by weight as it dries in still air while mounted in the recovery tester. Curve 1 shows the recovery of a spun fabric of 100% Dacron, which recovers so completely while still wet that it does not show this delay. The check marks on these curves indicate the time required for the drying fabric to reach 5% water retention. For most samples it was found that the weight loss was linear in time until the fabric reached about 5% water retention. According to the accepted interpretation, this loss represented the evaporation of surface water. For most fabrics the rapid recovery started at 5% water retention and was complete by the time the fabric reached equilibrium water content, as indicated by the crosses on these curves. Curve 2 represents a filament fabric of 85% Dacron and 15% nylon. It shows only a slight effect. Curves 3 and 4 represent identical specimens of a spun fabric of 65% Dacron and 35% rayon. Both of these specimens show the same large increase in recovery but after different periods of time.

This difference between Curves 3 and 4 was achieved by rewetting Sample 4 by dipping it in water to make it soaking wet at the start of the recovery period. All of the specimens except Sample 4 had been spun dried and were damp at the start of the recovery period. As shown, Sample 4 required somewhat more than two hours to complete its recovery. Curve 5 represents a spun fabric of Orlon; no change in rate was observed at the end of the drying period, but the recovery increased steadily with time. Curve 6 represents a resin-treated cotton suiting. We conclude that this phenomenon involves a restraint imposed on fabric recovery by the presence of liquid water; it possibly involves swelling and friction. We have found the effect only with fabrics containing cellulosic fibers but have not studied enough fiber types to generalize. Presumably this effect occurs during the drying of laundered fabrics. To obtain the true recovery of a wet-creased fabric, therefore, one must continue to measure its recovery until it has dried completely.

Conclusions

Wash and wear describes garments which maintain a neat appearance during wear and after home laundering. Freedom from wrinkles is only one of the many criteria of a good wash and wear garment, but it is the key fabric property and is the one which is receiving extensive study.

Freedom from wrinkles depends on the inherent ability of a fabric to recover from wear and laundering conditions. As shown in Table II, these are dependent on the wearer and the laundering procedure.

TABLE II. Summary of Wrinkling Factors

Wear	Laundry
Body movement (flexing)	Agitation (wrinkle recovery)
Body weight (compression)	Spinning (wrinkle formation)
Perspiration	Temperature (removal)
Temperature	Chilling (setting)
Compressibility	Wash load (pressure)
Ambient conditions	Loss of moisture

Wear produces two types of wrinkles, one due to the flexing movement of the body and the other to compression by the weight of the body. The temperature and humidity conditions are similar for both types, but the applied pressure is less for the movement wrinkle. The skin temperature, perspiration rate, and body compressibility, as well as ambient conditions, are variables which materially influence the amount of the wrinkling of fabrics during wear.

The wrinkling which occurs in machine washing occurs primarily in the spinning operations. The actual washing operation helps to remove wear wrinkles from wash and wear garments. It is important during washing to have good mechanical agitation of the garments and a water temperature of 95° F. or higher.

The use of warm water is desirable during agitation but undesirable during spinning. During spinning fabric temperatures decrease; this causes a setting of wrinkles in fabrics which contain thermoplastic fibers. Similarly, the decrease in water content which occurs during drying causes a setting of spin-wrinkles in fabrics which contain hydrophilic fibers. The pressure which deforms fabrics during spinning varies with the type of garment being laundered, the water retention of the fabric, and the design of the washer. The average pressure is about 2 psi.

The severity of the wrinkling produced during wear may be either less than or greater than that produced during laundering, depending on the home laundry procedure used. Wear wrinkles differ from spin-wrinkles, however, in that the latter, if present, are distributed over the entire garment whereas wear wrinkles are normally confined to small areas in specific locations.

Laboratory tests must employ realistic conditions in order to give results which can be correlated with actual use. Several such modified procedures under development have been described. These include a modified crease recovery procedure for evaluating the effect of wear on fabrics and a technique for measuring machine spin-wrinkling on small fabric specimens. Such tools can help place the evaluation of the wash and wear performance of a fabric on a quantitative basis.

Manuscript received February 12, 1959.

Procion Dye Staining for Differentiation of Skin and Core of Viscose Rayon Fibers

Koichi Kato

Research Department, Toyo Rayon Co. Ltd., Otsu, Japan

Abstract

A new microscopical technique for differentiating the skin–core structure of viscose rayon fibers is described. Slide preparations mounting fiber cross sections are stained with an alkaline solution of Procion Black HGS, which is a Procion dye recently marketed by ICI as a chemically reactive dye for cellulose fibers. This technique is found to furnish a staining entirely selective for the skin area in a simple and rapid way.

Since it is well established that Procion dyes do react chemically with cellulose molecules under alkaline conditions, it is highly probable that the differential staining produced by the present technique is due to a definite difference existing between the skin and the core with respect to the chemical reactivity toward the dye employed. This differentiation mechanism appears to be quite different from that which is generally accepted to be the case in the previously described techniques using ordinary dyes.

Typical results are presented for several types of cellulose rayons showing various staining behaviors. It is seen that these results are in good agreement with those obtained by other stain methods.

The same procedure, when applied to a variety of fibers other than cellulosics, is found to give positive staining reactions only to wool, silk, regenerated protein, and Vinylon fibers. Although most of these findings are as yet not satisfactorily explained, reactive dye staining of this kind seems to be of much promise in the field of fiber microscopy.

Introduction

Several staining techniques have been described for revealing microscopically the skin–core effect characteristic of viscose rayons [1, 2, 5, 8, 9, 11–14], where either direct or basic dye is employed to stain cross section preparations. It is generally accepted that the skin–core differentiation in every case takes place solely by virtue of physical phenomena such as diffusion and adsorption of dye molecules.

The silver staining developed by E. C. Jolliff [3] can also be used for the same purpose. This method gives excellent skin staining, although it is not simple to operate, but needs considerable practice if consistent results are to be obtained.

In a previous paper [5] the author described a direct dye technique with some of its applications; in another paper [6] he examined in detail the silver method referred to above, in order to make clear its character as a chemical stain. Throughout these studies chief interest was to elucidate the internal structures of regenerated cellulose fibers, especially the skin–core effect of viscose rayons, mainly by means of light microscopical methods.

In the course of investigation along this line it has recently been found that an excellent differentiation between the skin and core can be obtained by the use of Procion Black HGS. This stain technique is apparently dependent upon chemical fixation of the dye to the cellulose material, therefore upon a mechanism different from that involved in any other technique so far reported.

Experimental Procedure and Results Obtained

The preparation of fiber cross sections about 5μ thick was described in a previous paper [5].

The staining solution is prepared as follows. Dissolve 10 g. of Procion Black HGS and 7 g. of urea in a small amount of hot distilled water. After cooling, add 2 g. of soda ash, then make to 100 g. with distilled water. This solution can be stored at room temperature without deterioration for several weeks or more.

The steps in the staining procedure are as follows. First flood the slide preparations with a proper amount of the above dye solution and gently heat over small flame or on a hot plate for several minutes,

taking care not to let the solution dry. Wash excess dye from the slides by rinsing with water. The slides are then ready for mounting and examination, any further differentiating process being unnecessary.

A deep black staining takes place only on the skin area, the inner core remaining almost unstained. Typical results obtained for textile rayon, all-skin type cord rayon, cuprammonium rayon, and Fortisan are shown in Figures 1–4 respectively, together with conventional tire cord rayon as control. It will be seen that these results are in good agreement with those given by other ordinary dye techniques.

It is shown in Figure 5 that cotton fibers have acquired relatively high stainability during the mercerization process, presumably owing to the well-known reduction in crystallinity due to the treatment. A similar change in the cross-sectional staining behavior of cotton fibers has already been described in the previous paper [5].

It should be noted here that the final results attained in the present technique are little affected by slight variations of the conditions concerned, such as staining time, dye concentration, pH, heating temperature, etc. It is surely an advantage as a procedure for routine use.

Fig. 1. A conventional tire cord rayon showing a typical skin–core effect and a textile rayon showing its core somewhat stained. 407 ×.

Fig. 2. An all-skin type cord rayon together with a conventional tire cord rayon as control. 500 ×.

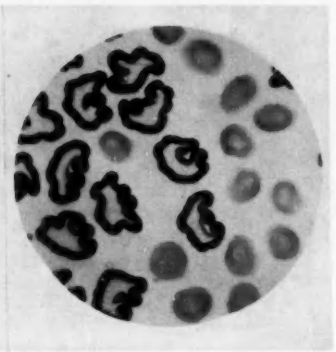

Fig. 3. Cuprammonium rayon together with a conventional tire cord rayon as control. 407 ×.

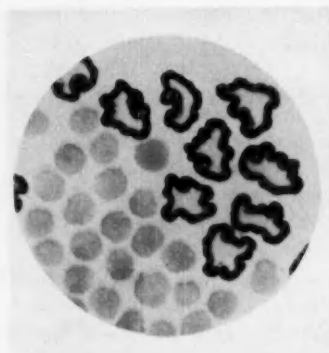

Fig. 4. Fortisan together with a conventional tire cord rayon as control. 407 ×.

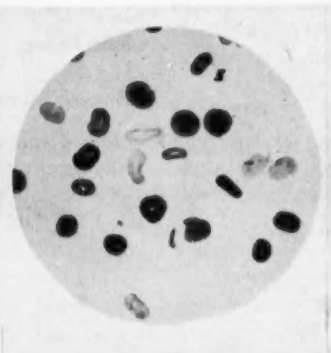

Fig. 5. Cotton fibers before and after mercerization, showing mercerized rounded fibers relatively well stained and untreated flat shaped fibers only slightly stained. 163 ×.

Fig. 6. Wool fibers showing a characteristic bilateral differentiation. 407 ×.

Fig. 7. Vinylon fibers showing a kind of skin–core differentiation. 407 ×.

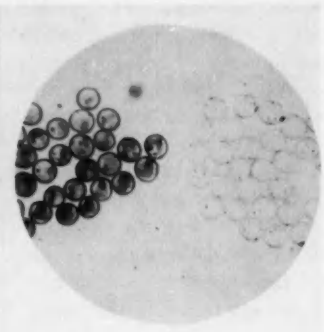

Fig. 8. Nylon 6 fibers before and after ultraviolet irradiation in Fadeometer, showing that originally unstained nylon fibers have acquired considerable stainability during the course of photodegradation. 203 ×.

Discussion

By the preliminary survey Procion Black HGS was found to be the most suitable for the present purpose among a number of Procion dyes examined. Other members, both so-called H type and cold type, were observed to produce too pale skin staining to be useful for microscopial work; at the same time the core is also slightly stained. In this respect Procion Black HGS is excellent; it gives a deep staining quite selectively on the skin area, leaving the core almost unstained, so that a good contrast between skin and core is furnished consistently.

The addition of alkali to the dye solution is essential; otherwise the desired staining does not occur at all. Sodium bicarbonate or trisodium phosphate may be used instead of soda ash; however, the first will be found to give somewhat too weak and the other somewhat too strong staining compared with soda ash under identical conditions.

Proper heating of the preparations flooded with the dye solution is also essential; otherwise fixation of the dye does not occur sufficiently at room temperature because of its relatively low reactivity. However, it is rather advantageous that the dye solution is stable enough to be stored for use at practically any time.

On the other hand, if the mounted solution is heated to dryness, the core area too becomes stained to a considerable extent; thus the contrast is destroyed.

It is already well known that the skin staining given by the previous techniques using regular dyes is a consequence of the differentiation process, when the absorbed dye is washed out selectively from the core of the wholly stained cross sections. Each technique involves a specific washing step, which is more or less critical. The present staining with Procion dye, as mentioned above, takes place on the skin area in a positive manner, therefore requiring no particular step to accomplish the differentiation.

The dyeing mechanism of Procion dyes for cellulose fibers has been discussed in many papers [15–19], and it appears to be well established that these dyes do react with hydroxyl groups of cellulose under certain conditions, thereby forming an integral part of the cellulose molecule itself. Accordingly, it is highly probable that the staining under observation depends on the fixation of the dye to the cross sections through chemical reaction with cellulose material. The selective skin staining with Procion Black HGS is not a simple result produced by the differential diffusion or absorption of the dye molecules, but just an indication that a definite difference in the chemical reactivity is present between the skin and the core in viscose rayons. The results observed for other types of cellulosic fibers, such as shown in Figures 1–5, should be accounted for similarly in terms of their chemical reactivities (or better, accessibilities) toward the cellulose-reactive dye used.

It has been shown [6] that the silver staining by Jolliff is a chemical stain associated with the reduc-

ing end groups of cellulose molecules. The present staining, though similarly of chemical nature, will be perhaps governed primarily by the hydroxyl groups along cellulose chains. As a consequence, we have had at least three types of stain methods with each different mechanism. It is desirable to make use of these techniques in a comparative manner, so as to throw additional light onto the structural features of regenerated cellulose fibers, including the skin–core effect of viscose rayons. Among others, the Procion dye technique presented here appears to be of particular interest, owing to its new principle of staining.

Further Applications

The same procedure was tested on a wide variety of fibers other than cellulosics. The staining reaction was found to be negative for cellulose acetate, polyamide, polyester, and polyacrylonitrile fibers and positive for wool, silk, regenerated protein, and Vinylon. Wool and Vinylon are worthy of note in that the former shows a bilateral staining analogous to that demonstrated by the previous workers using basic or acid dyes [4, 7, 10], while the latter exhibits a marked skin–core type differentiation, as illustrated in Figures 6 and 7.

Nylon 6 fiber, originally not at all stained, was found to become stainable to an increasing extent as it was more severely degraded by ultraviolet irradiation, as shown in Figure 8.

Of course, whether or not these positive staining reactions are due to some chemical linkages having occurred between the dye and the fiber materials is still questionable, and for the present it is impossible to explain all such findings on a reasonable basis. Although much remains to be studied, further application of reactive dyes in the field of fiber microscopy seems to be full of promise from various points of view.

Acknowledgment

The author wishes to express his thanks to Dr. K. Hoshino, Director of the Research Department of Toyo Rayon Co. Ltd., for permission to publish this paper. Sincere thanks are due to Mr. K. Yoshimura for his assistance throughout this investigation.

Literature Cited

1. Berry, W. R., TEXTILE RESEARCH JOURNAL **24**, 397 (1954).
2. Hermans, P. H., TEXTILE RESEARCH JOURNAL **18**, 9 (1948).
3. Heyn, A. N. J., "Fiber Microscopy," New York, Interscience, 201 (1954).
4. Horio, M. and Kondo, T., TEXTILE RESEARCH JOURNAL **23**, 373 (1953).
5. Kato, K., TEXTILE RESEARCH JOURNAL **27**, 803 (1957).
6. Kato, K., TEXTILE RESEARCH JOURNAL **29**, 407 (1959).
7. Mercer, E. H., TEXTILE RESEARCH JOURNAL **23**, 388 (1953).
8. Morehead, F. F. and Sisson, W. A., TEXTILE RESEARCH JOURNAL **15**, 443 (1945).
9. Ohara, K., *Sci. Pap. Inst. Phys. Chem. Res.* **25**, 152 (1934).
10. Ohara, K., *Melliand Textilber.* **19**, 407 (1938).
11. Preston, J. M., *J. Soc. Chem. Ind.* **50**, T199 (1931).
12. Preston, J. M. and Joshi, G. D., *Kolloid-Z.* **122**, 6 (1951).
13. Schramek, W. and Helm, J., *Kolloid-Z.* **85**, 291 (1938).
14. Taylor, G. G. and Brown, J. C., *J. Soc. Dyers Colourists* **69**, 396 (1953).
15. Vickerstaff, T., *J. Soc. Dyers Colourists* **73**, 237 (1957).
16. Vickerstaff, T., *Am. Dyestuff Reptr.* **47**, 33 (1958).
17. Vickerstaff, T., *Melliand Textilber.* **39**, 765 (1958).
18. Vickerstaff, T., *Melliand Textilber.* **39**, 905 (1958).
19. Wegmann, J., *Melliand Textilber.* **39**, 1006 (1958).

Manuscript received October 27, 1958.

Letter to the Editor

Short communications in the form of Letters to the Editor are intended to provide prompt publication of significant new research results and to permit an exchange of views on papers previously published in the Journal. These communications are not submitted to formal review as are research papers, and the editors do not assume any share of the author's responsibility for the information given or the opinions expressed. When work previously published in the Journal is the subject of critical comment, the authors of the original paper are given an opportunity to submit a reply, which will be published concurrently when possible.

The Effect of Alkali on the Extractability of Wool Proteins; Evidence Against Disulfide Exchange as an Explanation for the Reduction in Solubility

Division of Protein Chemistry
(formerly Biochemistry Unit)
C.S.I.R.O. Wool Research Laboratories
343 Royal Parade
Parkville, N2. (Melbourne)
Victoria, Australia
February 22, 1959

To the Editor
Textile Research Journal

Dear Sir:

Mild treatment of wool in dilute alkaline solutions causes a marked reduction or even complete loss of the subsequent solubility in urea-bisulfite solution [6]. In a recent letter Kessler and Zahn [4] have discussed this phenomenon and offered an explanation in terms of a disulfide-exchange mechanism, the interchanges being supposed to replace intrachain by interchain disulfide bonds.

I also have been studying this effect of alkali; my results agree with those of Kessler and Zahn in that the conversion of cystine to lanthionine [6] is not sufficient to explain the insolubility, since conditions can be found (for example 1–2 hr. heating in 0.05 *M* K_2CO_3 at 50°, 1–3 hr. in 0.5 *M* K_2CO_3 at 25°, or even 14 days in pH 7.0 phosphate buffer at 50°) where the subsequent solubility is markedly reduced while the cystine content remains virtually unchanged. However, my results give no support to the disulfide-exchange hypothesis.

Kessler and Zahn's explanation depends on the assumption that only about one half of the disulfide bonds are broken in the urea-bisulfite test solution. If all the disulfide bonds were broken the solubility should return to the original or an even greater value, since disulfide interchange merely replaces one set of disulfides by another. Leach [5] has shown that the reaction of sulfite with proteins, including intact wool, can be driven rapidly to completion if the solution contains an organic mercurial (RHgCl) or mercuric chloride. The equations are

$$PSSP + RHgCl + SO_3^{--} \rightarrow PSHgR + PSSO_3^- + Cl^- \quad (1)$$

$$2PSSP + HgCl_2 + 2SO_3^{--} \rightarrow PSHgSP + 2PSSO_3^- + 2Cl^- \quad (2)$$

When neohydrin (3-chloromercuri-2-methoxypropylurea) was added to the urea-bisulfite test solution, the solubility of untreated wool was hardly affected, but alkali-treated wools still showed greatly reduced solubilities. A similar picture emerged when mercuric chloride was present, except that the solubility of untreated wool was somewhat lower, due possibly to the formation of —S—Hg—S— cross links; some results are shown in Table I. The disulfide contents of the insoluble residues from these urea-bisulfite-mercury solutions were measured by an amperometric method which does not require prior hydrolysis of the protein [5] and were found to be in the

TABLE I

Treatment of Merino 64's wool (solvent scoured)	Addition to standard urea-bisulfite extractant [6]	Wt. loss in extraction test, %
Nil	Nil	56
	0.56% neohydrin	50
	0.2% $HgCl_2$	37
Heated 30 min. at 50° in 0.05 *M* K_2CO_3; liquor ratio 1:100	Nil	37
	0.56% neohydrin	22
	0.2% $HgCl_2$	11
Heated 1 hr. at 50° in 0.05 *M* K_2CO_3; liquor ratio 1:100	Nil	18
	0.56% neohydrin	−1 (wt. increase)
	0.2% $HgCl_2$	−3 (wt. increase)

TABLE II. Urea-Bisulfite Solubility (% Wt. Loss) of Wools

Time of heating in 0.05 *M* K_2CO_3 at 45°, liquor ratio 1:100	A*	B	C	D
0	55.0	58.5	53.8	57.1
15 min.	52.2	57.5	50.9	54.3
30 min.	44.6	49.6	42.8	49.8
1 hr.	25.6	39.6	30.0	41.9
2 hr.	13.6	25.8	14.6	21.7
3 hr.	9.0	14.6	9.2	8.5

* A—Merino 64's wool; –SS–, 470 μmole/g.; –SH, 30 μmole/g.; values determined by amperometric methods [5]. B—Wool treated with N-ethylmaleimide, 100 hr., 30°, pH 3.5. Final –SH value, 15 μmole/g. C—Wool treated with methylmercuric iodide, pH 7.0, and washed exhaustively. Final –SH value, Nil. D—Wool treated as in C, then with N-ethylmaleimide, 17 days, 30°, pH 3.5. Final –SH value, Nil.

range 0–20 μmole/g., showing that Reactions 1 and 2 were virtually complete under the conditions of the test.

Those wools modified by heating at pH 11 also showed reduced solubility in a standardized solubility test using 0.2 *M* thioglycollate at pH 10.4 (0.5 *M* carbonate buffer) for 1 hr. at 65°. In this solution, unlike urea-bisulfite, the extent of reduction is virtually complete both for normal and modified wools. Thus the untreated wool (—SS—, 470 μmole/g.) dissolved to the extent of 50–55%, and the insoluble residue, after reaction with iodoacetate to block —SH groups, contained only 26 μmole cystine/g. The same wool, previously heated 1 hr. at 50° in 0.05 *M* K_2CO_3 (residual —SS—, 460 μmole/g.), was only 12% soluble in the thioglycollate test; the insoluble

TABLE III. Urea-Bisulfite Solubility of Wool Heated in K_2CO_3 Solutions

Time of heating in solution A or B at 50°, liquor ratio 1:100	Solution A*	Solution B
0	51.3	51.3
15 min.	40.4	46.8
30 min.	23.0	36.8
1 hr.	9.6	22.0
2 hr.	3.0	9.4
3 hr.	1.7	8.7

* Solution A—0.05 *M* K_2CO_3, 0.05 *M* potassium acetate, pH 11.2. Solution B—0.05 *M* K_2CO_3, 0.05 *M* potassium iodoacetate, pH 11.2.

residue after reaction with iodoacetate contained less than 20 μmole cystine/g. Since the alkali-treated wools remain insoluble even under conditions where all or nearly all the disulfide bonds are broken, it is clear that disulfide exchange as proposed by Kessler and Zahn does not explain the effect of alkali in lowering the solubility. Confirmatory evidence has been found in a study of wools in which the disulfide contents have been reduced to very low values by various chemical means. On heating in alkali the same effect, a reduction in the subsequent solubility in urea-bisulfite, is still found.

An alternative hypothesis is that mild heating at pH 11 causes configurational changes in at least the more readily extractable wool proteins, leading to new hydrogen-bonded structures which are no longer easily soluble. Protein configurational changes have been invoked to explain the reduced solubility of wool in thioglycollate after being heated in boiling water [7], the increased trypsin digestibility of wool after being heated in alkaline buffers [1], the enhanced extractability of the proteins in supercontracted wool [3], and the permanent set acquired by wool after various physical and chemical treatments [2]. It can be suggested that the action of all chemical reagents on wool and other proteins must be interpreted with caution, since the effects observed may be due as much to concomitant configurational changes as to the formation of new covalent bonds between protein and reagent.

It is possible that some disulfide interchange occurs during the heating in K_2CO_3, and such exchange might even be an important aspect of the denaturation, so that chemical reagents that can retard or prevent disulfide exchange might thereby retard the effect of alkali on wool. In my view, however, such

interchange would be merely a facet of the process and not an explanation for the altered solubility. I have confirmed Kessler and Zahn's result that wool pretreated with N-ethylmaleimide is somewhat less affected by subsequent heating in 0.05 *M* K_2CO_3 than is control wool, although the differences in solubility in my case are much less than those reported [4]; see Table II. However, even this result can be accepted as evidence for a disulfide exchange only with caution, because wool treated with methylmercuric iodide under conditions known to convert *all* the —SH groups to —$SHgCH_3$ [5] fails to show a similar phenomenon. Moreover, this mercurated wool should no longer be capable of reacting with N-ethylmaleimide, but if wool is treated first with methylmercuric iodide, then with N-ethylmaleimide, and then heated as before in K_2CO_3, the same result is found as for wool treated with N-ethylmaleimide alone; it is now less affected by the alkali treatment as measured by the solubility in urea-bisulfite (Table II). This would indicate that the effect of N-ethylmaleimide, whatever it may be, is not necessarily due to its reaction with primary —SH groups.

Clear evidence that it is possible to retard the "denaturation" of wool by a chemical reagent is obtained on heating wool in 0.05 *M* K_2CO_3 also containing 0.05 *M* iodoacetate, pH 11.2. The subsequent urea-bisulfite solubilities are higher than those for wools heated similarly in a carbonate-acetate solution at the same pH value (Table III.) This result is not necessarily evidence for disulfide exchange, because iodoacetate at pH 11.2 is not specific for —SH groups. More importantly, it seems to be further evidence against Kessler and Zahn's hypothesis, because if the effect of alkali were *solely* due to intrachain–interchain rearrangements, then such disulfide reactions might be expected to be almost completely inhibited in the presence of a high concentration of iodoacetate. In fact the "heating time required to cause the urea-bisulfite solubility to fall by half" is still only 50 min. for the iodoacetate solution as compared to 30 min. for the control.

Literature Cited

1. Crewther, W. G., *Proc. Int. Wool Text. Res. Conf. Aust. 1955* **C**, 227 (1956).
2. Farnworth, A. J., TEXTILE RESEARCH JOURNAL **27**, 632 (1957).
3. Gillespie, J. M. and Lennox, F. G., *Aust. J. Biol. Sci.* **10**, 95 (1957).
4. Kessler, H. and Zahn, H., TEXTILE RESEARCH JOURNAL **28**, 357 (1958).
5. Leach, S. J., *Biochim. Biophys. Acta* **33**, 264 (1959).
6. Lees, K. and Elsworth, F. F., *Proc. Int. Wool Text. Res. Conf. Aust. 1955* **C**, 363 (1956).
7. Lennox, F. G., *Proc. Int. Wool Text. Res. Conf. Aust. 1955* **B**, 22 (1956).

J. M. SWAN

Book Reviews

Perkin Centenary London. New York, Pergamon Press, 1958. XII + 136 pages. Price $7.50.

Reviewed by Emery I. Valko, Lowell Technological Institute, Lowell, Mass.

This small volume contains the lectures given at the Perkin Centenary Celebrations held in 1958 in Perkin's native country. In contrast to the monumental "Proceedings of the Centennial" sponsored By the American Association of Textile Chemists and Colorists and edited by H. J. White, Jr., the emphasis of the British publication is entirely on the historical aspect. The life and work of Perkin is described by John Read, Clifford Paine reports the development of the dye industry, J. G. Evans gives a brief account of the "Tinctorial Arts Today," and Sir Alexander Todd reviews the "Development of Organic Chemistry since Perkin's Discovery." The volume concludes with a joint tribute to Perkin by spokesmen of the British Government, the Royal Society, the Deutsche Chemische Gesellschaft, and the Worshipful Company of Dyers. An appendix gives a report on the organization of the Celebrations and of the Perkin Centenary Fund.

Physical Methods in Chemical Analysis, Volume III. Edited by Walter G. Berl New York, Academic Press, 1956. 652 pages. Price $15.00.

Reviewed by Edmund M. Buras, Jr., Harris Research Laboratories, Washington 11, D. C.

In this, the third volume of a series, the editor indicates again his intent to describe modern methods for physical measurements and their application as tools in analytical chemistry, stressing principles and indicating areas of usefulness as well as limitations. His intentions have been accomplished with remarkable success. Each of eleven chapters on physical methods provides a thorough yet balanced treatment providing sufficient background, essential theory, descriptions of apparatus and experimental methods, typical applications, and discussions of advantages and limitations. Thus, all the information is given which an experienced chemist needs for the selection of a method suitable to a specific analytical problem, and even for the selection of suitable apparatus and procedures to carry out the required work. A twelfth chapter deals lucidly and pointedly with sampling theory and procedures which apply to all analytical work. A few inadequacies, such as an unjustifiably brief index covering only broad topics, and the absence of illustrations to describe devices for disintegration of solids and the mixing of all types of materials, are more than amply compensated for by copious references and rigorous yet readable treatments of the subject matter.

The volume contains twelve comprehensive articles, many of which are veritably books within a book. The topics are Gas Chromatography, by C. S. B. Phillips; Electrochromatography, T. Wieland and K. Dose; Electroanalytical Methods in Trace Analysis, W. D. Cooke; High-Frequency Method of Chemical Analysis, W. J. Blaedel and D. L. Petitjean; Field Emission Microscopy, E. W. Muller; Theory and Principles of Sampling for Chemical Analysis, A. A. Benedetti-Pichler; Flame Photometry, K. W. Gardiner; Microwave Spectroscopy, B. T. Dailey; Analytical Applications of Nuclear Magnetic Resonance, H. S. Gutowsky; Fluorescent X-Ray Spectrometric Analysis, G. L. Clark; Analytical Distillation, W. J. Podbielniak and S. T. Preston; and Neutron Spectroscopy and Neutron Interactions in Chemical Analysis, T. I. Taylor and W. W. Havens, Jr. When this imposing list of topics is considered together with the coverage provided by the two earlier volumes, the entire field of physical methods used in chemical analysis appears to be well covered, at least for the present.

This series of volumes is recommended without reservation to anyone who would develop an understanding of the methods of modern analytical chemistry so that he might contemplate their possible applications in his own field.